*A tutti coloro che credono in **m**e*

*e **a** tutti colo**r**o in cui **c**red**o**...*

Contents

Foreword

The huge biosynthetic potential of plants as a renewable source of fine chemicals and pharmaceuticals has long been recognized. Identification of biologically active compounds from plants and improvement of the isolation methods are of great interest for their therapeutic applications. Moreover, they are a huge source of inspiration for the design of new active compounds, not only for their structure, carrying the features responsible for drug's biological activity, but also for the biosynthetic pathways that Nature has established for them, often a suggestion for an easier synthetic access to the targeted molecule. Therefore, the future demands for pharmaceuticals is dependent on a detailed understanding of the biologically active compounds, of their biosynthetic pathways as well as the complex mechanisms regulating the development of diseases. Thus in both sections of this work two biologically active compounds and their therapeutic properties are discussed in relation to their methods of synthesis.

The first part of this work deals with the synthesis of a potential inhibitor of the hedgehog signaling pathway, a key regulator of multiple developmental processes of embryogenesis as well as in adult tissue maintenance and repair. Since its aberrant activation has been linked to the development of severe malignancies, the hedgehog signaling inhibitors has emerged as a valuable tool for cancer treatment. Several modulators have been reported so far, including cyclopamine, the first known inhibitor identified in 1968. Since its discovery, only in 2009 the first synthetic route to cyclopamine was established by Giannis et al. using a biomimetic and diastereoselective approach. This flexible synthetic strategy provides access to several structural modifications leading to multiple potential analogues of cyclopamine that do not exist in nature. Exploiting this route, in order to have new insights into the biological activity of the natural compound, the first synthetic analogue of cyclopamine was designed and partially synthesized.

In the second part of this work the catalytic activity of (S)-norcoclaurine synthase was investigated and used to set up a method for an easy access to (S)-norcoclaurine, the first common intermediate of all benzylisoquinoline alkaloids. Recently (S)-norcoclaurine gained a widespread interest in both organic and medicinal chemistry for its well recognized rich pharmacological potential in the treatment of several diseases. So far, several synthetic strategies have been employed based on asymmetric catalytic approaches involving the use of a chiral metal catalyst. Even though these synthetic routes are highly efficient and guarantee a very good enantioselectivity, they entail extensive use of organic solvents and metal catalysts. In order to develop a clean and green synthetic process towards (S)-norcoclaurine without using organic solvents and

metal catalysts, an efficient one pot-two steps synthesis was set up, starting from tyrosine and dopamine in the presence of (S)-norcoclaurine synthase providing the first attempt to exploit the potential of a “Pictet-Spengler” enzyme in the direct synthesis of chiral benzylisoquinolines.

Part A - Synthesis of IR-analogue of cyclopamine

Die vorgelegte Arbeit wurde von October 2009 bis Juni 2010 im Institut für Organische Chemie der Fakultät für Chemie und Mineralogie der Universität Leipzig unter Betreuung von Prof. Dr. Athanassios Giannis angefertigt.

Chapter 1

Introduction: the discovery of cyclopamine and hedgehog signaling

1.1. Newborn lamb malformations led to *Veratrum californicum*

Veratrum californicum (Figure 1.1), commonly known as the California false hellebore, is a lily of the family of melanthiaceae that grows throughout the mountains of the western United States. In the middle of the 20th century up to 25% of pregnant ewes that grazed in that area gave birth to lambs suffering from serious craniofacial defects. These anomalies termed holoprosencephaly (HPE) varied from the extreme of cyclopia (Figure 1.2), the presence of only one eye in the middle of the forehead accompanied with malformations of the brain, to deformed upper jaws. Furthermore, ewes carrying malformed lambs had a prolonged gestation period of about 60% (87 days) during which the lambs continued to grow in utero (the normal gestation period of a healthy sheep is 147 to 152 days).[1] Since this disease meant a huge economic loss, the sheep herders asked the *Department of Agriculture* for help. It took three summers living with sheep for the scientist Lynn F. James before discovering that in times of drought the sheep moved to higher grounds where they could graze huge amounts of *Veratrum californicum.*

a  b 

Figure 1.1 *Veratrum californicum:* plant (a) and flower (b).

Later the connection between plant and malformations was proved by Richard F. Keeler of the Poisonous Plant Research Laboratory feeding ewes of *Veratrum californicum* and observing occurrence of cyclopia in their offspring[2]; from that time on, with much relief,

the losses of newborn animals from deformities were avoided by keeping sheep away from false hellebore during early gestation.

Figure 1.2 Cyclopic malformation in lamb induced by maternal consumption of *V. californicum.*

Although the problem was solved there was still no idea concerning the causative agent of such malformations and the mechanism of action. Keeler's attempt to isolate the biological active compounds of *Veratrum californicum* led to identify three alkaloids able to induce cyclopia in embryos of pregnant sheep[3,4]: jervine, cycloposine and a third more active compound resembling jervine lately named cyclopamine after the one-eyed giant described in Homer's Odyssey.

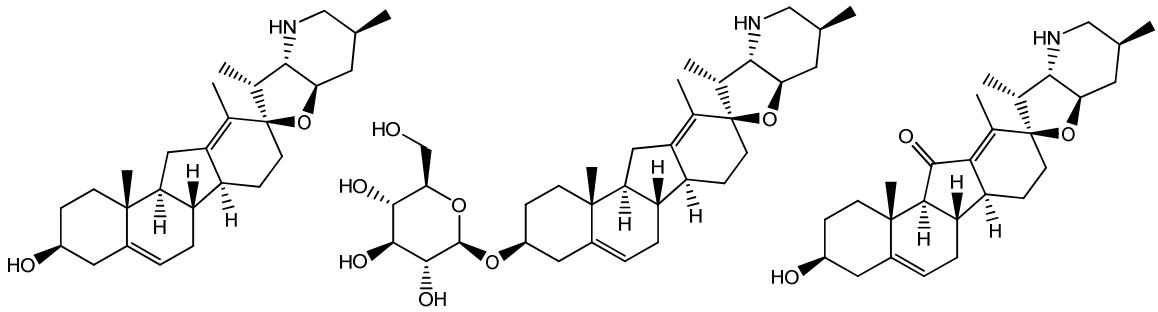

Scheme 1.1 Structures of *Veratrum* alkaloids cyclopamine, cycloposine (3-glucosyl cyclopamine) and jervine.

1.2. From *Drosophila* mutants to the hedgehog pathway

Until the 1970s very little was known about the construction of complex organism from similar repeating units. At that time Christiane Nüsslein-Volhard and Eric F. Wieschaus undertook systematic studies to understand how a relatively simple egg can give rise to a

complex segmented body plan.[5] They used lethal mutants of the fruit fly *Drosophila melanogaster* to identify the loci which, when mutated, alter the segmental pattern of the larva. In these studies more than 50 different genes involved in segmental pattern formation were identified and one of them was named *hedgehog* (*hh*), because its mutation was found to cause *Drosophila* embryos to develop as spiny balls reminiscent of hedgehogs (Figure 1.3). The number of segments of the larvae did not change, but in each segment a defined area was deleted and the remaining segments showed the phenotype of a mirror-image duplication.

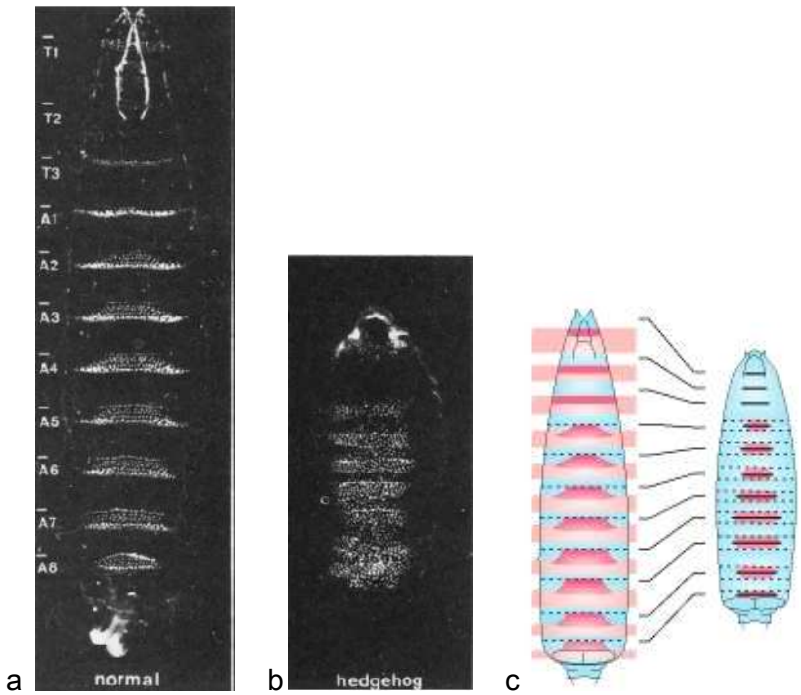

Figure 1.3 (a) Wild-type ventral larva cuticle showing its regular pattern of denticles; (b) *hh* mutant ventral cuticle: the back is covered by chitinous spines and a defined area of each segment is deleted; c) a diagram depicting the mutant larval phenotype due to mutation in the class of zygotically acting gene controlling segment number Patched in Drosophila. The boundary of each segment is the dotted line. On the left, the pink regions indicate, on a diagram of a wild-type larva, the domains of the larva that are missing in the mutant.

From this abnormal segmentation it was deduced that *hedgehog* gene could be a key regulator in embryonic development and later his activity was found to be central to the growth, patterning, and morphogenesis of many different regions within the body plans of vertebrates and insects: it produces protein signals in specific cells, and these signals establish the patterns of embryonic tissues by instructing neighboring cells to divide or to become a particular type of differentiated cell. Moreover, although the final outcome might look quite different (e.g., a fly vs. a mouse), there is a striking conservation in gene families involved in the development of these seemingly quite different organisms.

Anyway mechanism of action and features of the hh components were still unclear. In 1996, Philip A. Beachy and coworkers undertook a series of mutagenic experiments in the mouse to understand which role *hh* gene plays in development of some embryonic tissues including the spinal cord and brain.[6] Mice lacking *Sonic hedgehog* gene (*Shh*), the most-studied member of this gene family in vertebrates, led to embryos with several anomalies, including lack of midline structures, such as the floor plate and the notochord, absence of the spinal column and most of the ribs, abnormal limbs and cyclopia (Figure 1.4).

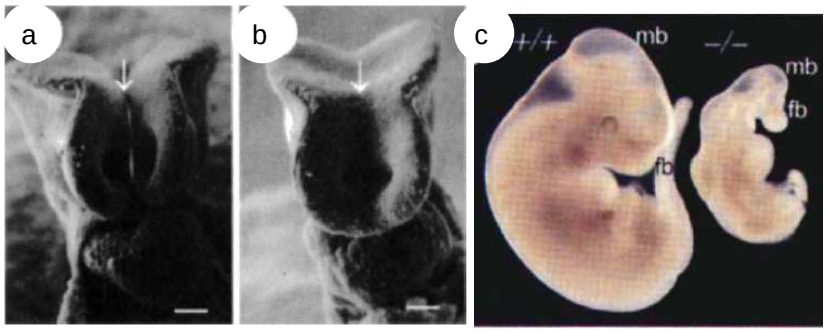

Figure 1.4 Comparison between wild-type (a) and mutant (b) embryos: in the latter is clearly missing a distinct midline, the overall size is reduced and the forebrain has an abnormal morphology (c).

The occurrence of these malformations, in particular of cyclopia, suggested a potential connection between embryonic disruption of hh signaling to previous epidemics of cyclopia in lambs fed of *V. californicum* and also to the most severe human cases of HPE. Subsequently, it was discovered that Shh undergoes a posttranslational addition of cholesterol that somehow is connected with the activity of the transmembrane receptor Patched (Ptch). Since perturbations in cholesterol metabolism are associated with holoprosencephaly in mammalian embryos, Beachy hypothesized that such abnormal phenotype in sheep was caused by interaction of cyclopamine with the Shh processing and/or cholesterol biosynthesis. His hypothesis was supported by cyclopian-type birth defects in the offspring of pregnant rats treated with AY-9944, an inhibitor of the final step of cholesterol synthesis catalyzed by 7-dehydrocholesterol (7-DHC) reductase, and some forms of Smith-Lemli-Opitz syndrome, a human disorder that results from genetic reduction in 7-DHC reductase activity. Later, a comparison of the effects of cyclopamine to those of HPE induction by AY-9944 in neural plate explants from mammalian embryos, showed that, although both compounds interrupt Shh signaling, they do so by different mechanism and cyclopamine doesn't interfere nor with cholesterol biosynthesis neither with its metabolism[7] but it's able to bind a transmembrane protein called Smoothened (Smo) resulting in a complete inhibition of hh signaling.

Since its discovery, *hh* gene was found to be involved in an increasing number of processes not only concerning normal and pathological roles in embryonic growth but also in adult tissue maintenance and in cancer development, as will be discussed later. Although many pieces in the puzzle of hh pathway are still missing, most of the components have been discovered and several inhibitors have been already identified and tested to threat some type of malignancies, opening a new and revolutionary strategy for cancer treatment.

Chapter 2

The hedgehog signaling pathway

2.1. Maturation of the hedgehog proteins

The hedgehog signaling pathway in vertebrates shares many common features with *Drosophila* hedgehog signaling, although there are several differences. While in Drosophila there is only one *hh* gene, in mouse three paralogous genes were identified: *Indian* (*Ihh*), *Desert* (*Dhh*) and *Sonic hedgehog*.[8,9] The first two were named after existing species of hedgehogs, while the third one was named after the video game character "Sonic the Hedgehog" because his icon possesses synophthalmia with a noselike structure below the eyes. These three proteins are ligands of the membrane-bound receptor Ptch and activate the hh signaling pathway, that is, they have an indirect influence on the transcription of *hh-response* genes. After translation, hh proteins undergo several posttranslational modification to generate and release the active ligand from the producing cell: the mechanism is conserved in vertebrates and invertebrates and consists in autocleavage of the precursor, addition of a cholesterol moiety and subsequent palmitoylation.[10,11,12,13]

A comparison between hh coding sequences and serine proteases gave some suggestions to understand the autocatalytic mechanism through which the initial 45-kDa precursor, after removal of a short signal sequence, yields a 19-kDa NH_2-terminal fragment (hh-N) and a 25-kDa COOH-terminal fragment (hh-C) containing the autoprocessing machinery: a conserved His residue acts as a general base in the catalytic process resulting in the autoproteolysis. First the peptide bond between the conserved residues glycine and cysteine is rearranged to form a thioester, then the hydroxyl moiety of a cholesterol attacks the carbonyl-group of the thioester. The sulphur is displaced resulting in an N-terminal signal domain that contains an ester-linked cholesterol at its C-terminus, and a C-terminal processing domain with no known activity yet. The cholesterol modification enables association of the hh-N with the plasma membrane. Subsequently, a palmitic acid moiety is added to the N-terminus of hh-N by the acyltransferase Ski, (Skinny hedgehog).[14] The resulting fully active hedgehog protein (for simplification termed hh) is then secreted from the producing cell. This step requires the activity of the 12-transmembrane protein Dispatched (Disp) which belongs to the bacterial RND (Resistance-Nodulation-Division) family of transport proteins.[15,16]

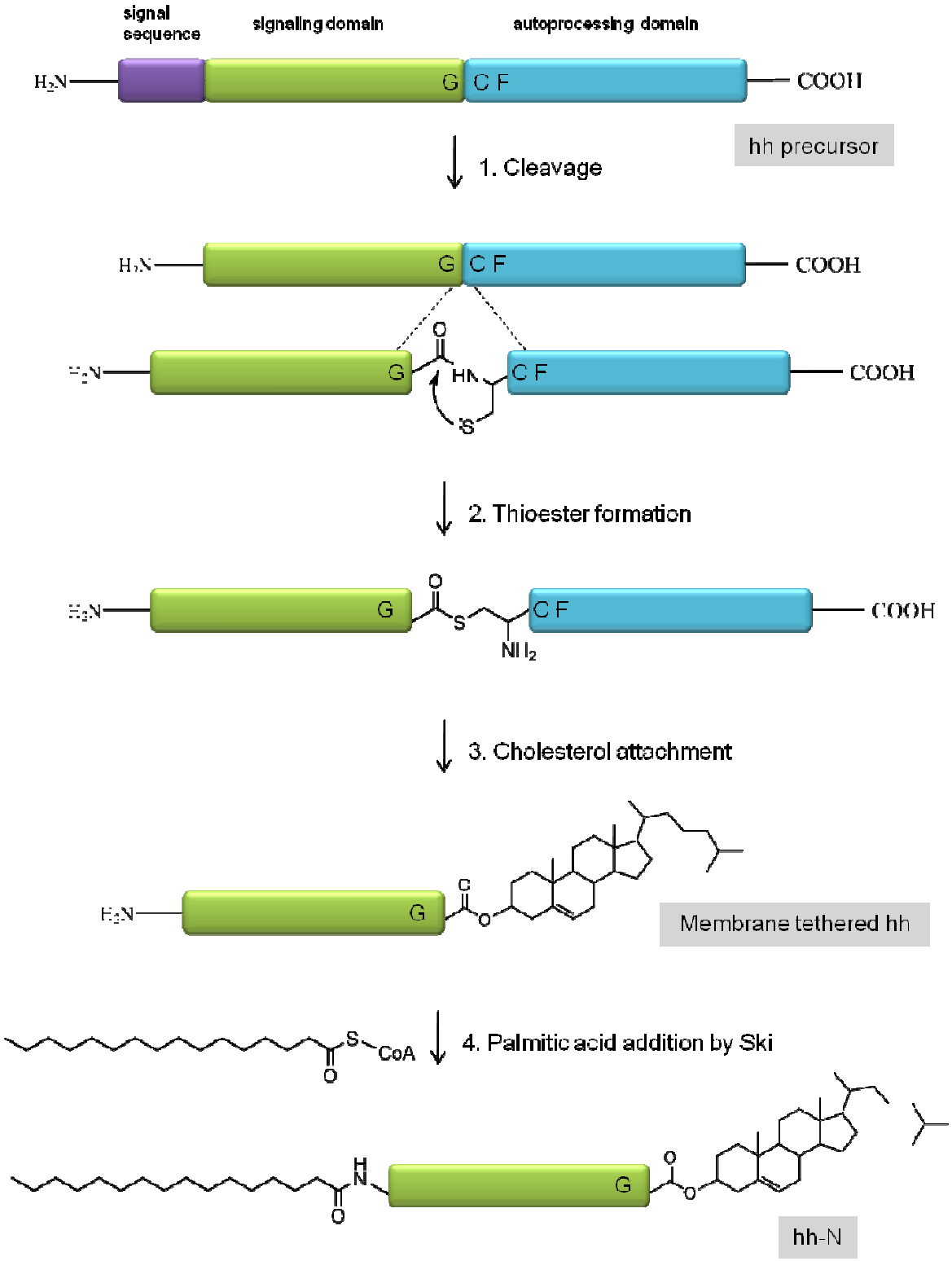

Scheme 2.1 Posttranslational modification of hedgehog protein. Hh, hedgehog protein; Ski, Skinny hedgehog; hh-N, N-terminal active hedgehog protein.

2.2. Role of lipids in hh transport

Distances over which hh has been shown to act are ~300 μm in vertebrates (Figure 3.2)[17] but how hh moves through tissues is still not clear, and could involve passive diffusion, active transport or transcytosis. A lot of hypotheses have been done, among which also a possible involvement of heparan sulphate proteoglycans. Another open question is whether hh moves as an individual molecule or if it's packed into larger structures: the physiologically relevant form of Shh in mammalian cells seems to be a stable multimeric form in which the palmitate and cholesterol moieties are responsible for the ability to associate with cellular membranes (Figure 2.1b). In addition, *Drosophila* hh was found to be transported in lipoprotein particles (Figure 2.1c).[18,19]

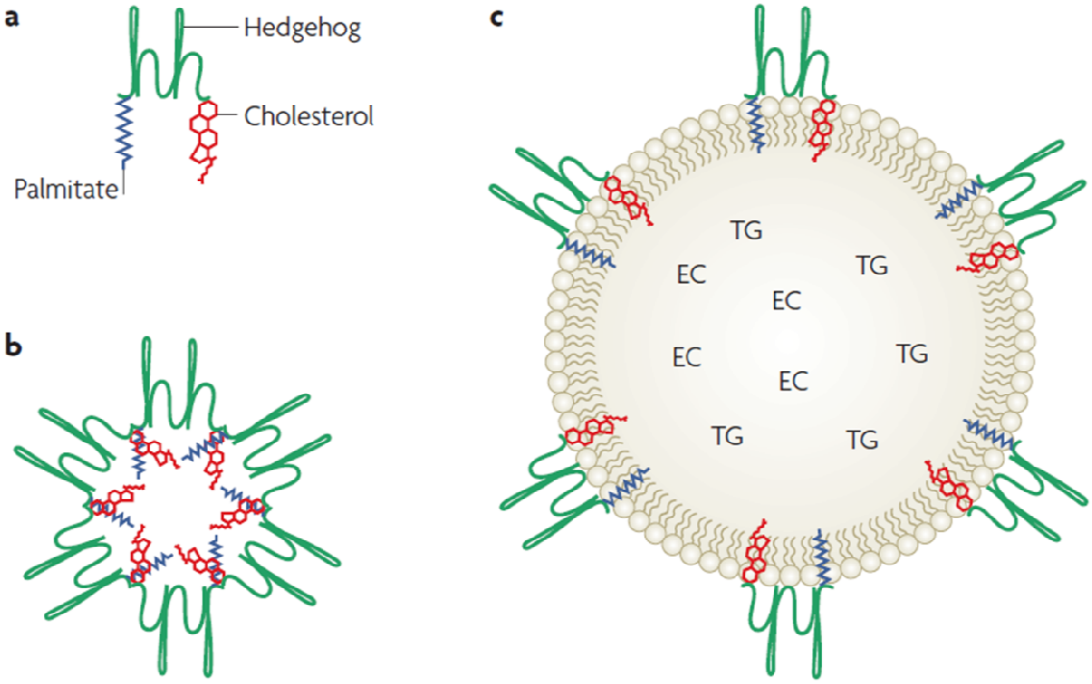

Figure 2.1 Proposed vehicles for Hedgehog release. (a) The fully active hedgehog protein covalently linked to cholesterol and palmitate. (b) Interaction of the hydrophobic moieties with each other drives the formation of hh multimers. (c) Lipoproteins carrying hh consist of an outer phospholipid monolayer that surrounds a core of esterified cholesterol (EC) and triglyceride (TG).

Recent studies suggested secretion of two different forms of proteins: the first is secreted for diffusion acting at a short-range and the second is "packaged" for long-range transport, and its formation requires the cytoplasmic membrane-scaffolding protein Reggie-1/flotillin-2.

With an outstanding mechanism, a single morphogen is able to induce distinct cellular responses in a concentration-dependent manner influencing the fate and the identity of cells through the establishment of a protein gradient (see section 3.1).[20]

2.3. The Patched receptor

The tumor-suppressor protein Patched is the receptor for the hh protein and can structurally be defined as 12-pass transmembrane protein with high degree of homology to the sterol-sensing domains of several proteins involved in cholesterol processing and trafficking, including 3-hydroxy-3-methyl-glutaryl coenzyme A (HMG-CoA) reductase. In vertebrates, Ptch exists as two isoforms (Ptch1 and Ptch2) of which Ptch1 is the functional ortholog of the well studied *Drosophila* Ptch. In the absence of hh ligand, Patched catalytically inhibits the downstream effector Smoothened (Figure 2.4). In Drosophila, Ptch keeps Smo in an unphosphorylated state, which results in its endocytosis and degradation in lysosomes. Upon binding of hedgehog, Ptch gets inactivated, resulting in the activation of Smo: Smoothened is hyperphosphorylated, leading to a block of its endocytosis and degradation.[21] It is undisputed that Patched does not directly bind to Smoothened in any possible way. The structural similarities of Patched to transporters using a proton gradient to flux small lipophilic molecules across the bilayer, like the RND protein family, have led to the hypothesis that a Smoothened ligand is pumped across the membrane thereby altering Smoothened activity. No such a molecule was found until now, however, exogenous small lipophilic molecules were reported to activate Smoothened by binding to it.[22] The involvement of primary cilia in the regulation of Patched-mediated Smoothened repression will be discussed in section 2.5.

2.4. Smoothened controls transcription of hh target genes

Smoothened is a seven-transmembrane protein with a high degree of similarity to the family of G-protein-coupled receptors (Figure 2.2). Its main effectors are Ci in *Drosophila* and Gli homologs in vertebrates.

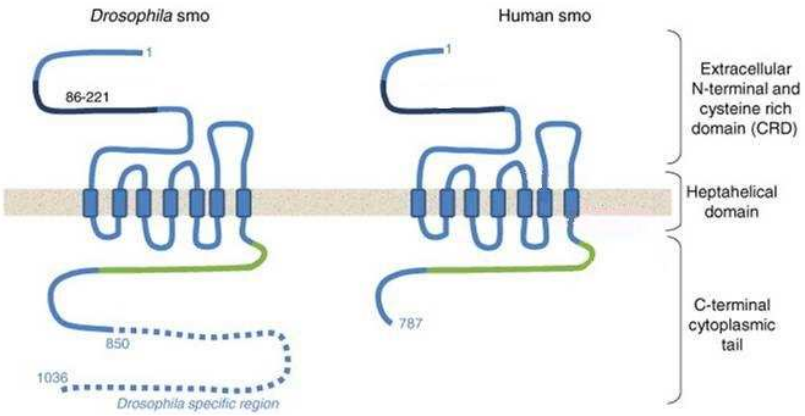

Figure 2.2 Structures of the *Drosophila* and Human Smo proteins. Numbers represent amino acids.

In *Drosophila*, a complex of proteins including Fused (Fu), Suppressor of Fused (SuFu) and Costal 2 (Cos2) mediates downstream signaling of Smoothened.[9] Several kinases, such as protein kinase A (PKA), glycogen synthase kinase 3 (GSK3), and casein kinase 1 (CK1) are participating as well.

After inhibition of Ptch by hh binding, Smo gets phosphorylated at the C-terminal region by PKA and CK1: phosphorylation neutralizes the positive charge of the Smo C-terminus and induces a conformational switch in the C-terminal cytoplasmic tail and consequent dimerization or multimerization of Smo which allows its exposure on the cell surface. Cos2 is able to bind to the phosphorylated domain and to directly relay the signal from the receptor bringing together multiple cytoplasmic components of the pathway including the transcription factor Ci (Figure 2.3).

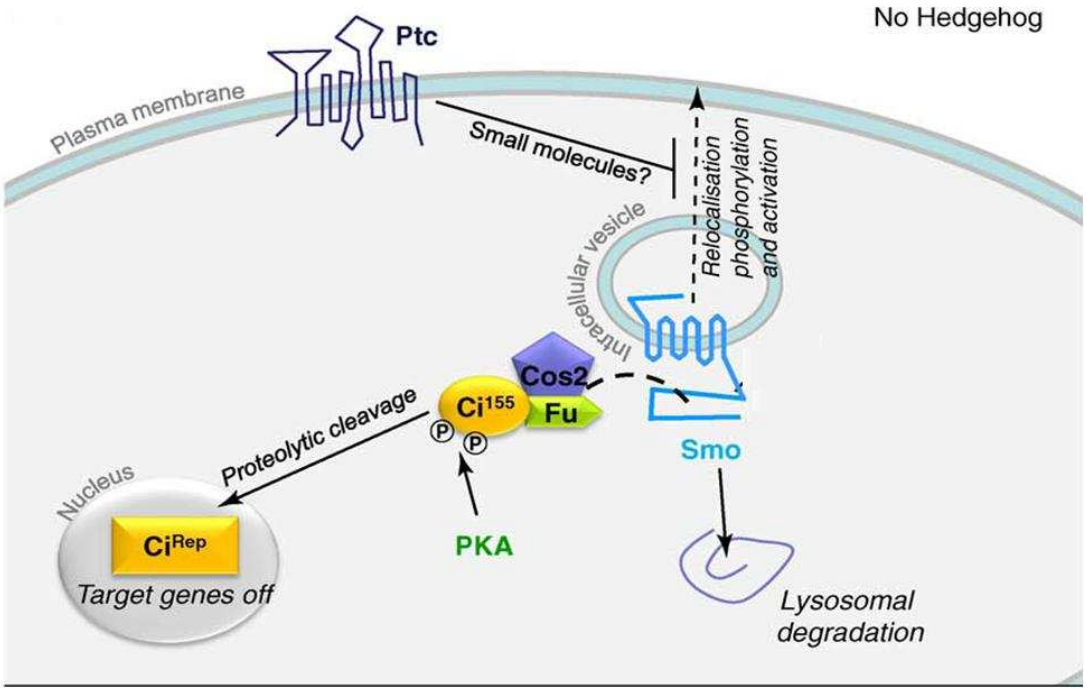

Figure 2.3 Smo inhibition in *Drosophila*. In the absence of hh, Ptch represses Smo by an unknown mechanism that could utilize small lipophilic molecule. This blocks Smo accumulation at the plasma membrane and allows its degradation. The pathway signaling complex, including Cos2 and Fu, allows phosphorylation of the transcription factor (Ci^{155}) by kinases such as PKA. This causes partial cleavage of Ci by the proteosome, releasing the repressive CiRep, that turns off signaling. (according to [25])

Some experimental evidences suggested that in vertebrates, as well as in *Drosophila,* Smo may exists in a balance between active and inactive forms.[23,24] As previously discussed, Ptch is probably able to induce a conformational change of Smo pumping small molecules across the membrane. In a similar manner, cyclopamine, through its

binding to the heptahelical bundle of Smo, acts as a negative regulator shifting the balance towards the inactive state of the protein.[26] However, the activity of all small molecules found to activate or inhibit Smo, including cyclopamine, appears to be specific for vertebrate Smo proteins, suggesting that mechanisms of action of *Drosophila* and mammalian Smo may be different. Moreover, some differences can be found in proteins downstream of Smo as Fused and Costal 2, not yet identified in mammals and probably substituted by MAP3K10 or SuFu, which role of repressor in the hh pathway was demonstrated to be central in mammals and irrelevant in *Drosophila.*

2.5. Transcription factor Gli

The Glioma associated transcriptor factor (Gli) is a member of the Krüppel zinc finger proteins acting directly downstream of hh signaling. In vertebrates three Gli proteins were found (Gli1, Gli2 and Gli3) corresponding to the *Drosophila* Ci (Cubitus interruptus). *Gli1* gene was found to be amplified about 50-fold in a malignant glioma and seems to be the major activator of hh target gene expression. Although they have some structural similarities, the functions of the Gli proteins differ.[27] The biggest difference is the existence of activator and repressor domains in Gli2 and Gli3. Consequently in the absence of upstream hh signal, Gli2 and Gli3 are cleaved to generate truncated repressor forms. This cleavage is inhibited by hh signaling which results in full-length Gli2 and Gli3 with activator function. Gli1, in contrast, does not undergo proteolytic cleavage and acts as constitutive activator. The transcription of *Gli1*, however, is initiated by hh and controlled by Gli3 which may act as a mediator of hh signaling. It was reported that Gli3, as does Ci, contains a CRE (cAMP response element)-binding protein (CBP) domain and phosphorylation sites of the known negative regulator of hh signaling, protein kinase A (PKA). N-terminus truncated Gli3 is inactive, but hh-dependent inhibition of its proteolysis and additional binding of coactivator CBP enables binding of Gli3 to the *Gli1* promoter. The expressed Gli1 then activates specific target genes as well as the *Gli1* gene itself in an hh-independent way.

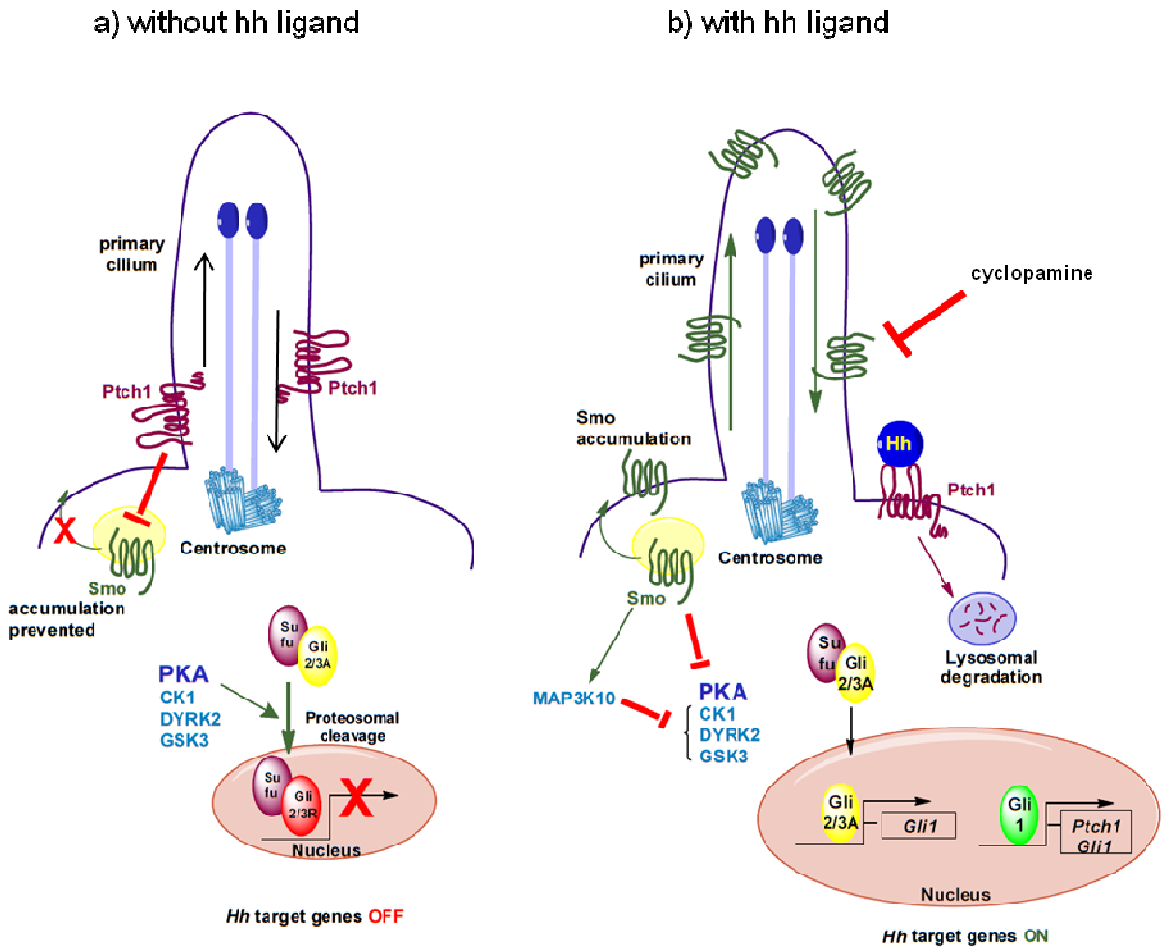

Figure 2.4 Proposed mechanism for hedgehog signaling in mammals. (A) In the absence of a ligand, Patched1 (Ptch1) prevents accumulation of Smoothened (Smo) in the cilia membrane. Phosphorylation of transcription factors Gli2 and Gli3 by Protein kinase A (PKA) and others (CK1, DYRK2, GSK3) results in cleavage to shorter inactive proteins. Additional, Suppressor of fused (SuFu) is stabilized by PKA and enhances proteosomal cleavage (Gli1 does not undergo cleavage). (B) Upon binding of a hedgehog ligand (hh), Patched1 transmitted inhibition of Smoothened is interrupted. Smoothened is translocated to the ciliary membrane and blocks the kinases-driven cleavage of Gli2/3. Binding of CRE-binding protein (CBP) in addition promotes binding of full-length Gli2/3 to the Gli1-promotor. Expressed Gli1 then activates specific target genes, including Ptch1 and Gli1. (scheme modified according to [28])

2.6. Cilia as signaling centers

Almost all vertebrate cells have protrusions extending from their surfaces called cilia. They are microtubule-based organelles and can be of two different types: motile cilia that are usually present in large numbers and beat in coordinated waves to generate a fluid flow across surfaces and non-motile cilia, or primary cilia, which usually occur one per cell and typically serve as sensory organelle. Primary cilium acts as a “signaling center” where the biochemical events of signal transduction take place. Since its discovery it was believed

that the cilium was a vestigial organelle without important functions. It took almost one century for scientists to understand its physiological roles in signal transduction and control of cell growth as well as its role in causing diseases.

Recently a role of cilia in hh signaling was reported.[29] Many components of hh pathway are localized to the primary cilium or its basal body, including Sonic hedgehog, Patched1, Smoothened, Suppressor of Fused and Gli transcription factors. In the absence of Shh, Ptch1 is enriched in the primary cilium, while its cilial localization is lost after binding of Shh. On the other hand, Smo becomes enriched on the primary cilium upon Shh binding to Ptch1. It was shown that Smo moves to cilia by lateral transport rather than being first recycled. This means, Smo follows a path from internal vesicles to the plasma membrane and finally to the cilium (Figure 2.5).

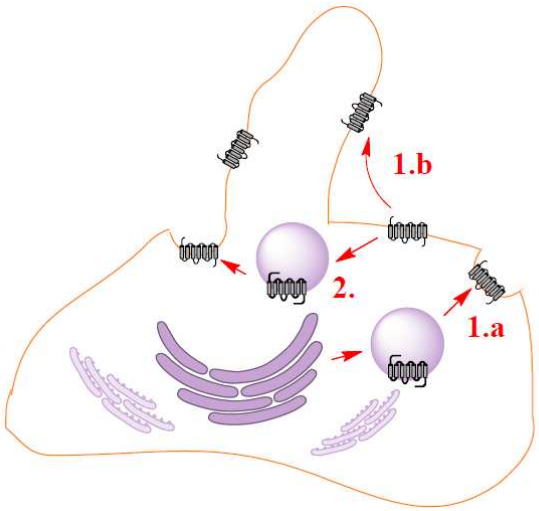

Figure 2.5 Model of hh-induced Smo transport to the primary cilium. (1) Lateral transport consisting of (a) trafficking to the plasma membrane and (b) lateral movement. (2) Recycling pathway (surface Smo > internal Smo > ciliary Smo) is not used for Smo transportation.

Surprisingly, not only Shh and other agonists induce Smo localization to the cilium, but also some antagonists, among them cyclopamine, increased cilia-localized Smoothened.

Chapter 3

Chemistry and Biology of hedgehog signaling inhibition

3.1. Role of hh signaling in animal development and tissue maintenance

The hh proteins act as morphogens controlling multiple different processes in embryogenesis.[9] All mammalian hh proteins are thought to have similar physiological effects, therefore the differences in their roles in development result from diverse pattern of expression (Figure 3.1).

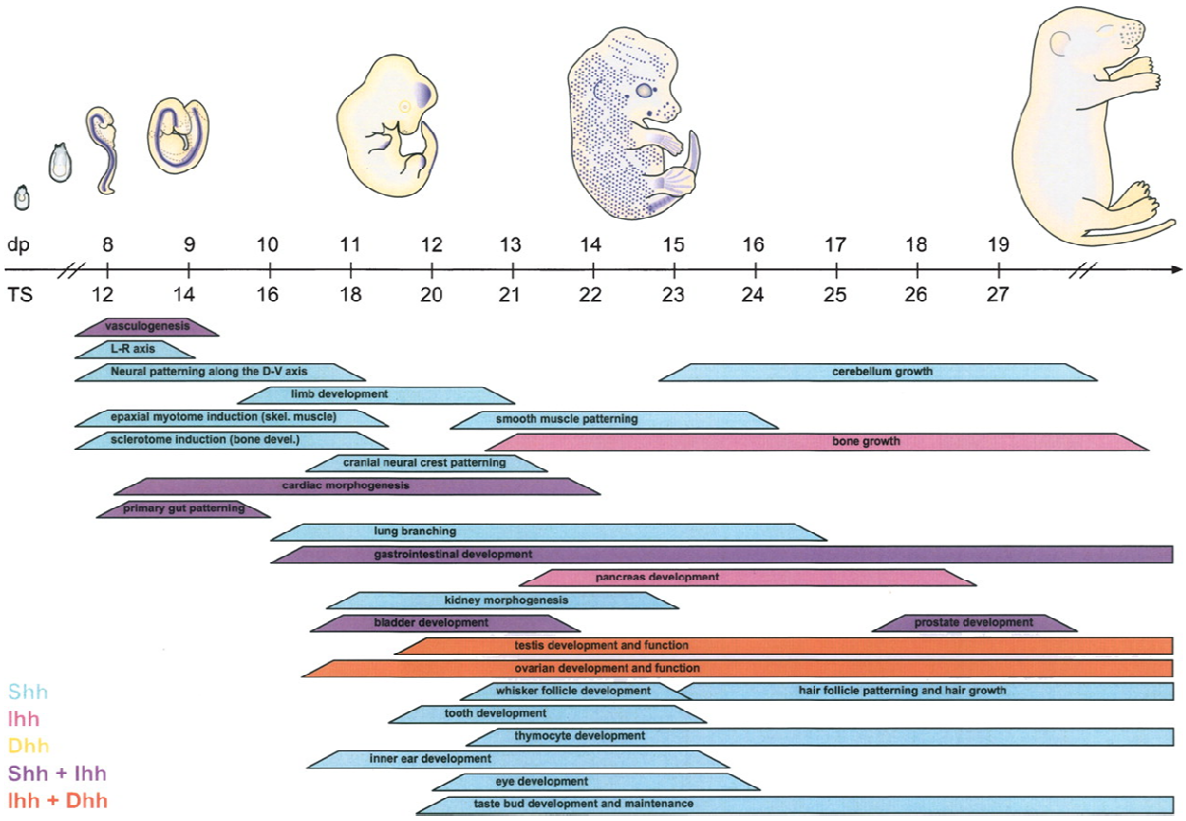

Figure 3.1 Shh controls mouse development from an embryo to an adult. (Top) The embryo cartoons show aspects of expression of the *hh* target gene Patched (blue) during mouse embryonic development. (Bottom) Bars show approximate embryonic stages when Shh, Ihh, and/or Dhh (color code in bottom left) control developmental processes in the indicated tissues or cell types.

Dhh expression is largely restricted to gonads, including sertoli cells of testis and granulosa cells of ovaries while Ihh is specifically expressed in a limited number of tissues, including primitive endoderm, gut, and prehypertrophic chondrocytes in the growth plates of bones. Shh is the most broadly expressed mammalian hh signaling molecule. Shh expression was found in nearly every development stage from very early embryogenesis to adult. In vertebrate, Shh is expressed in midline tissues (node, notochord, floor plate), hence controlling patterning of the left-right and dorso-ventral axes

of the embryo during early embryogenesis. Furthermore, Shh expression in the zone of polarizing activity (ZPA) of the limb bud is necessary for limb development (Figure 3.2). In later development stages, during organogenesis, Shh is mostly expressed and affects epithelial tissues.

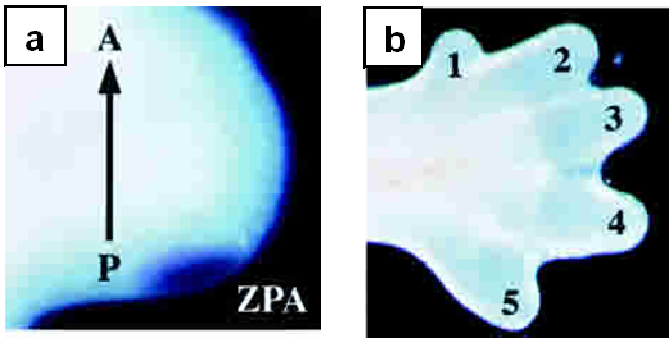

Figure 3.2 Shh journey in the developing vertebrate limb bud. (a) Shh is produced in the posterior limb bud, a region known as the Zone of Polarizing Activity (ZPA). (b) High concentrations of Shh (in deep blue) promote posterior digit formation (digits 4 and 5), with successively lower amounts promoting more anterior digit patterning (digits 2 and 3). The most anterior digit (digit 1) is formed due to the absence of Shh signaling from the ZPA.

The ability of a single morphogen to affect almost every part of the vertebrate body plan is made possible by the fact that cellular responses to hh depend on the type of responding cell, the dose of hh received, and the time the cell is exposed to hh. At the molecular level, this means that many different sets of target genes are induced downstream of hh protein binding.

Hedgehog signaling is known to be crucial in embryonic development. Less is known about its role in adult tissue. Here hh signaling is silenced in most cells except those important for maintaining homeostasis. An important role was demonstrated in restraining growth in the nervous system and other tissues and in maintenance of stem cells. It seems also relevant hh participation in bone growth and homeostasis of osteoblasts. Until today, the best-characterized role for hh signaling in adult is in the reproductive system: it was reported that hh acts specifically on stem cells in Drosophila ovaries and that these cells cannot proliferate in the absence of hh. Furthermore, in mammals Dhh is known to be responsible for the regulation of development and function of somatic cells in testis.

3.2. Hh signaling in cancer

While disruption of hedgehog signaling during embryonic development can lead to severe developmental abnormalities, uncontrolled activation of the hh pathway during aging can lead to several cancers. About 25% of all cancer deaths are estimated to involve aberrant hh pathway activation. Tumorigenesis or tumor growth can result from abnormal up-regulation of hh ligand or from deregulation of the expression or function of downstream components by, for example, loss of Ptch, activating mutations of Smo, loss of SuFu, alteration of Gli1 function.[30,31] Several kinds of cancer have been linked to these mutations including basal-cell carcinoma (BCC), medulloblastoma, rhabdomyosarcoma and pancreatic cancer. Hh is further supposed to promote also various other cancers, such as glioma, esophageal, endometrial, ovarian, gastric, breast, prostate, and small-cell lung carcinoma although the mutational basis of hh pathway activation in these types of cancer has not been unraveled.

3.3. Three models for the development of cancer

There are three different models for the mechanism of hedgehog pathway induced cancers.[28] (Figure 3.3)

Type 1 cancer is ligand-independent: it was the first to be identified and is caused by a congenital mutation in hedgehog pathway components. Patients with the so-called Gorlin syndrome (nevoid basal-cell carcinoma syndrome, NBCCS) have a high incidence for basal-cell carcinoma, medulloblastoma or rhabdomyosarcoma. Absence of the hedgehog pathway repressor Patched leads to ligand independent hh signaling. Patients with this syndrome are perfect candidates for the therapy with modulators inhibiting smoothened or further downstream components.

Type 2 was suggested to depend on autocrine-secreted hedgehog ligands. These will be produced and accepted by the same tumour cell. Only recently, it was demonstrated conclusively that this type of hh signaling exists in human cancer cell lines of the colon.

Type 3 cancers are dependent on paracrine-secreted hh ligands. Recent studies demonstrated that hh is overproduced in most of the hedgehog-dependent tumors. Hh proteins stimulate nearby stromal cells (endothelial cells, epithelial cells, fibroblasts and cells of immune system), thereby supporting tumor growth by i.e. stimulation of cancer stem cells, stimulation of angiogenesis, influencing extracellular matrix and secretion of other signaling pathway components involving insulin-like growth factor (IGF) and Wnt.

A variant of this type of hh signaling is the so-called “reverse-paracrine” signaling (type 3b), where hh ligands are secreted from stromal cells to receiving cells in a tumor.

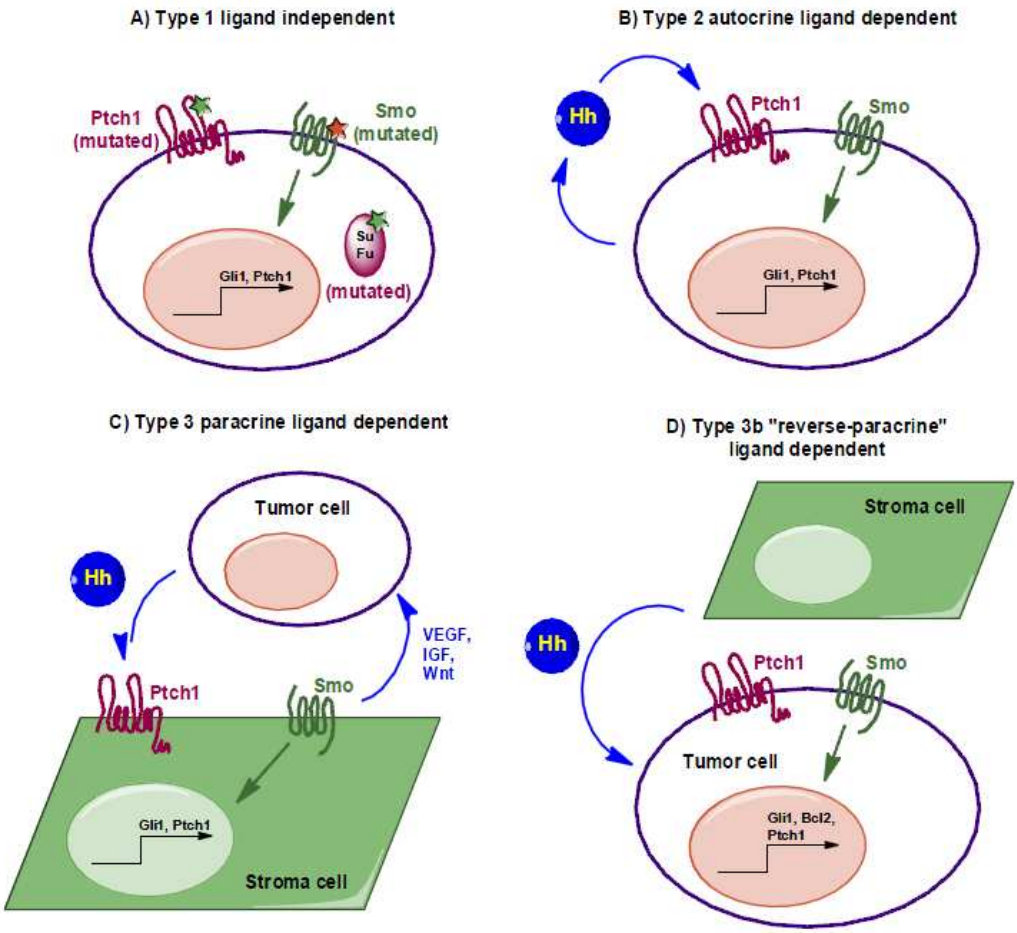

Figure 3.3 Model for the development of cancer due to aberrant hh signaling.

3.4. Inhibition of hh pathway as anticancer therapy

Along with the proceeding knowledge about molecular signaling, cancer therapy is rapidly changing: until now the common treatment was based on cytotoxic agents targeting all rapidly dividing cells while the new therapies are focused on a specific mechanism or molecule. Therefore, inhibition of hh signaling pathway provides a new route to novel and selective anticancer therapies. The first identified hh inhibitor was cyclopamine and it is currently used for some application (vide infra). Anyway, since its clinical development has a lot of limitations, several other inhibitors of hh signaling, in particular of Smo, have been synthesized in recent years. Some of them bear structural elements or are chemical derived from cyclopamine, others have completely different chemical scaffolds. Among them, pyridyl (**101**-**103**) and quinoxaline (**104**-**106**) compounds were reported by Curis[24]:

the small GDC-0449 Smo inhibitor **101** (Scheme 3.1) is currently in phase I/II clinical trials for advanced BCC and breast cancer[32] while the heterogeneous class of SANT, Smo antagonists (Scheme 3.2),[22] was found to inhibit Smo activity at a concentration lower than cyclopamine.[26]

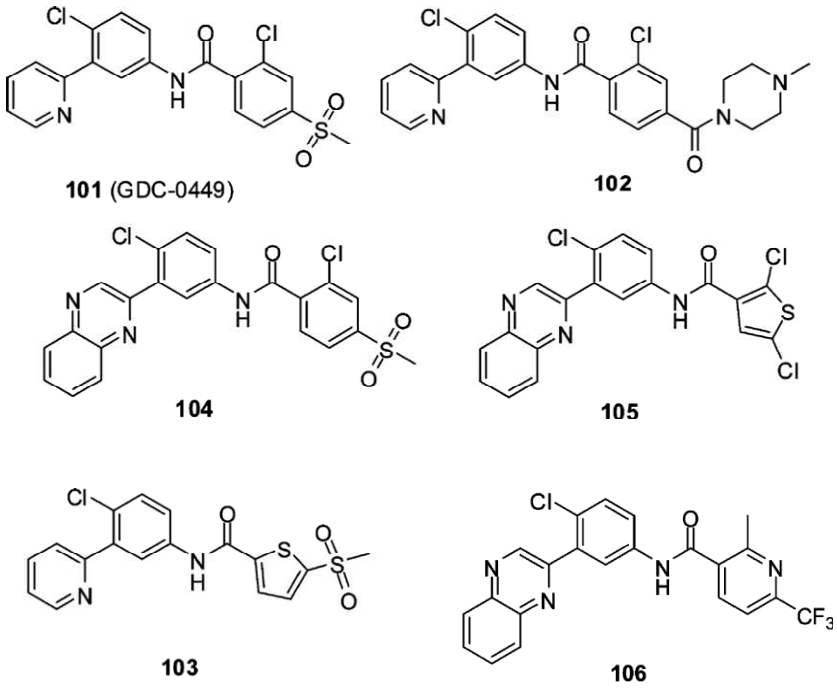

Scheme 3.1 Pyridyl and quinoxaline Smo inhibitors.

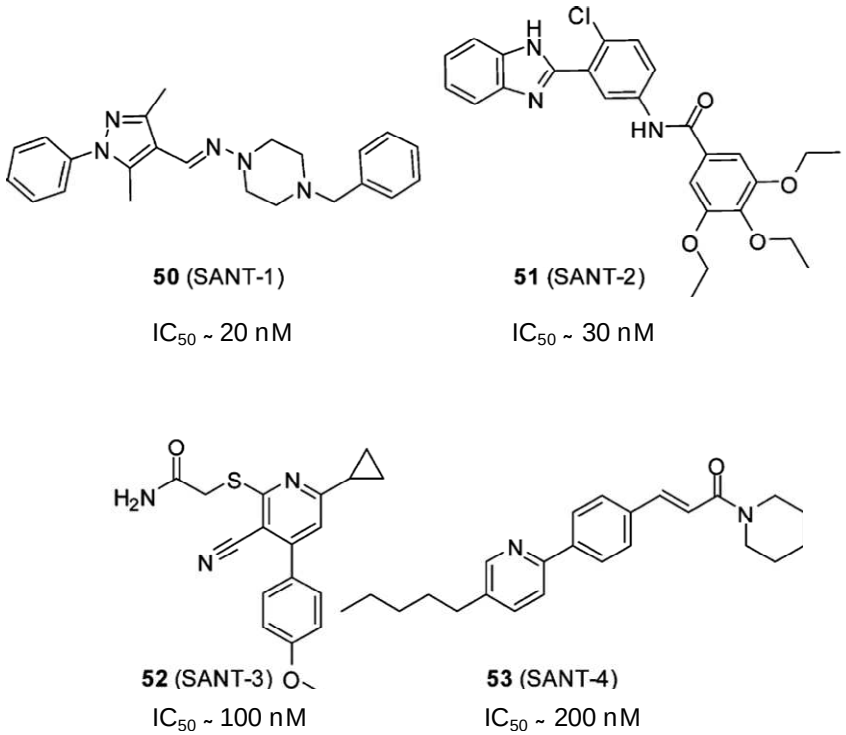

Scheme 3.2 Structures of the SANT Smo inhibitors. IC_{50} values were obtained in a Shh-LIGHT II assay.

In table 3.1 the activities of some Smo inhibitors are reported.

Inhibitor name	*Gli*-luc IC_{50} μM (potency compared with cyclopamine)	*in vivo* activity	Dosing	Tested in human
Cyclopamine	~0.5 (1x)	yes	SQ, IT, topical	Limited, topical only
Jervine	~0.7 (0.7x)	yes	PO	No
KAAD-cyclopamine	~0.08 (10–20x)	n.d.	NA	No
SANT1-SANT4	~0.02–0.2 (2.5–20x)	n.d.	NA	No
GDC-0449	~0.003 (~ 170x)	yes	PO	Phase II
IPI-269609*	0.6 (~1x)	Limited	PO	No
IPI-926*	0.015 (~30x)	yes	PO	Phase I

Table 3.1 Activities of some Smo inhibitors. Abbreviations: *Gli*-luc, *Gli*-luciferase assay; IT, intratumoral injection; NA, not applicable; n.d. not determined or not disclosed; PO, oral administration; SQ, subcutaneous injection.

*see chapter 4.3.

Chapter 4

Cyclopamine and its derivatives as anticancer agents

4.1. Cyclopamine

Cyclopamine is an isosteroid ("6-6-5-6 system") consisting of a hexacyclic structure made by four annulated carbocycles, all of which are six-membered rings except for the C ring, and a spiro-connected E-F annulated system (Scheme 4.1).

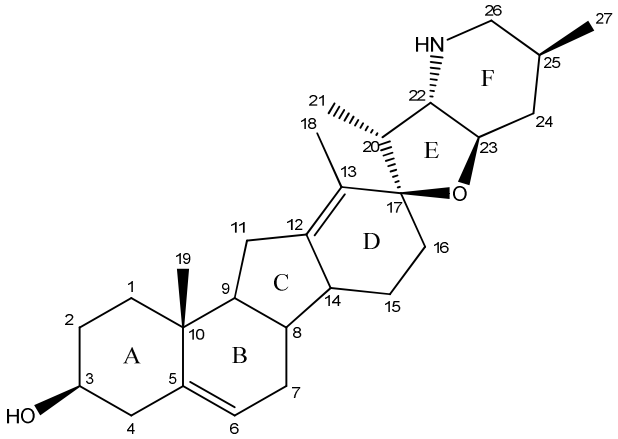

Scheme 4.1 Structure of cyclopamine.

The structure has an inherent instability that arises from the C12-C13 double bond which renders the oxygen atom allylic: treatment of cyclopamine with Lewis acid or with the low pH value of the stomach, leads to loss of the D-E spiro connection and, in contrast to which postulated by Keeler, causes formation of the C17-epimer and another non-aromatic elimination product, both of which show no hh inhibitory properties.[33] The small amount of unaffected cyclopamine is anyway still able to induce the malformations described in the pregnant sheep after consumption of *V. californicum* leading to the discovery of this teratogenic compound. On the other hand, from a pharmaceutical point of view, the dramatic reduction of cyclopamine due to acid lability, represents the biggest problem for a clinical application.

4.2. Biosynthesis and first total synthesis of cyclopamine

The biosynthetic pathway of cyclopamine is still not completely elucidated but it was ascertained that begins from cholesterol and through a series of oxidative and reductive processes, sometimes only hypothesized, leads to epirubijervine: one hydroxyl group of this intermediate is converted to a phosphate leaving group that allows a Wagner-Meerwein type rearrangement into the *C*-nor-*D*-homostreroid skeleton (Scheme 4.2).[34]

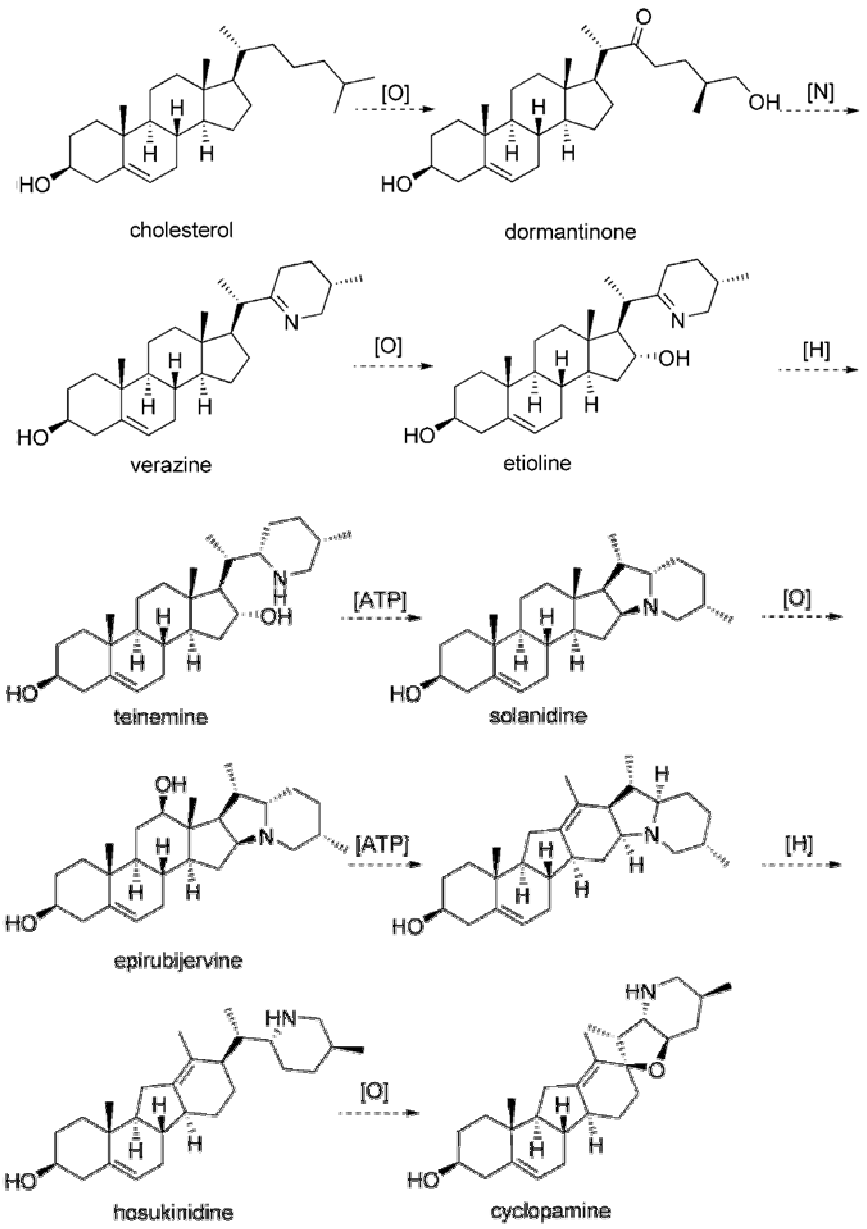

Scheme 4.2 Biosynthesis of cyclopamine.

The total synthesis of cyclopamine was performed only in 2009 from Giannis et al. using a biomimetic and completely diastereoselective synthetic route (Scheme 4.3).[35] The synthesis starts from the hydroxylation at the 12-β position of the intermediate **4** from the commercially available dehydroepiandrosterone in three steps by a C-H activation and oxidation with a copper catalyst and molecular oxygen.[36] This material is then transformed in four more steps into the lactone **9C** which, after deprotection, proceeds through a Wagner-Meerwein rearrangement,[37] i.e., ring contraction/expansion by conversion of this alcohol function into a leaving group, resembling completely the biosynthetic pathway for the *C*-nor-*D*-homo system construction.

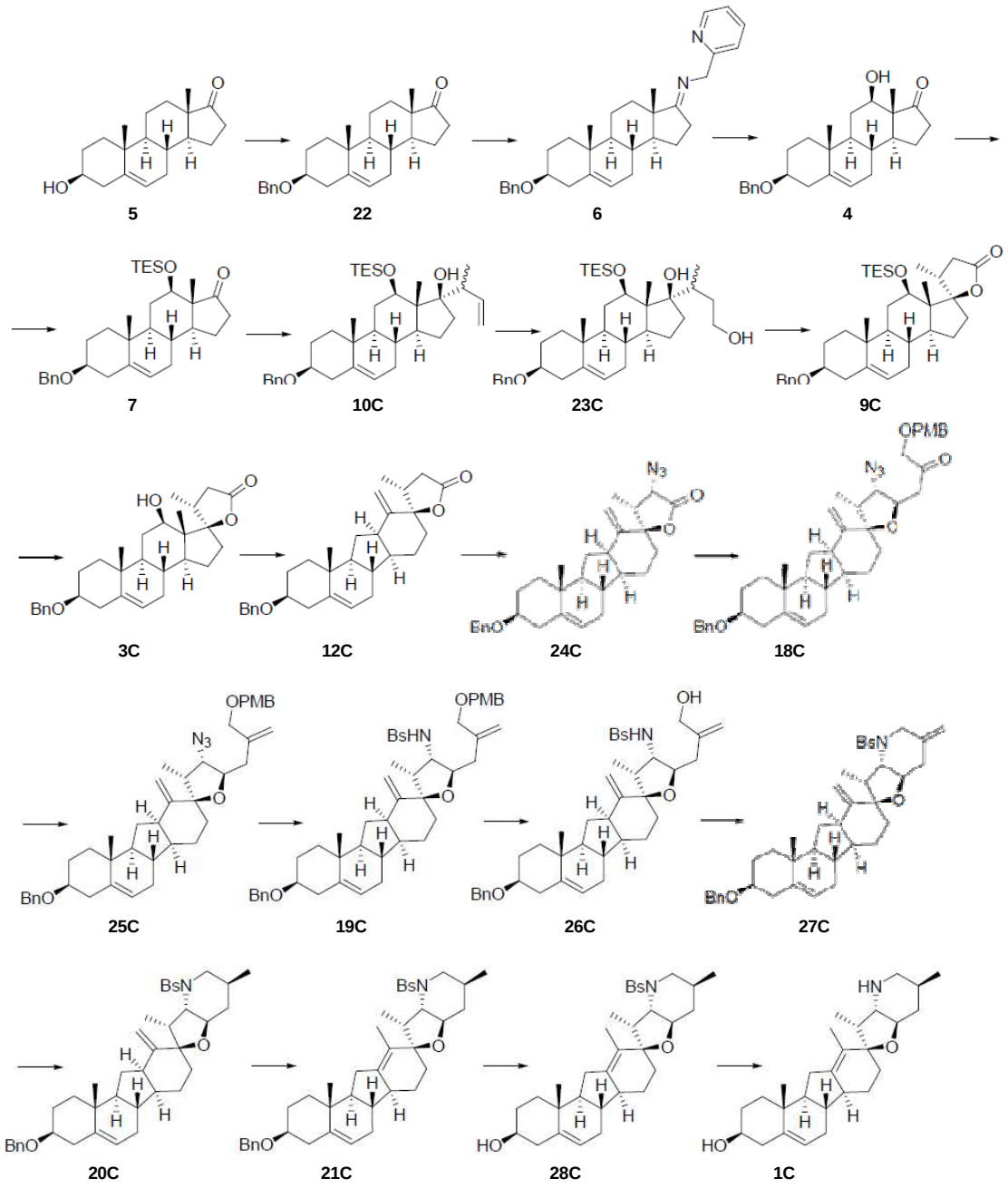

Scheme 4.3 Total synthesis of cyclopamine.

This step provides access to the exo- and endo-isomers of the *C*-nor-*D*-homo structures (section 4.4) but, since the attempt to construct the furan ring using the endo-isomer failed, it was decided to proceed with the exo-derivative **12C** which was treated with LDA and trisyl azide[38] to give the azidolactone **24C**. The furan ring was introduced in the molecule using a tandem Horner–Wadsworth–Emmons reaction (HWE)[39] and intramolecular Michael addition between a β-ketophosphonate and the azidolactol obtained from the reduction of **24C**. The piperidine ring was completed in seven steps proceeding through the Peterson olefination,[40] Staudinger reduction[41] followed by amine

sulfonylation, and alcohol deprotection allowing a modified Mitsunobu procedure[42] for the ring closure. The regioselective hydrogenation of **27C** furnished the exo-cyclopamine derivative which was then converted in the endo-isomer through an Alder-ene reaction followed by desulfurization[43,44]. Subsequent deprotection affords cyclopamine in 20 steps and a total yield of 1%. This linear approach avoids the diastereoselectivity problems of the former convergent strategy based on a low yielding coupling between a *C*-nor-*D*-homosteroid intermediate and a precursor of the F-ring.[45] The development of a synthetic strategy provides also access to cyclopamine analogues with different configurations, thus making it possible to establish fundamental structure–activity relationships.

4.3. Structure-activity relationship of cyclopamine

From the analogues of cyclopamine it was possible to identify which parts of the molecule bear the activity, and which could be modified without loosing the anticancer properties. Except for the Winkler analogue (Scheme 4.4),[46] all the other derivatives synthesized to date are semisynthetic thanks to the high yield extraction method developed in the last years that improved the commercial availability of cyclopamine coming from the plant.[47] In scheme 4.4 are reported the structures of some analogues of cyclopamine.

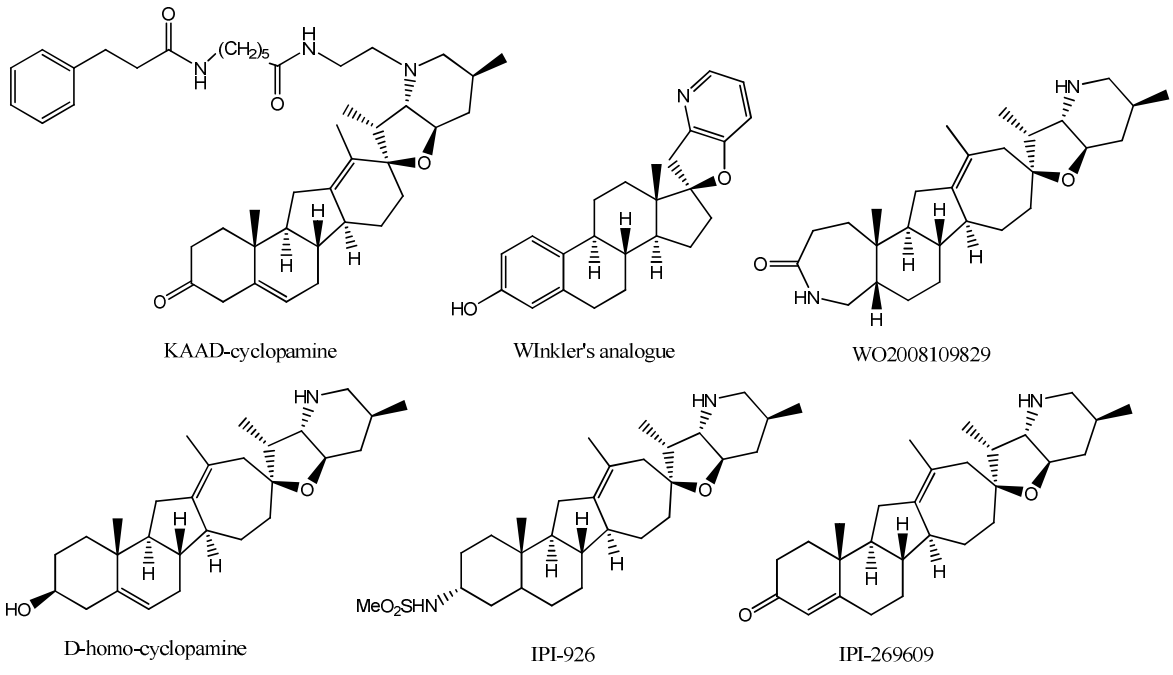

Scheme 4.4 Derivatives of cyclopamine

KAAD-cyclopamine, a derivative that exhibited better solubility and an increased biological potency by a factor of 10 to 20, was obtained in five steps from natural cyclopamine.

Other derivatives showed in scheme 4.4 have been obtained in few steps from the natural compound: these derivatives do not inherit the instability of cyclopamine, since cleavage of the allyl ether system cannot occur.[48] Several D-*homo*-derivatives of this type have been synthesized and also patented, and their biological profiles have been determined. Winkler et al. prepared a simplified cyclopamine analogue from estrone in which the C-*nor*-D-homosteroid structure was substituted with a conventional steroid system, a pyridine was used in place of the piperidine ring, and a phenol used for the homoallyl alcohol. Although these modifications have great influence on the structure, polarity, and acidity, biological activity was still evident in a μM range. From the reduced or improved activity of these and other analogues it was possible to deduce some information about the structure-activity relationships of cyclopamine as reported in scheme 4.5.[24,49]

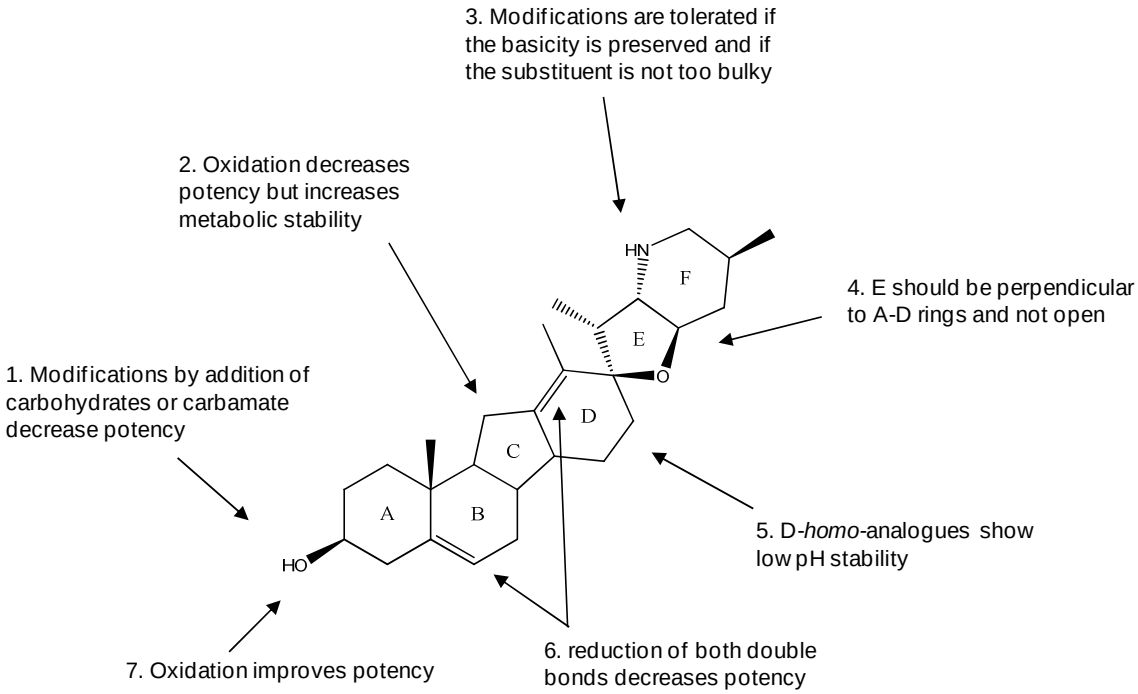

Scheme 4.5 Structure-activity relationship of cyclopamine.

However, insights into the presence and the stereochemistry of several functional groups are still missing.

4.4. Serendipity in the cyclopamine synthetic route: the exo-cyclopamine

As previously discussed, since the first attempt to perform the tandem HWE reaction/intramolecular Michel addition from the endo-azidolactone failed, it was decided to try with the by-product of the Meerwein reaction, the exocyclic-derivative **12C** which

gave easily access to compound **18C** and subsequently to **24C** (Scheme 4.6). After the synthesis was completed, a small amount of the intermediate **20C** was deprotected without performing the double bond shift: this led to an isomer of cyclopamine which shows a different conformation.

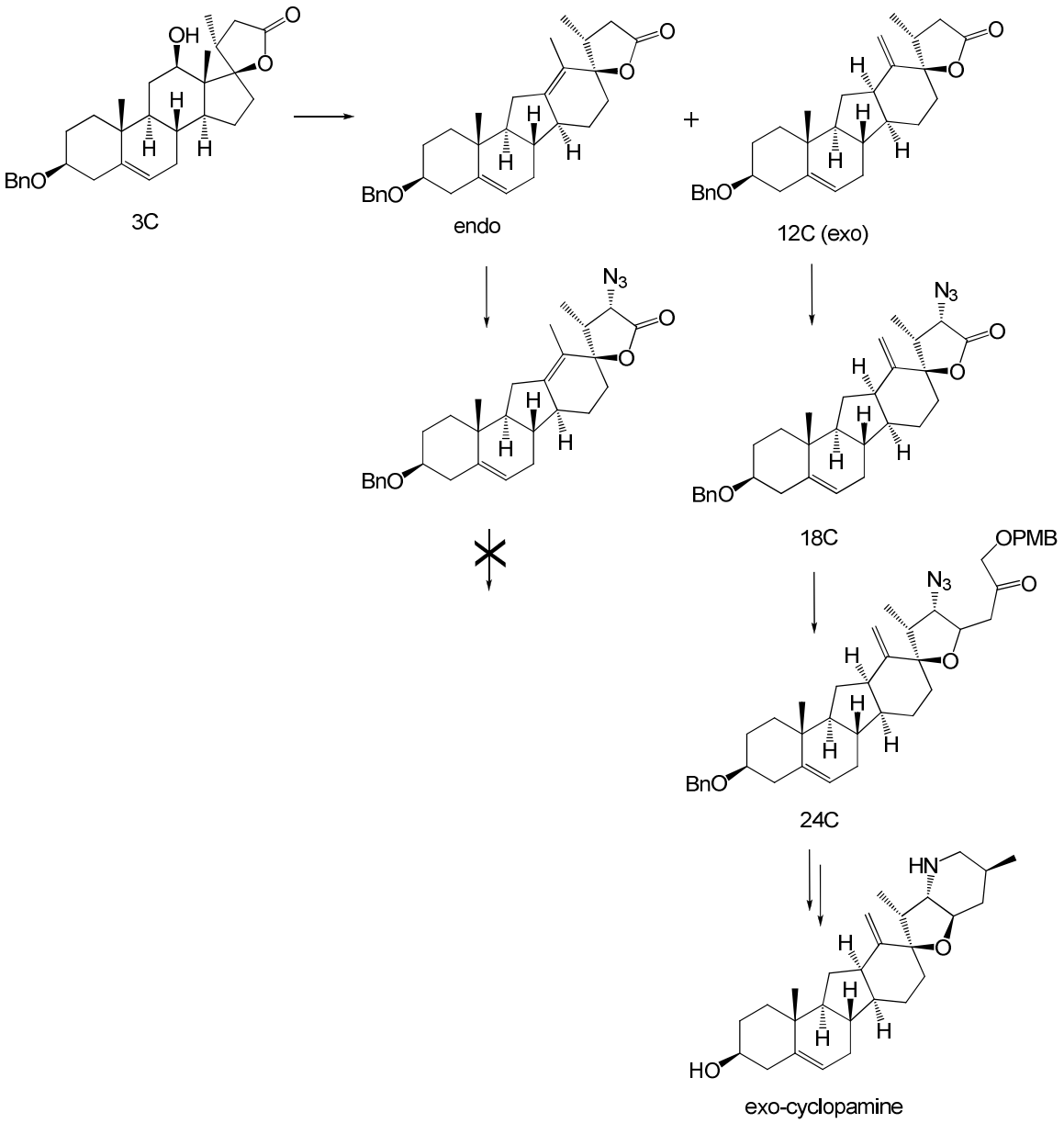

Scheme 4.6 The Wagner- Meerwein rearrangement furnished the exo- and endo-derivatives. Only the exocyclic-double bond allows the F ring construction.

The exo-double bond might prevent the acid lability of cyclopamine. With this little structural change, a noteworthy increasing of stability could be introduced. Exo-cyclopamine, synthetical derived cyclopamine as well as commercially available cyclopamine (purified from *V.californicum*) were examined for their potency to inhibit Gli1-

dependent luciferase expression in the reporter gene assay in the laboratories of Professor Giannis from the PhD student Anita Büttner. Synthesized and commercially obtained cyclopamine showed an IC_{50} of 5µM. Exo-cyclopamine was 10-fold more active with an IC_{50} of 0.5µM (Figure 4.1). Consequently, exo-cyclopamine is a more potent inhibitor of Shh signaling than cyclopamine.[50]

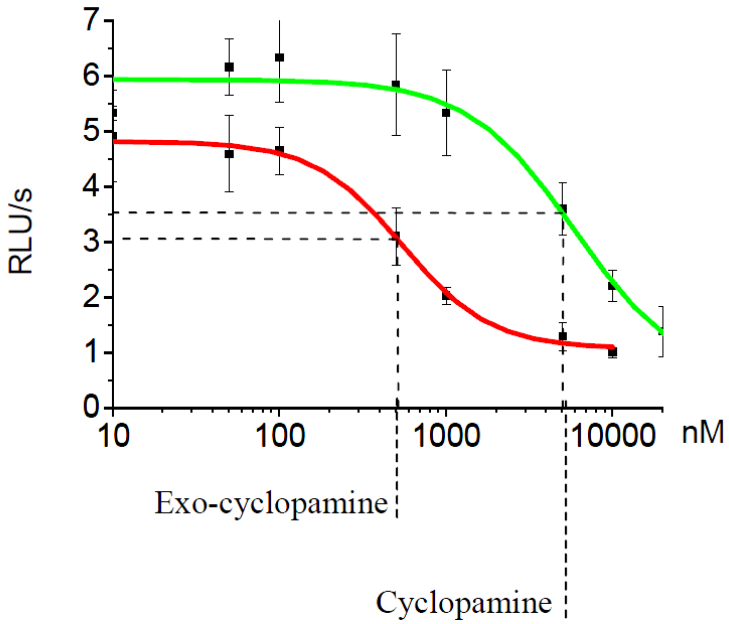

Figure 4.1 Comparison of IC_{50}-values of Shh inhibition by exo-cyclopamine (IC_{50} =0.5µM) and cyclopamine (IC_{50} = 5µM) in a Gli1- reporter gene assay. Obtained from three independent experiments. Data represent mean ± standard deviation.

4.5. Medical relevance of cyclopamine

Cyclopamine has been a significant pharmacological tool to validate the hh pathway in cancer. It is currently used in clinical trials in the therapy of basal-cell carcinoma. BCC is the most common type of nonmelanoma skin cancer and is usually caused by exposure to UV radiation. A cream containing cyclopamine was applied to basal-cell carcinoma in patients who were scheduled to have their tumors excised; all of the tumors treated with cyclopamine regressed rapidly. Recent studies showed that cyclopamine could be also a powerful tool in pancreatic cancer treatment: even in cases in which surgical resection with curative intention can be done, the majority of patients develop local recurrence or metastases in distant organs, and finally die. Inhibition of hh signaling with cyclopamine has enhanced the survival rate in a genetically engineered mouse model of pancreatic cancer and abrogated the systemic metastases arising from orthotopic xenografts. Although cyclopamine has a high potential anti-cancer activity, its pharmacological and

physicochemical properties are not ideal: it exhibits only a moderate inhibition of transcription of the hh-target-genes Gli1 and Ptch1, with an EC_{50} of 300 nM. Additionally, it has very poor aqueous solubility and it's metabolically unstable because of its lability to acid conditions as previously discussed.

4.6. Aim of the study

Inhibition of the hh signaling pathway is an attractive target for anticancer treatment. The synthetic route to cyclopamine, the first known inhibitor, offers several possibilities to clarify which moieties are essential and which could be modified in the molecule to have new compounds synthetically accessible with increased activity and stability. Moreover, this is the way to have information about the binding site of the Smo receptor. Starting from the synthetic strategy of cyclopamine it was possible to design and partially synthesize a new analogue of cyclopamine, the first completely synthetic analogue.

Chapter 5

Results and discussion

5.1. Design of the first synthetic analogue of cyclopamine

All the cyclopamine-like structures synthesized to date, except for the exo-cyclopamine, are semisynthetic derivatives, that is, derivatives synthesized from natural cyclopamine by chemical modification of the natural product. Therefore, starting from the natural compound, just some structural features could be changed providing access to structure-activity relationships information only of few parts of cyclopamine. Thus, the role of the methyl groups or the stereochemistry of some functional groups is still not known: these structural features could be not required for the biological activity leading to develop a more concise and cheap synthetic approach to obtain a new cyclopamine analogue. The synthetic route to cyclopamine[35] allows several modifications of the structure like configuration and existence of methyl groups 21 and 27 or different heteroatoms in E or F rings. Among the possible modifications, it was decided not to introduce the methyl group 21 and to simplify the construction of the F ring removing the methyl group 27 and reducing the ring size, that means it was possible to avoid several steps using a smaller phosphono-derivative for the HWE reaction. Since the exo-cyclopamine was demonstrated to be more active than the natural compound, it was also decided to maintain the exocyclic double bond in the final compound resulting in the IR-analogue **1** of cyclopamine showed in scheme 5.1.

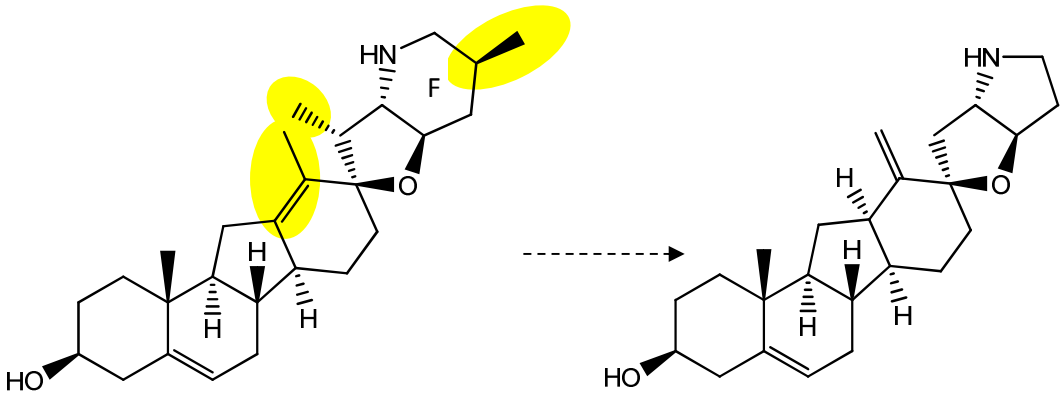

Cyclopamine

IR-analogue of cyclopamine

1

Scheme 5.1 Design of the IR-analogue of cyclopamine: the moieties in evidence are different in the IR-analogue.

5.2. Retrosynthesis of IR-analogue

In a retrosynthetic analysis of **1** (Scheme 5.2), the pyrrolidine ring (ring F) is dissected into the cyclization precursor **17**, which would be readily accessible in a stereospecific manner from of the appropriate E ring unit installed in **14**. Finally, the 12β-hydroxyketone **4** would serve to create the correct ABCD framework from the commercially available dehydroepiandrosterone **5**.

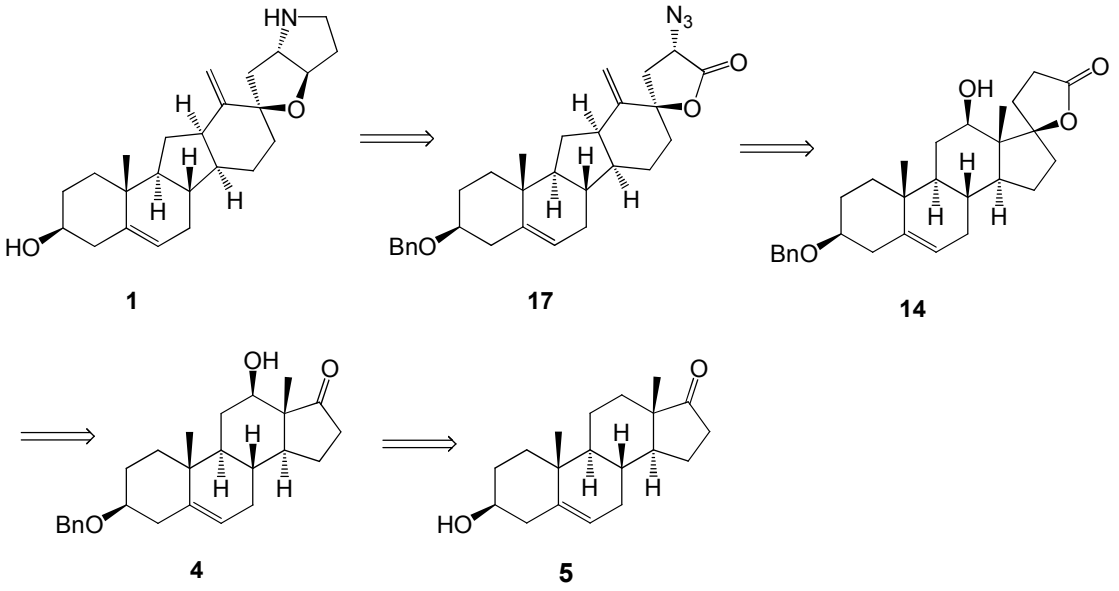

Scheme 5.2 Retrosynthetic analysis of IR-analogue.

5.3. Construction of the C-*nor*-D-*homo* skeleton

To build the correct cyclopamine ABCD ring system it was decided to adopt the cationic rearrangement of the 12β-hydroxy steroids which is a much more convenient and easy approach than performing the total synthesis of the C-*nor*-D-*homo* structure. Since 12β-hydroxy steroids are rare and a properly functionalized one (like **4**) resembling the cyclopamine ABCD skeleton was not available, it was decided to introduce the hydroxyl moiety on the commercially available dehydroepiandrosterone **5** at position 12 by C–H activation. The total synthesis based on the above-mentioned plan was therefore initiated with known protection of 70 grams of dehydroepiandrosterone as a benzyl ether by reaction with Dudley's pyridinium triflate[51] followed by formation of 2-picolylimine at position 17 by treatment of the ketone with 2-picolylamine under azeotropic removal of water which afforded **6** in high yield (85%).

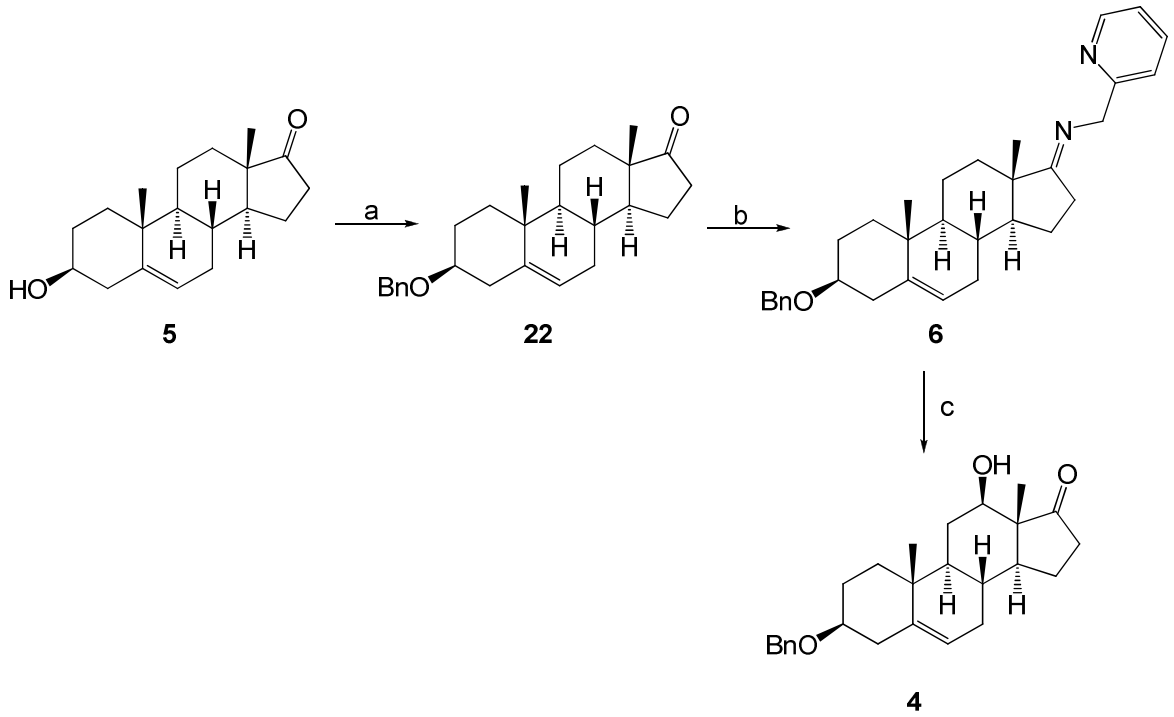

Scheme 5.3 Synthesis of the 12β-hydroxy ketone **4**: reaction conditions: a) 2-benzyloxy-methyl-pyridinium triflate, MgO, $PhCF_3$, 85°C, 95%; b) 2-picolyl amine, *p*-TsOH (2.4 mol%), toluene, reflux, 85%; c) $[Cu(MeCN)_4]PF_6$, acetone, then O_2 (1 atm), then NH_4OH, then AcOH, MeOH, 49% of **4** and 9% of recovered **22**.

The picolyl amine was introduced at C17 position to set up the molecule for the regio- and diastereoselective oxidation of the next step. This biomimetic procedure was recently published by Schoenecker et al.[36] and proceeds through the use of the copper salt tetrakis(acetonitrile)copper(I) hexafluorophosphate and molecular oxygen: the mechanism consists of an oxidation driven by the 2-(aminomethyl)pyridine able to form a complex with the copper-catalyst as showed in scheme 5.4.

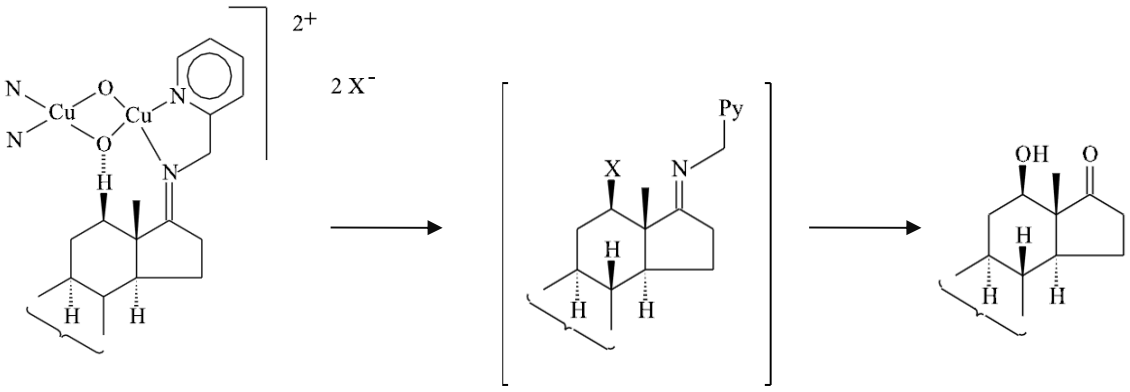

Scheme 5.4 Copper mediated C-H activation followed by hydroxylation and deprotection of the imino group. X= OH.

The distances and the positions of the atoms involved in the complex allow only the C-H activation that lead to the 12β-hydroxy diastereomer. The tetrakis(acetonitrile)copper(I) hexafluorophosphate was prepared as described in the experimental section following a convenient and easy procedure and, once is prepared, it can be stored for a long time. The 12β-hydroxilation affords **4** in an acceptable yield of 49% and recovered **22** in 9% yield. The hydroxyl moiety of **4** was subsequently protected in mild conditions to avoid enolate formation at C17, using 2,6 lutidine at 0°C and triethylsilyl triflate dropwise giving rise to derivative **7** (91%, Scheme 5.5).

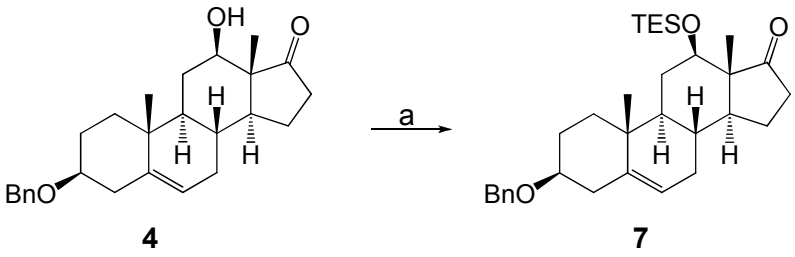

4 **7**

Scheme 5.5 Protection of **4**. Reaction conditions: a) TESOTf, 2,6-lutidine, CH_2Cl_2, 0°C, 91%.

The next task was to create the lactone with the spiro-connection in C17. The attack at the carbonyl site of **7** by an appropriate functionalized allyl C-nucleophile followed by hydroboration/oxidation, would proceed smoothly to convert the quaternary center (C17) to the spiro connection of the new-formed ring (Scheme 5.6). So the crucial point of this route was to establish the correct stereochemistry at position 17.

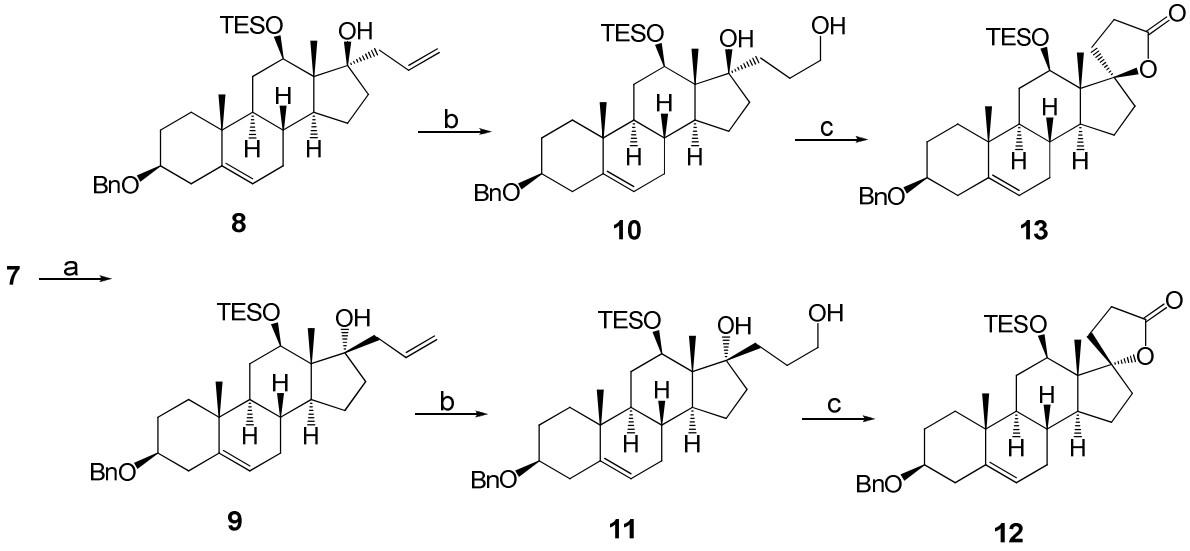

8 **10** **13**

9 **11** **12**

Scheme 5.6 The lactone formation. a) allylcerium bromide, THF, 0°C, 93% and 7% of recovered **7**; b) 9-BBN, THF, reflux, then $NaBO_3$, H_2O, 50°C, 91%; c) BAIB, TEMPO, CH_2Cl_2, 73% **13** and 5% **12** (overall yield of 66% over three steps).

The most convenient way to proceed would have been to perform the Barbier reaction: an easy one pot reaction in which a mixture of magnesium, allyl bromide, iodine, and **7** in diethyl ether was refluxed for 1,5 h. These mild conditions furnished the tertiary alcohol in 84% yield but, unfortunately, as a mixture of the two diasteroisomers in a not encouraging 1,8 : 1 ratio as estimated from the ^{1}H NMR spectrum. Even though the stereospecificity of this reaction was uncertain, the distinctly different steric environment of the two faces was expected to favor the attack from the slightly less crowded one. Therefore the attack of the nucleophile should have occurred predominantly from the α-face since the methyl 18 shields the β-access to the carbonyl group (Figure 5.1).

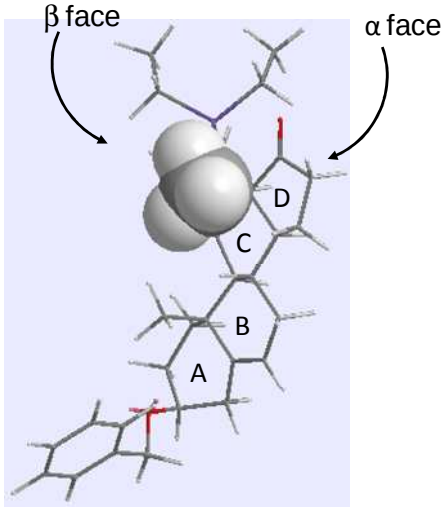

Figure 5.1 Stick model of **7**: the methyl 18 is represented as a “space filling” model.

An alternative to the Barbier reaction is the classical Grignard procedure that was performed at -10°C to change the ratio of the two diasteroisomers and obtain the kinetically favored product. Although the yield was improved to 99%, the ^{1}H NMR spectrum shows the same ratio of diastereoisomers obtained through the Barbier method. Finally it was concluded that, in order to prevent the undesired diastereoisomer formation, it would be necessary to use a bulky nucleophile not able to attack from the β-face of **7**. The last and successful attempt was accomplished using the organocerium(III) reagent generated by the reaction of Cerium(III) halides with a Grignard reagent.[52] The long and tedious procedure consists of drying the $CeCl_3$ heptahydrate (the commercially available dry one was proved to be less effective than the freshly prepared one) to remove any possible trace of water, add freshly distilled THF to form the white creamy suspension that will stir at room temperature for 2 h and, after cooling to 0°C, adding dropwise the previously prepared Grignard reagent allyl-magnesium bromide that turns the colour of the suspension from white to deep yellow-orange. When the organocerium specie has been

formed (2h), the solution of **7** in THF can be added and it will rapidly react. The inseparable mixture of the alcohols **8** and **9** obtained in a good yield of 93% underwent hydroboration/oxidation with 9-borabicyclo[3.3.1]nonane (9-BBN) and sodium perborate, and, finally, the oxidative cyclization of the intermediate diols using TEMPO (2,2,6,6-tetramethylpiperidinoxy radical) and BAIB ([bis(acetoxy)iodo]benzene)[53] gave the lactones **12** and **13** as a mixture of epimers at C20 in a 66% yield over three steps. These in turn were easily separable by chromatography. Thus the desired 20R lactone **13** was obtained from the last step in 73% yield and the 20S-configurated lactone **12** was isolated in 5% yield. With a suitable lactone intermediate in hand, it was possible to rearrange the steroid skeleton. Cleavage of the triethylsilylether with hydrofluoric acid yielded the free alcohol **14**, which, in turn, was subjected to the Wagner–Meerwein-type rearrangement (Scheme 5.7).[46]

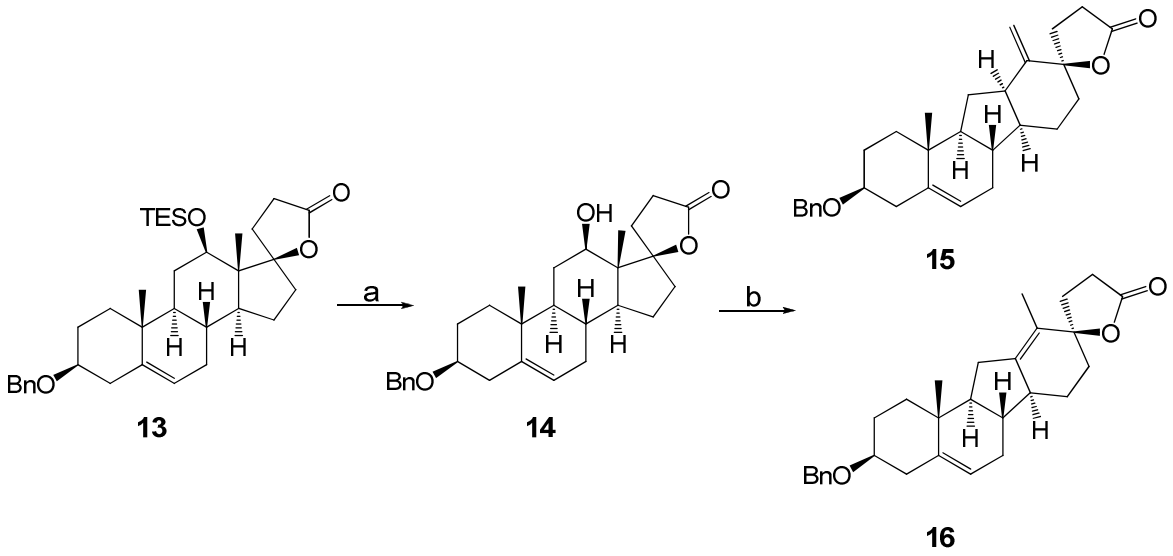

Scheme 5.7 Reaction conditions: a) HF, MeCN, H_2O, 87%; b) Tf_2O, pyridine, 0°C → 50°C, 61% (46% of **15** and 15% of **16**).

Typically, 12-hydroxy-17-keto-steroids give only elimination products or extensive degradation in these conditions but when **14** was treated with trifluoromethanesulfonic anhydride (Tf_2O) in pyridine at elevated temperature it gave the desired C-*nor*-D-*homo* skeleton in an acceptable yield of 61% as a 3:1 mixture of regioisomers **15** and **16** which were separable by chromatography.

5.4. Construction of the furan motif

The next task was the introduction of the azide at C21 (Scheme 5.8). The possibility of introducing such functionality directly in the lactone ring following the Evans' method was

so entertained.[38] The lithium diisopropylamide (LDA) promoted enolization of **15** and the subsequent attack to the trisyl azide followed by the intermediate triazine decomposition, afforded a mixture of the two epimers in a 53% yield. The chromatographic separation provided the azide **17** in 43% yield and the epimeric azide **18** in 10% yield. Spectroscopic analysis confirmed their structures and revealed that fortunately the major isomer was the desired one.

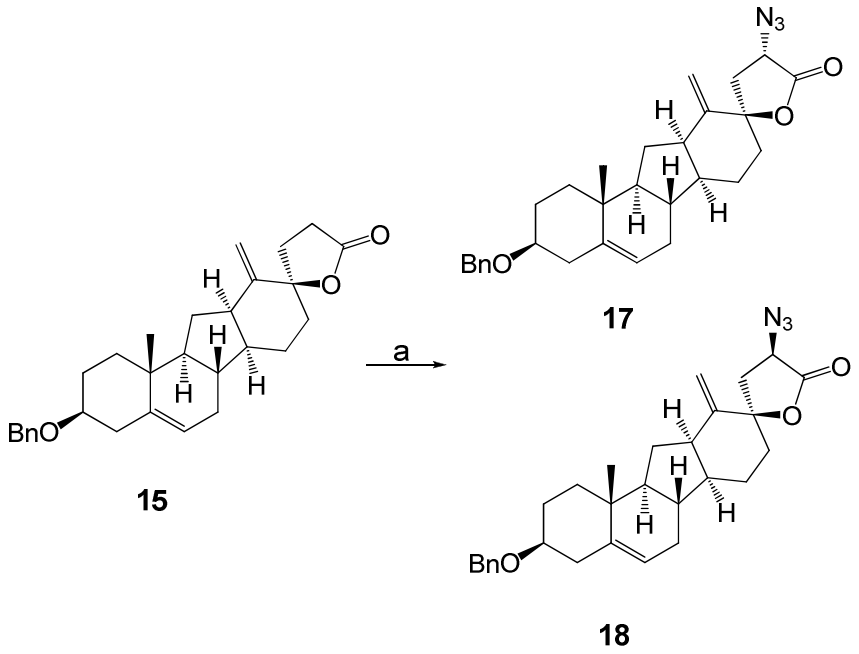

Scheme 5.8 Reaction conditions: a) LDA, THF, -78°C, then trisyl azide, -78 °C, then AcOH, -78°C → 22°C, 53% (d.r.4:1).

Once the nitrogen had been incorporated, it was necessary to introduce the suitable side chain in position 22 needed to form the pyrrolidine ring. To correctly functionalize the furan ring, the possibility to use the tandem Horner–Wadsworth–Emmons reaction/intramolecular Michael addition between the β-ketophosphonate showed in scheme 5.9 and the azidolactol **19** was therefore envisioned.

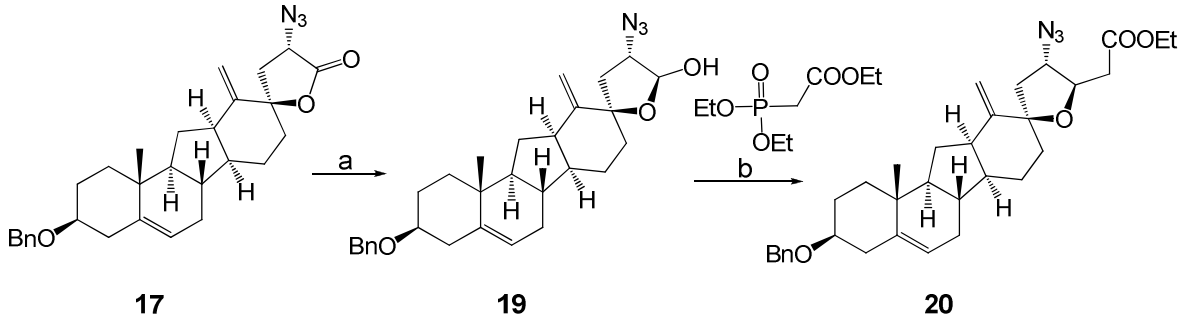

Scheme 5.9 Reaction conditions: a) DIBAH, THF, -78°C→-65°C, 88%; b) $Ba(OH)_2$, THF, H_2O, then **19**, 80°C, 55%.

This previously adopted strategy for cyclopamine, successfully led to isolate the desired compound in 48% yield and the recovered starting material in 11% yield using the β-ketophosphonate showed in scheme 5.10.

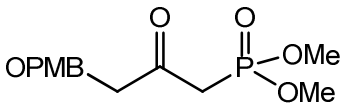

Scheme 5.10 [3-(4-methoxy-benzyloxy)-2-oxo-propyl]-phosphonic acid dimethyl ester used in the synthesis of cyclopamine.

In the synthesis of the IR-analogue it was so expected to obtain the desired furan **20** with a slightly improved yield due to the higher reactivity of the triethyl phosphonoacetate in comparison with the one used for cyclopamine. The long and laborious procedure consists of reducing the carbonyl moiety of **17** to obtain the highly unstable lactol **19** which has to be immediately added to a previously prepared suspension of triethyl phosphonoacetate and dried $Ba(OH)_2$ in THF after prolonged sonication. After the low yielding first reaction conditions due essentially to the low solubility of the phosphonoacetate, several attempts to find the ideal conditions using high temperatures and also a more soluble trimethyl phosphonoacetate, the HWE reaction/Michael addition furnished the furan **20** in an encouraging yield of 55% without any remaining starting material.

5.5. The pyrrolidine ring closure

Continuing the sequence from the azidoester **20**, with a suitable ring precursor in hand, it was possible to test the feasibility for the proposed aza-Wittig strategy toward the pyrrolidine formation: reduction of the ester to aldehyde and subsequent Staudinger reduction of the azide would directly provide the imino-derivative which could have been reduced to form the F ring. This approach would have been an interesting and elegant way to perform a ring closure in a concise few steps synthesis (Scheme 5.11). After the reduction of **20** to **22**, the planned Staudinger reaction afforded the amine from which, unfortunately, was not possible to obtain the desired amine **24** neither trying to reduce the hypothetic imino-derivative with sodium cyanoborohydride ($NaBH_3CN$) in acetic acid or $NaBH_4$, nor using the classical DIBAH.

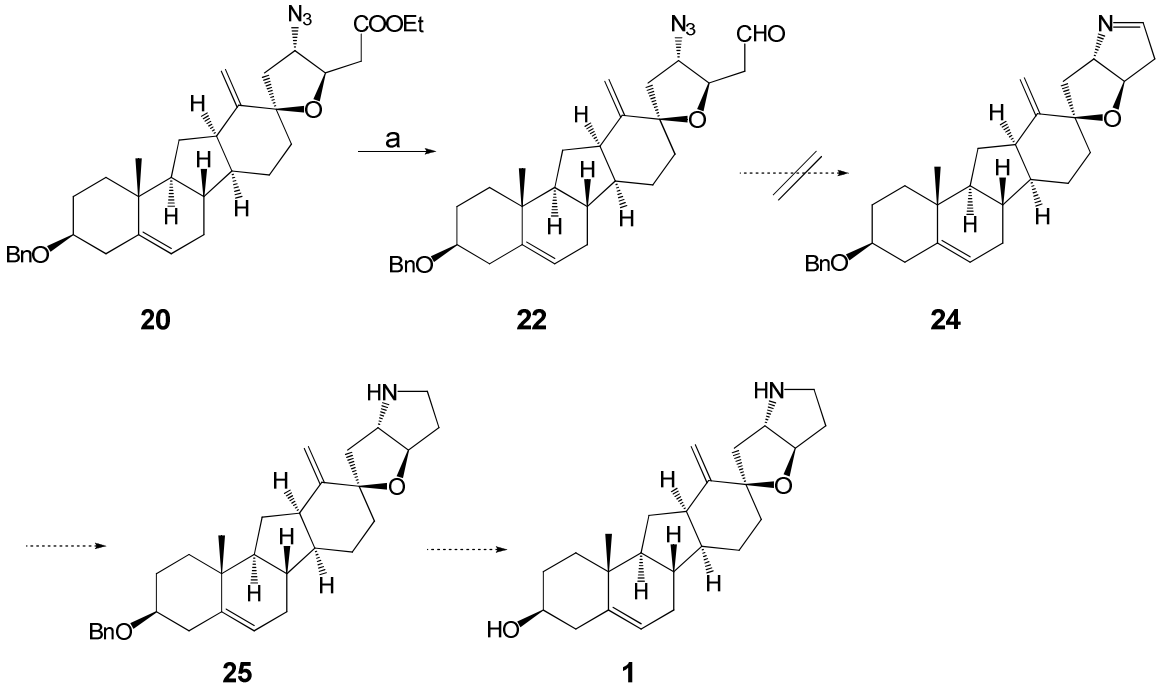

Scheme 5.11 Tandem Staudinger/aza-Wittig strategy toward the pyrrolidine ring formation. Reaction conditions: a) DIBAH, THF, -78°C→-65°C, 78%.

Since the tandem Staudinger/aza-Wittig route was not successful, it was then decided to proceed with the Staudinger reduction and subsequent direct lactam formation to obtain the precursor of the F ring which should have been reduced to the corresponding amine as showed in scheme 5.12.

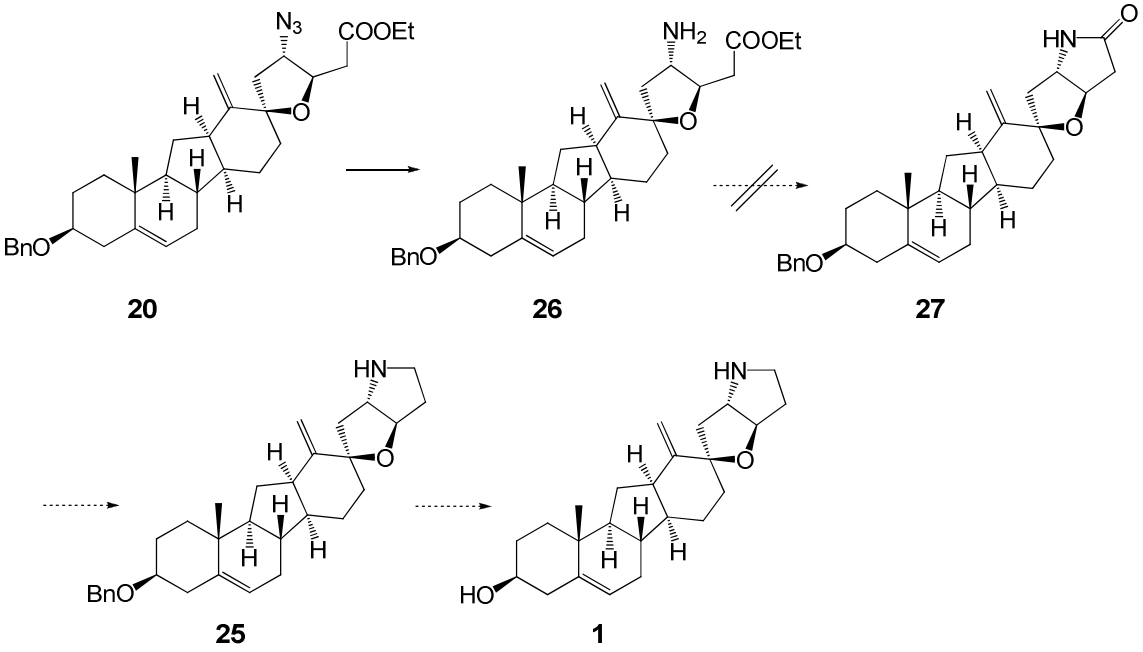

Scheme 5.12 Proposed Staudinger/lactam formation to create the pyrrolidine ring.

The initial Staudinger reduction afforded, as planned, the amine **26** which unfortunately could not be converted in the corresponding lactam, neither activating the ester as a more reactive acyl chloride. Therefore, after considerable experimentation it was concluded that compounds **22** and **26** are highly strained systems possessing a fusion of two-membered rings which implies a high energy barrier to their formation. Since the mentioned ring closure conditions didn't lead to the pyrrolidine formation, it was necessary to find a new synthetic strategy.

Continuing the sequence from the azidoester **20** (Scheme 5.13), the strategy toward IR-analogue **1** proceeded with an intermediate which bears no sp^2 carbon in the pyrrolidine ring formation.

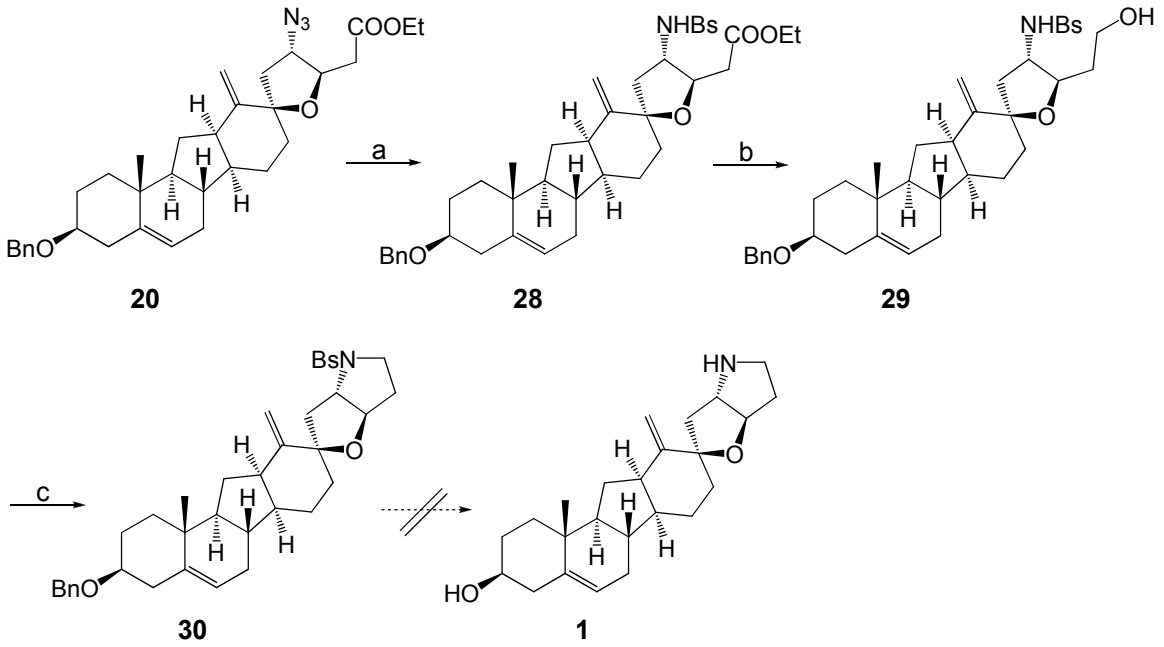

Scheme 5.13 Formation of the pyrrolidine ring. Reaction conditions: a) PPh_3, H_2O, toluene, 50°C, then BsCl, Et_3N, CH_2Cl_2, 40°C; 78%; b) DIBAH, THF, -78°C → -40°C, 97%; c) Bu_3P, ADDP, toluene, 81%.

After the Staudinger reduction, protection of the amine with benzenesulfonyl chloride furnished the sulfonamide **28**, which in turn was treated with DIBAH to give the corresponding alcohol **29**. Ring closure by a modified Mitsunobu protocol,[54] consisting of treatment of **29** with tributylphosphine and azodicarboxylic dipiperidide at 0°C, proceeded with high efficiency and furnished the pyrrolidine **30** in a 81% yield. With the protected IR-analogue in hand it was tried to easily obtain the desired compound **1** removing in one step both protective groups, the benzyl ether and the benzenesulfonamide moiety, using the Birch reduction, but lithium and ethanol in liquid ammonia, unfortunately, gave only

extensive degradation of pyrrolidine **30**, hampering so far the access to the targeted compound **1**.

This unfortunate outcome led once again to change the planned synthetic route and to follow the previously established protocol viable for cyclopamine synthesis. The final deprotection will be therefore done removing at first the benzyl ether by Raney nickel in refluxing ethanol and then the benzenesulfonamide moiety by sodium naphthalenide at -78°C.[55]

Summary

The synthetically challenging IR-analogue with its six skeletal rings and complex stereochemistry, particularly around its spiro connection, provided several obstacles to be overcome. The stereochemically controlled E-ring lactone formation was optimized via a Cerium reagent, while the completely diastereoselective and biomimetic 12β-hydroxylation set the stage for the not common *C*-nor-*D*-homo skeleton construction. The nitrogen introduction followed by the laborious procedure of reduction and Horner–Wadsworth–Emmons reaction/intramolecular Michael addition led to obtain the correctly functionalized furan motif. The subsequent challenging pyrrolidine ring closure required considerable experimentation and even with a fine tuning of the functional groups for proper elaboration of the synthetic intermediates, the much more convenient planned route had finally to be changed. Therefore the Mitsunobu approach was a viable alternative to overcome the problematic highly strained pyrrolidine formation, consisting in more steps than the ones planned but necessary to close the five membered ring. Moreover, even the final step of deprotection was not so obvious: the Birch reduction would have led in one step to the targeted compound **1** but this attempt was, however, thwarted by failure to remove the protective groups without the concomitant degradation of the pyrrolidine **30** leading to choose a different deprotection procedure. So far, even after extensive experimentation, it was not possible to gain access to the final goal: the first synthetically accessible analogue of cyclopamine will be therefore obtained with two more steps promising fundamental insights into structure-activity relationships from the evaluation of its biological potency.

Experimental Part

General procedures. All reactions were run under an atmosphere of argon unless otherwise indicated. Room temperature refers to 22°C, ambient pressure to 1013 hPa.
Reagents and anhydrous solvents were transferred via oven-dried syringe or cannula. Flasks were flame-dried under vacuum and cooled under a constant stream of argon. Tetrahydrofuran was distilled under argon from potassium, dichloromethane from SICAPENT (phosphorus pentoxide on solid support with indicator), and diisopropyl amine and triethylamine from calcium hydride. Toluene, dimethoxyethane, acetone, acetonitrile and pyridine were purchased from Acros, Aldrich or Fluka (anhydrous over molecular sieves).
All other chemicals were purchased from ABCR, Acros, Aldrich, Alfa Aesar, Fluorochem, Fluka, Merck and TCI Europe at highest commercially available purity and used as such.
Reactions were monitored by thin layer chromatography using Merck silica gel 60 F_{254} TLC aluminium sheets and visualized with ceric ammonium molybdate or vanillin staining solution. Chromatographic purification was performed as flash chromatography on Acros silica gel 35-70, 60 Å, using a forced flow of eluent (method of Still).
Concentration under reduced pressure was performed by rotary evaporation at 40°C at the appropriate pressure.
NMR spectra were recorded on a Varian Mercury plus 400 (operating at 400 MHz for ^{1}H, 100 MHz for ^{13}C and 162 MHz for ^{31}P acquisitions), a Varian Mercury plus 300 (operating at 300 MHz for ^{1}H and 75 MHz for ^{13}C acquisitions) and a Varian Gemini 2000 (operating at 200 MHz for ^{1}H and 50 MHz for ^{13}C acquisitions) spectrometer. Chemical shifts δ are reported in ppm with the residual solvent signal as the internal standard (d_1-chloroform: 7.26 (^{1}H-NMR), 77.16 (^{13}C-NMR); d_2-dichloromethane: 5.32 (^{1}H-NMR), 53.44 (^{13}C-NMR). ^{31}P-NMR shifts are reported in ppm relative to 85% H_3PO_4 in water. Coupling constants *J* are given in Hertz (Hz). Multiplicities are classified by the following abbreviations: s = singlet, d = doublet, t = triplet, q = quartet and combinations thereof, or m = multiplet.
Where 2D-spectra were recorded and allowed complete assignment of all hydrogen- and carbon-atoms of a compound, spectral data include this assignment using common steroid numbering. Where this is not the case, all hydrogen-signals below 2 ppm are omitted and only methyl groups in this range are listed.
High resolution mass spectra were obtained on a Bruker Daltonics ESI-FT-ICR-MS APEX II. IR spectra were obtained on an ATI/MATTSON Genesis FT-IR as thin film (in CCl_4) or KBr-disk. Absorbance frequencies are reported in reciprocal centimetres (cm^{-1}).
Melting points were measured on a Boetius-micro hot stage.

Optical rotation data was obtained with a Schmidt+Haensch Polartronic MHZ-8 at the sodium-D line (589 nm) using a 50 mm path-length cell in the solvent and concentration indicated.

Synthesis overview

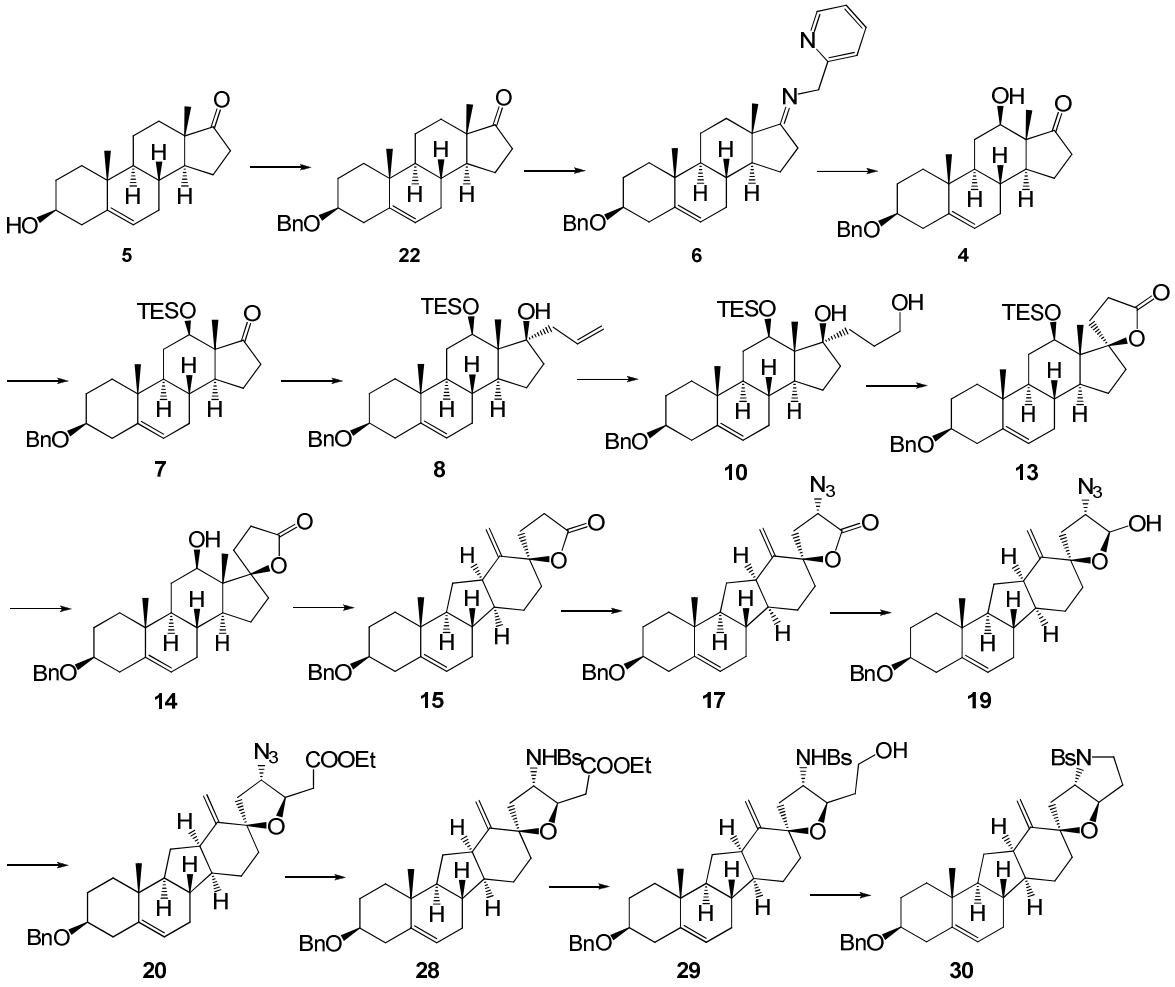

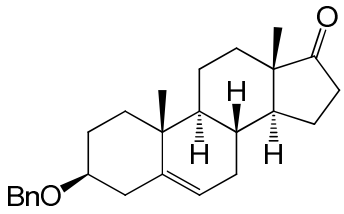

22

(+)-*O*-benzyl-dehydroandrosterone 22: A suspension of magnesium oxide (19.57 g, 485.0 mmol), dehydroandrosterone **5** (70.00 g, 242.7 mmol) and 2-benzyloxy-methylpyridinium triflate (169.43 g, 485.0 mmol) in α,α,α-trifluorotoluene (1 L) was heated to 85°C for 24 h. The suspension was allowed to cool to room temperature, filtered through a pad of Celite and washed with CH_2Cl_2 (3 x 250 mL). The solvents were removed by rotary evaporation and the resulting crude **22** was recrystallised from hot *n*-hexane/CH2Cl2 (app. 15:1) to yield **22** (85.44 g, 225.7 mmol, 95%, containing 5% of starting material) as a white solid. An analytically pure sample was obtained by silica gel chromatography (CH2Cl2/*n*-hexane, 5:1 v/v); m.p. 151-153°C; TLC (CH_2Cl_2/*n*-hexane, 10:1 v/v): R_F = 0.24; $[\alpha]_D^{22}$ (deg cm^3 g^{-1} dm^{-1}) = +17.8 (c = 0.0102 g cm^{-3} in $CHCl_3$); IR (KBr): ν_{max} 1737, 742, 699 cm^{-1}; ^1H NMR (400 MHz, $CDCl_3$) δ 7.37-7.30 (m, 4 H), 7.30-7.24 (m, 1 H), 5.38 (m, 1 H), 4.57 (s, 2 H), 3.29 (tt, *J* = 11.2, 4.5 Hz, 1 H), 2.46 (m, 2 H), 2.30 (m, 1 H), 2.12 (m, 2 H), 1.04 (s, 3 H), 0.89 (s, 3 H); ^{13}C (100 MHz, $CDCl_3$) δ 221.2, 141.3, 139.1, 128.5, 127.7, 127.5, 120.9, 78.5, 70.1, 51.9, 50.4, 47.7, 39.3, 37.3, 37.2, 36.0, 31.6, 31.6, 31.0, 28.5, 22.0, 20.5, 19.5, 13.7; HRMS (*m/z*): $[M+Na]^+$ calcd for $C_{26}H_{34}O_2Na$: 401.24529, found: 401.24494, $[2M+Na]^+$ calcd for $C_{52}H_{68}O_4Na$: 779.50098, found: 779.50034.

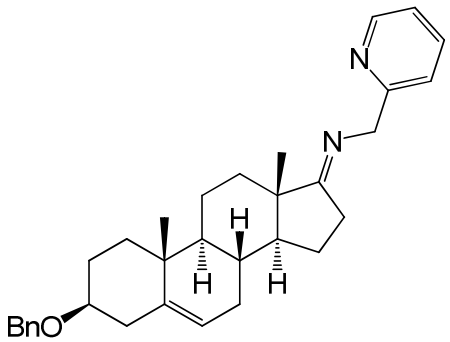

6

(-)-*O*-benzyl-17-iminomethylpyridyl-dehydroandro-sterone 6: A solution of **22** (37.29 g, 98.5 mmol), picolyl amine (50.2 mL, 493 mmol) and p-tolyl sulfonic acid (444 mg) in toluene (0.926 L) was heated to reflux for 3 h with azeotropic removal of water using a dean-stark apparatus when another portion of picolyl amine (15.1 mL, 148 mmol) was added and reflux was continued for 2 h. The reaction mixture was allowed to cool to room temperature, diluted with EtOAc (1.1 L), washed with saturated aqueous $NaHCO_3$ (2 x 370 mL), brine (370 mL) and dried (Na_2SO_4). The solvents were rotary evaporated and the

crude **6** was recrystallised from EtOAc (app. 10 mL per g crude **6**) (39.26 g, 83.7 mmol, 85%); colourless needles; m.p. 149-150°C; $[\alpha]_D^{22}$ (deg cm^3 g^{-1} dm^{-1}) = -20.7 (c = 0.0116 g cm^{-3} in $CHCl_3$); IR (KBr): ν_{max} 1672, 763, 696 cm^{-1}; ^1H NMR (400 MHz, $CDCl_3$) δ 8.52 (d, *J* = 4.3 Hz, 1 H), 7.64 (dt, *J* = 7.7, 1.6 Hz, 1 H), 7.42 (d, *J* = 7.8 Hz, 1 H), 7.37-7.30 (m, 4 H), 7.30-7.23 (m, 1 H), 7.13 (dd, *J* = 7.0, 5.3 Hz, 1 H), 5.37 (m, 1 H), 4.59 (q, *J* = 16.5 Hz, 2 H), 4.56 (s, 2 H), 3.29 (tt, *J* = 11.1, 4.4 Hz, 1 H), 2.44 (m, 2 H), 2.30 (m, 2 H), 2.06 (m, 2 H), 1.05 (s, 3 H), 0.92 (s, 3 H); ^{13}C (100 MHz, $CDCl_3$) δ 186.0, 160.6, 149.1, 141.4, 139.2, 136.7, 128.5, 127.7, 127.5, 121.7, 121.7, 121.2, 78.6, 70.1, 58.1, 53.4, 50.7, 45.7, 39.3, 37.3, 37.2, 34.2, 31.7, 31.5, 28.5, 28.1, 23.5, 20.9, 19.6, 16.4; HRMS (*m/z*): $[M+Na]^+$ calcd for $C_{32}H_{41}N_2ONa$: 469.32134, found: 469.32140, $[2M+Na]^+$ calcd for $C_{64}H_{80}N_4O_2Na$: 959.61735, found: 959.61794.

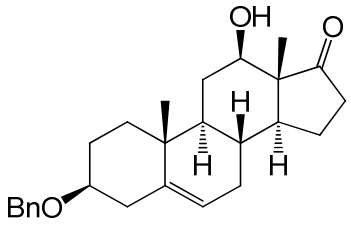

4

(+)-3-benzyl-12β-hydroxy-dehydroandrosterone 4: To a suspension of **6** (19.11 g, 40.8 mmol) in acetone (500 mL) was added tetrakis(acetonitrile)copper(I) hexafluorophosphate (18.24 g, 48.9 mmol). The light-green solution was stirred for 1 h when dry oxygen was bubbled through the suspension for 45 min and the resulting dark-green solution was stirred under an atmosphere of oxygen for another 36 h. The solvent was removed by rotary evaporation and the resulting green solid was taken up in EtOAc/Et_2O/NH_3(aq. 25%) (1 L, 1:2:1), the layers were separated and the organic layer was washed with aqueous ammonia (2 x 100 mL) and brine (75 mL), dried (Na_2SO_4) and the solvents were again rotary evaporated. The residue was redissolved in MeOH/AcOH (0.375 L, 1:1) and heated to 90°C for 6 h. The solvents were rotary evaporated and the brown residue was taken up in EtOAc (0.75 L) washed with brine (2 x 50 mL), dried ($MgSO_4$) and rotary evaporated. Purification by silica gel chromatography (*n*-hexane/EtOAc, 3:1→ 2:1 v/v) yielded pure **4** (7.87 g, 19.9 mmol, 49%) as colourless needles and recovered **22** (1.40 g, 3.70 mmol, 9%); m.p. 165-166°C; TLC (*n*-hexane/EtOAc, 2:1 v/v): R_F = 0.36; $[\alpha]_D^{22}$ (deg cm^3 g^{-1} dm^{-1}) = +6.6 (c = 0.0104 g cm^{-3} in toluene); IR (KBr): ν_{max} 3350, 1717, 736, 698 cm^{-1}; ^1H NMR (400 MHz, $CDCl_3$) δ 7.36-7.25 (m, 5 H), 5.37 (m, 1 H), 4.56 (s, 2 H), 3.80 (dd, *J* = 11.3, 4.7 Hz, 1 H), 3.27 (tt, *J* = 11.2, 4.5 Hz, 1 H), 3.06 (br, 1 H), 2.46 (m, 2 H), 2.29 (m, 1 H), 2.12 (m, 2 H), 1.05 (s, 3 H), 0.96 (s, 3 H); ^{13}C (75 MHz, $CDCl_3$) δ 223.0 (C-17), 141.5 (C-5), 139.2 (ipso-C Bn), 128.6 (meta-C Bn), 127.8 (ortho-C Bn), 127.7 (para-C

Bn), 120.8 (C-6), 78.5 (C-3), 72.9 (C-12), 70.2 (benzyl. C), 51.6 (C-14), 49.8 (C-13), 49.4 (C-9), 39.3 (C-4), 37.4 (C-10), 37.4 (C-1), 36.0 (C-16), 30.8 (C-8), 30.6 (C-7), 28.5 (C-11), 28.4 (C-2), 21.9 (C-15), 19.6 (C-19), 8.3 (C-18); HRMS (*m/z*): $[M+Na]^+$ calcd for $C_{26}H_{34}O_3Na$: 417.24002, found: 417.23969, $[2M+Na]^+$ calcd for $C_{52}H_{68}O_6Na$: 811.49081, found: 811.49056.

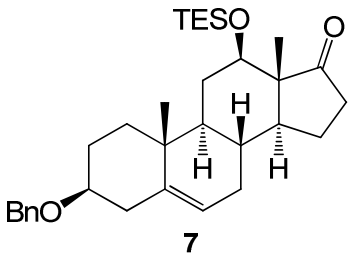

7

(-)-3-benzyl-12β-(triethylsilyloxy)-dehydroandrosterone 7: To a stirred solution of **4** (5.25 g, 13.3 mmol) and 2,6-lutidine (3.09 mL, 26.6 mmol) in CH_2Cl_2 (423 mL) was added triethylsilyl triflate (3.30 mL, 14.6 mmol) dropwise over a period of 30 min at 0°C. After stirring for 1 h at this temperature the reaction mixture was quenched with saturated aqueous $NaHCO_3$ (200 mL), the phases were separated and the aqueous layer was extracted with CH_2Cl_2 (2 x 100 mL). The combined organic layers were washed with brine (200 mL), dried ($MgSO_4$) and the solvents were rotary evaporated. Purification by silica gel chromatography (*n*-hexane/EtOAc, 22:1 v/v) yielded pure **7** (6.14 g, 12.1 mmol, 91%) as a slight yellow oil; TLC (*n*-hexane/EtOAc, 10:1 v/v): R_F = 0.39; $[\alpha]_D^{22}$ (deg cm^3 g^{-1} dm^{-1}) = -11.3 (c = 0.0131 g cm^{-3} in $CHCl_3$); IR (KBr): ν_{max} 1742, 739, 697 cm^{-1}; ^1H NMR (400 MHz, $CDCl_3$) δ 7.37-7.24 (m, 5 H), 5.37 (m, 1 H), 4.57 (s, 2 H), 3.73 (dd, *J* = 10.8, 4.8 Hz, 1 H), 3.28 (tt, *J* = 11.2, 4.5 Hz, 1 H), 2.44 (m, 2 H), 2.29 (m, 1 H), 2.09 (m, 2 H), 1.04 (s, 3 H), 0.98 (t, *J* = 7.9 Hz, 9 H), 0.94 (s, 3 H), 0.65 (dq, *J* = 14.9, 7.9 Hz, 6 H); ^{13}C (100 MHz, $CDCl_3$) δ 218.2, 141.2, 139.1, 128.5, 127.7, 127.6, 120.9, 78.5, 72.2, 70.1, 52.0, 50.4, 49.3, 39.2, 37.3, 37.1, 35.8, 31.7, 30.6, 30.5, 28.5, 21.2, 19.5, 8.4, 7.2, 5.4; HRMS (*m/z*): $[M+Na]^+$ calcd for $C_{32}H_{48}O_3SiNa$: 531.32649, found: 531.32605, $[2M+Na]^+$ calcd for $C_{64}H_{96}O_6Si_2Na$: 1039.66376, found: 1039.66401.

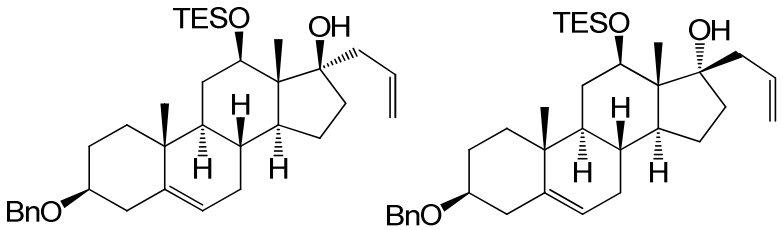

8 **9**

(-)-alkene 8: Ceriumchloride heptahydrate (35.2 g, 94.5 mmol) was heated under vacuum (0.5 mbar) at 150°C for 3 h then at 0.05 mbar and 300°C stirring overnight. After cooling to room temperature THF (144 mL) was added and the suspension was stirred for 2 h at room temperature and then cooled to 0°C. A solution of allylmagnesium bromide (1 M in THF; 94.5 mL, 94.5 mmol,) was added dropwise and the reaction mixture was stirred at this temperature for 1.5 h. Then **7** (4.79 g, 9.41 mmol) in THF (17 mL) was added very fast and stirring was continued for another 30 min. The reaction was quenched with saturated aqueous NH_4Cl (200 mL), extracted with EtOAc (2 x 70 mL) and the combined organic extracts were washed with brine (130 mL) and dried ($MgSO_4$). The solvents were rotary evaporated and the crude product was purified by silica gel chromatography (*n*-hexane/EtOAc, 22:1 v/v) to yield an inseparable mixture of the epimeric alcohols **8** and **9** (4,84 g, 8,78 mmol, 93%) as a colourless oil and recovered **7** (335 mg, 0.66 mmol, 7%); TLC (*n*-hexane/EtOAc, 10:1 v/v): R_F = 0.38; $[\alpha]_D^{22}$ (deg cm^3 g^{-1} dm^{-1}) = -50.4 (c = 0.0100 g cm^{-3} in $CHCl_3$); IR (CCl_4): ν_{max} 3574, 732, 697 cm^{-1}; NMR data of the main isomer: ^{1}H NMR (400 MHz, $CDCl_3$) δ 7.35-7.26 (m, 5 H), 6.05 (dddd, *J* = 17.1, 10.1, 8.4, 5.5 Hz, 1 H), 5.36 (m, 1 H), 5.15 (d, *J* = 9.6 Hz, 1 H), 5.10 (d, *J* = 17.2 Hz, 1 H), 4.57 (d, *J* = 2.6 Hz, 2 H), 3.85 (dd, *J* = 11.0, 4.7 Hz, 1 H), 3.28 (tt, *J* = 11.2, 4.5 Hz, 1 H), 2.46 (m, 2 H), 2.26 (m, 2 H), 1.05 (s, 3 H), 0.99 (t, *J* = 7.9 Hz, 9 H), 0.95 (s, 3 H), 0.62 (m, 6 H); ^{13}C (100 MHz, $CDCl_3$) δ 140.8, 139.1, 135.6, 128.5, 127.6, 127.5, 121.5, 117.5, 83.2, 78.5, 74.9, 70.1, 50.7, 49.8, 49.6, 41.9, 39.1, 37.5, 37.1, 32.4, 32.0, 31.5, 30.4, 28.6, 23.7, 19.5, 9.6, 7.2, 5.9; HRMS (*m/z*): $[M+Na]^+$ calcd for $C_{35}H_{54}O_3SiNa$: 537.37344, found: 537.37288, $[2M+Na]^+$ calcd for $C_{70}H_{108}O_6Si_2Na$: 1123.75767, found: 1123.75776.

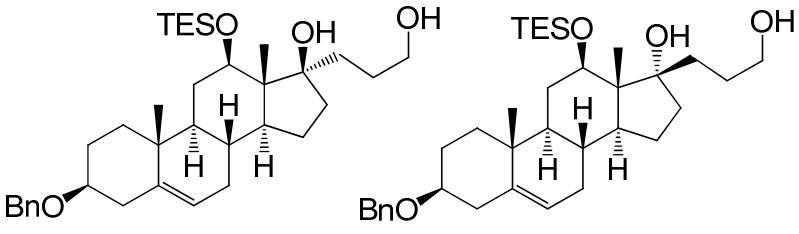

10 **11**

(-)-diol 10: To a stirred solution of **8** and **9** (5.07 g, 9.20 mmol) in THF (40 mL) was added a solution of 9-BBN (0.5 M in THF; 73.6 mL, 36.8 mmol) dropwise at room temperature. After stirring for 6 h under reflux the reaction mixture was cooled to 0°C and water (45 mL) was added carefully. Then sodium perborate (21.23 g, 138.0 mmol) were added sequentially and stirring was continued at 50°C for 12 h. The reaction was quenched with water (43 mL), extracted with EtOAc (3 x 90 mL) and the combined organic extracts were washed with brine (60 mL) and dried ($MgSO_4$). The solvents were rotary evaporated and the crude product was purified by silica gel chromatography (*n*-hexane/EtOAc, 4:1 v/v) to yield an inseparable mixture of the epimeric alcohols **10** and **11** as a colourless oil (4.78 g, 8.41 mmol, 91%); TLC (*n*-hexane/EtOAc, 6:4 v/v): R_F = 0.42; $[\alpha]_D^{22}$ (deg cm^3 g^{-1} dm^{-1}) = -56.0 (c = 0.0101 g cm^{-3} in $CHCl_3$); IR (CCl_4): ν_{max} 3573, 3424, 744, 697 cm^{-1}; NMR data of the main isomer: ^{1}H NMR (300 MHz, $CDCl_3$) δ 7.35-7.26 (m, 5 H), 5.34 (m, 1 H), 4.56 (d, *J* = 1.5 Hz, 2 H), 3.87 (dd, *J* = 10.9, 4.8 Hz, 1 H), 3.67 (t, *J* = 5.8 Hz, 2 H), 3.27 (m, 1 H), 2.44 (m, 1 H), 2.25 (m, 1 H), 1.04 (s, 3 H), 0.97 (m, 9 H), 0.93 (s, 3 H), 0.61 (m, 6 H); ^{13}C (75 MHz, $CDCl_3$) δ 140.8, 139.1, 128.5, 127.7, 127.6, 121.5, 83.6, 78.5, 74.8, 70.1, 63.9, 50.9, 49.6, 49.6, 39.1, 37.5, 37.2, 33.6, 32.1, 32.1, 31.6, 30.3, 28.6, 27.4, 23.8, 19.5, 9.6, 7.2, 5.9; HRMS (*m/z*): $[M+Na]^+$ calcd for $C_{35}H_{56}O_4SiNa$: 591.38401, found: 591.38366.

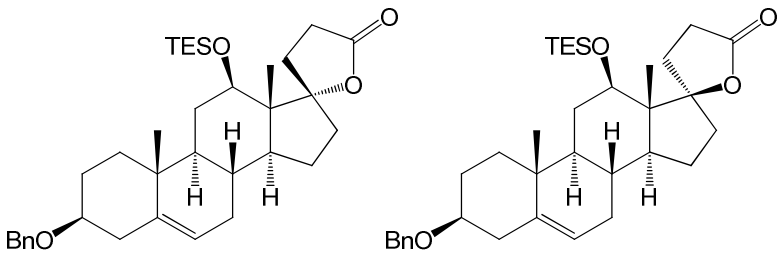

12 **13**

(-)-spirolactone 12 and (-)-spirolactone 13: A stirred solution of the alcohols **10** and **11** (4.60 g, 8.07 mmol) in CH_2Cl_2 (58 mL) was treated with iodobenzene diacetate (12.8 g, 39.7 mmol) and 2,2,6,6-tetramethylpiperidine-1-oxyl (252 mg, 1.61 mmol) at room temperature. The reaction mixture was treated with saturated aqueous $Na_2S_2O_3$ (30 mL) and CH_2Cl_2 (30 mL). The phases were separated and the organic phase was washed with saturated aqueous $NaHCO_3$ (20 mL) brine (20 mL) and dried ($MgSO_4$). The solvent was rotary evaporated and the crude product was purified by silica gel chromatography (*n*-

hexane/EtOAc, 9:1 v/v) to yield pure **12** (250 mg, 0,442 mmol, 5 %) and **13** (3.36 g, 5.94 mmol, 73%) both as a colourless foam; **12**: TLC (*n*-hexane/EtOAc, 8:2 v/v): R_F = 0.29; $[\alpha]_D^{22}$ (deg cm^3 g^{-1} dm^{-1}) = -68.0 (c = 0.0100 g cm^{-3} in $CHCl_3$); IR (CCl_4): ν_{max} 1773, 735, 697 cm^{-1}; ^{1}H NMR (300 MHz, $CDCl_3$) δ 7.35-7.25 (m, 5 H), 5.35 (m, 1 H), 4.56 (s, 2 H), 4.05 (dd, *J* = 11.1, 4.8 Hz, 1 H), 3.29 (tt, *J* = 11.1, 4.5 Hz, 1 H), 2.77 (m, 1 H), 2.54 (m, 2 H), 2.45 (ddd, *J* = 13.2, 4.6, 2.2 Hz, 1 H), 2.27 (m, 1 H), 1.03 (s, 3 H), 0.95 (t, *J* = 7.9 Hz, 9 H), 0.81 (s, 3 H), 0.55 (m, 6 H); ^{13}C (100 MHz, $CDCl_3$) δ 177.2, 140.8, 139.1, 128.5, 127.7, 127.5, 121.5, 97.8, 78.5, 72.8, 70.1, 50.5, 50.3, 49.2, 39.2, 37.9, 37.4, 36.9, 31.5, 30.9, 29.6, 29.0, 28.5, 23.9, 19.5, 9.2, 7.1, 5.7; HRMS (*m/z*): $[M+Na]^+$ calcd for $C_{35}H_{52}O_4SiNa$: 587.35271, found: 587.35208, $[2M+Na]^+$ calcd for $C_{70}H_{104}O_8Si_2Na$: 1151.71619, found: 1151.71518; **13**: TLC (*n*-hexane/EtOAc, 8:2 v/v): R_F = 0.18; $[\alpha]_D^{22}$ (deg cm^3 g^{-1} dm^{-1}) = -52.0 (c = 0,0102 g cm^{-3} in $CHCl_3$); IR (CCl_4): ν_{max} 1773, 735, 697 cm^{-1}; ^{1}H NMR (300 MHz, $CDCl_3$) δ 7.36-7.33 (m, 5 H, ortho-, meta-H Bn), 7.27 (m, 1 H, para-H Bn), 5.35 (m, 1 H, H-6), 4.56 (s, 2 H, benzyl. H), 3.84 (dd, *J* = 10.9, 4.7 Hz, 1 H, H-12), 3.28 (tt, *J* = 11.2, 4.5 Hz, 1 H, H-3), 2.58 (m, 1 H, H-20), 2.49 (m, 1 H, H-20), 2.45 (m, 2 H, H-4, H-21), 2.28 (m, 1 H, H-4), 2.23 (m, 1 H, H-16), 2.03 (m, 1 H, H-7), 1,99 (m, 1 H, H-2), 1.87 (m, 1 H, H-21), 1.81 (m, 1 H, H-1), 1.80 (m, 1 H, H-16), 1.75 (m, 1 H, H-11), 1.66 (m, 1 H, H-15), 1.55 (m, 2 H, H-2, H-11), 1.49 (m, 1 H, H-8), 1.47 (m, 1 H, H-7), 1.45 (m, 1 H, H-15), 1.05 (m, 1 H, H-1), 1.04 (s, 3 H, H-19), 1.02 (m, 1 H, H-9), 1.01 (m, 1 H, H-14), 1.00 (s, 3H, H-18), 0.97 (t, *J* = 7.9 Hz, 9 H, CH_3 TES), 0.58 (q, *J* = 7.9 Hz, 6H, CH_2 TES); ^{13}C (75 MHz, $CDCl_3$) δ 176.3 (C-22), 140.5 (C-5), 138.7 (ipso-C Bn), 128.1 (meta-C Bn), 127.3 (ortho-C Bn), 127.2 (para-C Bn), 120.8 (C-6), 95.5 (C-17), 78.1 (C-3), 74.2 (C-12), 69.7 (benzyl. C), 49.6 (C-14), 49.1 (C-13), 48.9 (C-9), 38.8 (C-4), 37.1 (C-1), 36.6 (C-10), 36.2 (C-16), 31.2 (C-8), 30.9 (C-7), 30.6 (C-11), 30.3 (C-21), 29.2 (C-20), 28.1 (C-2), 22.3 (C-15), 19.2 (C-19), 9.3 (C-18), 6.8 (CH_3 TES), 5.7 (CH_2 TES); HRMS (*m/z*): $[M+Na]^+$ calcd for $C_{35}H_{52}O_4SiNa$: 587.35271, found: 587.35270, $[2M+Na]^+$ calcd for $C_{70}H_{104}O_8Si_2Na$: 1151.71619, found: 1151.71706.

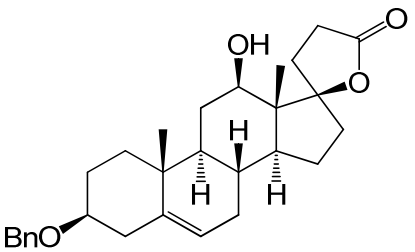

14

(-)-hydroxylactone 14: To a solution of the lactone **13** (2.80 g, 4.96 mmol) in MeCN (100 mL) was added a solution of hydrofluoric acid (50 wt% in H_2O; 15 mL) in MeCN (100 mL) under stirring at room temperature. After stirring for 20 min the reaction was diluted with

EtOAc (100 mL) and saturated aqueous $NaHCO_3$ (200 mL) was introduced very carefully under vigorous stirring until no further CO_2 evolution was detectable. The phases were separated, the aqueous phase was extracted with EtOAc (4 x 150 mL) and the combined organic extracts were washed with brine (150 mL) and dried ($MgSO_4$). The solvents were rotary evaporated and the crude product was purified by silica gel chromatography (*n*-hexane/EtOAc, 2:1 v/v) to yield pure **14** (1.95 g, 4.34 mmol, 87%) as a white solid; m.p. 215-219°C; TLC (*n*-hexane/EtOAc, 2:8 v/v): R_F = 0.50; $[\alpha]_D^{22}$ (deg cm^3 g^{-1} dm^{-1}) = -54.0 (c = 0.0101 g cm^{-3} in $CHCl_3$); IR (KBr): ν_{max} 3489, 1759, 735, 698 cm^{-1}; ^{1}H NMR (400 MHz, $CDCl_3$) δ 7.35-7.26 (m, 5 H), 5.34 (m, 1 H), 4.56 (s, 2 H), 3.69 (td, *J* = 10.7, 5.2 Hz, 1 H), 3.27 (tt, *J* = 11.2, 4.4 Hz, 1 H), 2.77 (m, 1 H), 2.52 (m, 2 H), 2.44 (ddd, *J* = 6.7, 5.0, 2.6 Hz, 1 H), 2.28 (m, 2 H), 1.04 (s, 3 H), 0.97 (s, 3 H); ^{13}C (100 MHz, $CDCl_3$) δ 177.3, 141.0, 139.1, 128.5, 127.6, 127.5, 121.0, 95.9, 78.4, 73.2, 70.1, 49.5, 49.5, 49.3, 39.1, 37.3, 37.1, 36.5, 31.5, 31.4, 31.2, 31.0, 29.7, 28.4, 22.6, 19.5, 9.0; HRMS (*m/z*): $[M+Na]^+$ calcd for $C_{29}H_{38}O_4Na$: 473.26623, found: 473.26637, $[2M+Na]^+$ calcd for $C_{58}H_{76}O_8Na$: 923,54324, found: 923.54277.

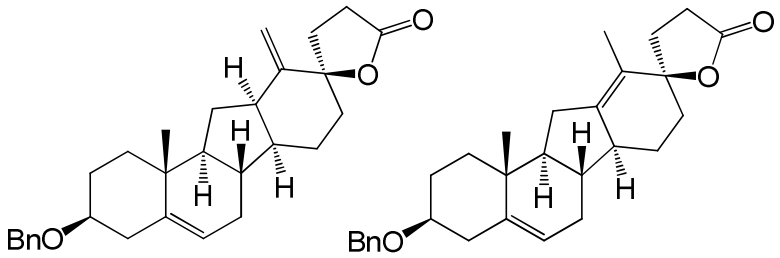

15 **16**

(-)-exo-C-*nor*-D-*homo*-lactone 15 and (-)-endo-C-*nor*-D-*homo*-lactone 16: To a stirred solution of the alcohol **14** (1.95 g, 4.34 mmol) in pyridine (62 mL) was added triflic anhydride (1.44 mL, 8.68 mmol) at 0°C. After stirring at this temperature for 10 min the reaction was warmed to 50°C and kept there for 1,5 h. The reaction was cooled again to 0°C, additional 2 equivalents of triflic anhydride (1.44 mL, 8.68 mmol) were added and stirring was continued at this temperature for 10 min and thereafter at 50°C for 2 h. After allowing the dark brown mixture to cool to room temperature, it was diluted with CH_2Cl_2 (186 mL) and washed several times with hydrochloric acid (0.5 M) and finally with saturated aqueous $NaHCO_3$ (62 mL) and brine (62 mL). The organic phase was dried ($MgSO_4$), the solvent was rotary evaporated and the crude product was purified by silica gel chromatography (*n*-hexane/EtOAc, 8.5:1.5 v/v) to yield pure exo-C-*nor*-D-*homo*-lactone **15** (0.86 g, 2.0 mmol, 46%) and pure endo-C-*nor*-D-*homo*-lactone **16** (0.28 g, 0.65 mmol, 15%) both as colourless needles; **15:** m.p. 94-102°C; TLC (*n*-hexane/EtOAc, 2:1 v/v): R_F = 0.46; $[\alpha]_D^{22}$ (deg cm^3 g^{-1} dm^{-1}) = -32.4 (c = 0.0100 g cm^{-3} in $CHCl_3$); IR

(KBr): ν_{max} 1767, 736, 697 cm^{-1}; ^1H NMR (400 MHz, $CDCl_3$) δ 7.35-7.26 (m, 5 H), 5.35 (m, 1 H), 5.18 (d, *J* = 2.1 Hz, 1 H), 4.93 (d, *J* = 1.8 Hz, 1 H), 4.56 (s, 2 H), 3.28 (tt, *J* = 11.4, 4.4 Hz, 1 H), 2.74 (m, 1 H), 2.50 (m, 3 H), 2.27 (m, 2 H), 2.09 (m, 4 H), 1.00 (s, 3 H); ^{13}C (100 MHz, $CDCl_3$) δ 177.0, 149.3, 142.2, 139.1, 128.5, 127.6, 127.5, 121.8, 108.2, 88.3, 78.7, 70.0, 53.7, 45.8, 41.2, 38.7, 38.6, 38.3, 37.5, 35.8, 33.1, 31.1, 28.3, 28.3, 26.8, 23.1, 19.0; HRMS (*m/z*): $[M+Na]^+$ calcd for $C_{29}H_{36}O_3Na$: 455.25567, found: 455.25541, $[2M+Na]^+$ calcd for $C_{58}H_{72}O_6Na$: 887.52211, found: 887.52285; **16:** m.p. 181-185°C; TLC (*n*-hexane/EtOAc, 2:1 v/v): R_F = 0.46; $[\alpha]_D^{22}$ (deg cm^3 g^{-1} dm^{-1}) = -109.6 (c = 0.0098 g cm^{-3} in $CHCl_3$); IR (KBr): ν_{max} 1759, 737, 696 cm^{-1}; ^1H NMR (400 MHz, $CDCl_3$) δ 7.34-7.26 (m, 5 H), 5.36 (m, 1 H), 4.57 (s, 2 H), 3.29 (tt, *J* = 11.1, 4.3 Hz, 1 H), 2.67 (m, 2 H), 2.51 (ddd, *J* = 13.3, 4.5, 2.0 Hz, 1 H), 2.39 (td, *J* = 13.2, 9.2 Hz, 1 H), 2.20 (m, 5 H), 1.60 (s, 3 H), 0.98 (s, 3 H); ^{13}C (100 MHz, $CDCl_3$) δ 177.0, 146.3, 141.9, 139.1, 128.5, 127.7, 127.5, 123.5, 121.7, 86.9, 78.6, 70.1, 52.2, 49.2, 41.9, 38.8, 38.5, 38.3, 37.0, 31.8, 31.1, 30.0, 28.9, 28.2, 24.1, 18.7, 13.2; HRMS (*m/z*): $[M+Na]^+$ calcd for $C_{29}H_{36}O_3Na$: 455.25567, found: 455.25609, $[2M+Na]^+$ calcd for $C_{58}H_{72}O_6Na$: 887.52211, found: 887.52275.

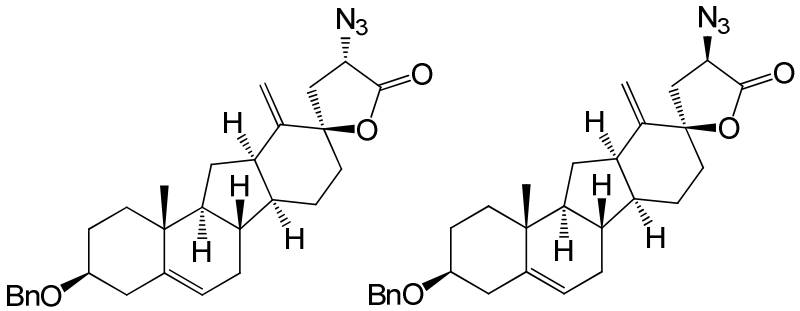

17 **18**

(-)-exo-C-*nor*-D-*homo*-azidolactone 17 and (+)-21-epi-exo-C-*nor*-D-*homo*-azidolactone 18: To a stirred solution of diisopropylamine (938 µL, 6.65 mmol) in THF (6.6 mL) was added *n*-BuLi (1.6 M solution in *n*-hexane; 4.04 mL, 6.46 mmol) at -78°C. After stirring for 40 min at this temperature a solution of the lactone **15** (1.60 g, 3.69 mmol) in THF (9 mL) was added dropwise and the temperature was risen to -30°C in the course of 1 h, kept at this temperature for 10 min and then lowered again to -78°C. Freshly prepared trisyl azide[2] (2.5 g, 8.08 mmol) in THF (13.2 mL) was added in one portion and stirring was continued for 1.5 h. The reaction mixture was quenched with glacial acetic acid (0.66 mL), warmed to room temperature and stirred there for another 30 min. After dilution with EtOAc (66 mL) and saturated aqueous NH_4Cl (33 mL), the phases were separated and the aqueous layer was extracted with EtOAc (2 x 66 mL). The combined organic extracts were washed with brine (33 mL), dried ($MgSO_4$) and the solvents were rotary evaporated. Purification by

silica gel chromatography (*n*-hexane/EtOAc, 12:1 v/v) yielded pure **17** (754 mg, 1.59 mmol, 43%) as colourless needles and the epimeric azide **18** (178 mg, 0.376 mmol, 10%) as a white solid; **17:** m.p. 144-146°C; TLC (*n*-hexane/EtOAc, 5:1 v/v): R_F = 0.46; $[\alpha]_D^{22}$ (deg cm^3 g^{-1} dm^{-1}) = -108.8 (c = 0.0100 g cm^{-3} in $CHCl_3$); IR (KBr): ν_{max} 2127, 1774, 737, 695 cm^{-1}; ^{1}H NMR (400 MHz, $CDCl_3$) δ 7.35-7.26 (m, 5 H), 5.35 (m, 1 H), 5.14 (d, *J* = 2.4 Hz, 1 H), 4.98 (d, *J* = 2.2 Hz, 1 H), 4.57 (s, 2 H), 4.29 (dd, *J* = 10.9, 8.4 Hz, 1 H), 3.28 (tt, *J* = 11.3, 4.4 Hz, 1 H), 2.77 (m, 1 H), 2.71 (dd, *J* = 12.6, 8.4 Hz, 1 H), 2.50 (ddd, *J* = 13.3, 4.6, 2.1 Hz, 1 H), 2.26 (m, 1 H), 2.10 (m, 2 H), 0.99 (s, 3 H); ^{13}C (100 MHz, $CDCl_3$) δ 173.1, 148.7, 142.1, 139.1, 128.5, 127.6, 127.5, 121.8, 108.8, 86.3, 78.6, 70.1, 57.2, 53.6, 45.9, 41.3, 38.8, 38.7, 38.5, 38.3, 37.5, 36.3, 31.0, 28.2, 26.7, 22.7, 19.0; HRMS (*m/z*): $[M+Na]^+$ calcd for $C_{29}H_{35}N_3O_3Na$: 496.25767, found: 496.25726, $[2M+Na]^+$ calcd for $C_{58}H_{70}N_6O_6Na$: 969.52401, found: 969.52406; **18:** m.p. 144-146°C; TLC (*n*-hexane/EtOAc, 5:1 v/v): R_F = 0.36; $[\alpha]_D^{22}$ (deg cm^3 g^{-1} dm^{-1}) = +50.0 (c = 0.0102 g cm^{-3} in $CHCl_3$); IR (CCl_4): ν_{max} 2113, 1780, 736, 687 cm^{-1}; ^{1}H NMR (300 MHz, $CDCl_3$) δ 7.35-7.26 (m, 5 H), 5.35 (m, 1 H), 5.31 (d, *J* = 2.3 Hz, 1 H), 4.98 (d, *J* = 2.2 Hz, 1 H), 4.57 (s, 2 H), 4.39 (t, *J* = 8.9 Hz, 1 H), 3.28 (tt, *J* = 11.2, 4.4 Hz, 1 H), 2.72 (m, 1 H), 2.62 (dd, *J* = 13.1, 8.8 Hz, 1 H), 2.50 (ddd, *J* = 13.2, 4.6, 2.2 Hz, 1 H), 2.27 (m, 2 H), 2.10 (m, 3 H), 1.00 (s, 3 H); ^{13}C (100 MHz, $CDCl_3$) δ 172.4, 149.1, 142.3, 139.1, 128.5, 127.7, 127.6, 121.8, 108.7, 86.4, 78.7, 70.1, 57.6, 53.7, 45.2, 41.3, 40.0, 39.2, 38.7, 38.3, 37.5, 35.4, 31.2, 28.3, 27.1, 23.6, 19.1; HRMS (*m/z*): $[M+Na]^+$ calcd for $C_{29}H_{35}N_3O_3Na$: 496.25732, found: 496.25726, $[2M+Na]^+$ calcd for $C_{58}H_{70}N_6O_6Na$: 969.52449, found: 969.52454.

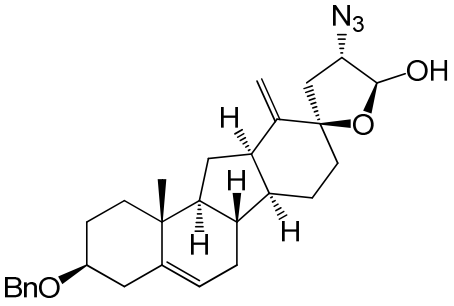

19

(-)-exo-C-*nor*-D-*homo*-azidolactol 19: To a stirred solution of azidolactone **17** (377 mg, 0.791 mmol) in THF (6.3 mL) at -78°C was added diisobutylaluminiumhydride (1.2 M in toluene; 3.32 mL, 3.98 mmol) dropwise and stirring was continued at this temperature for 1 h and thereafter at -65°C for 1 h. The reaction mixture was quenched with MeOH (1.60 mL), diluted with CH_2Cl_2 (42 mL) and Rochelle-salt (10 wt% in H_2O) (42 mL) and warmed to room temperature. After stirring for 1 h the phases were separated and the aqueous layer was extracted with CH_2Cl_2 (2 x 42 mL). The combined organic extracts were dried

($MgSO_4$) and the solvents were rotary evaporated. Purification by silica gel chromatography (*n*-hexane/EtOAc, 5:1 v/v) yielded a mixture of the two epimers of **19** (333 mg, 0.700 mmol, 88%) as a colourless oil: TLC (*n*-hexane/EtOAc, 3:1 v/v): R_F = 0.46; $[\alpha]_D^{22}$ (deg cm^3 g^{-1} dm^{-1}) = -64.0 (c = 0.0100 g cm^{-3} in $CHCl_3$); IR (CCl_4): ν_{max} 2105, 734, 697 cm^{-1}; HRMS (*m/z*): $[M+Na]^+$ calcd for $C_{29}H_{37}N_3O_3Na$: 498.27271, found: 498.27272, $[2M+Na]^+$ calcd for $C_{58}H_{74}N_6O_6Na$: 973.55621, found: 973.55694.

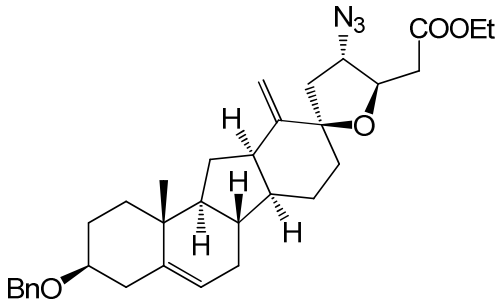

20

(-)-furane 20: Finely ground bariumhydroxide octahydrate (336 mg, 1.06 mmol) was activated in a constant stream of dry argon at 140°C stirring for 2 h and then, after breaking the big stones, for additional 20 min. The powder was allowed to cool to room temperature and after adding a solution of triethyl phosphonoacetate (537 mg, 2.40 mmol) in THF (7.10 mL), the suspension was warmed to 60°C under vigorous stirring for 45 min and thereafter sonicated for 10 min at room temperature. A solution of lactol **19** (126 mg, 0.266 mmol) in THF:H_2O (7.10 mL, 40:1) was introduced in one portion and after sonication for 10 min, the reaction mixture was brought to reflux and THF was evaporated slowly (by inserting a fine cannula through the septum, oil bath temperature 80°C) over the course of 12 h. The remaining viscous orange oil was dissolved in EtOAc (30 mL), washed with saturated aqueous NH_4Cl (13 mL) and the phases were separated. The aqueous phase was reextracted with EtOAc (13 mL) and the combined organic phases were washed with brine (13 mL), dried ($MgSO_4$) and the solvent was rotary evaporated. Purification by silica gel chromatography (*n*-hexane/EtOAc, 7:1 v/v) yielded pure **20** (80.3 mg, 0.147 mmol, 55%) as a colourless oil; TLC (*n*-hexane/EtOAc, 6:1 v/v): R_F = 0.43; $[\alpha]_D^{22}$ (deg cm^3 g^{-1} dm^{-1}) = -15 (c = 0.0100 g cm^{-3} in $CHCl_3$); IR (CCl_4): ν_{max} 2103, 1736, 735, 697 cm^{-1}; ^{1}H NMR (400 MHz, $CDCl_3$) δ 7.35 (m, 2 H, ortho-H Bn), 7.33 (m, 2 H, meta-H Bn), 7.28 (m, 1 H, para-H Bn), 5.35 (m, 1 H, H-6), 5.28 (m, 1 H, H-18), 4.85 (m, 1 H, H-18), 4.56 (s, 2 H, benzyl. H), 4.18 (m, 1 H, H-22), 4.17 (q, *J* = 7.1 Hz, 2 H, CH_2 Et), 3.82 (q, *J* = 7.2 Hz, 1 H, H-21), 3.28 (tt, *J* = 11.1, 4.5 Hz, 1 H, H-3), 2.68 (m, 1 H, H-12), 2.65 (m, 2 H, H-23), 2.49 (ddd, *J* = 13.1, 4.6, 2.0 Hz, 1 H, H-4), 2.31 (m, 1 H, H-20), 2.25

(m, 1 H, H-4), 2.11 (m, 1 H, H-7), 1.99 (m, 1 H, H-20), 1.95 (m, 1 H, H-2), 1.81 (m, 1 H, H-11), 1.77 (m, 1 H, H-16), 1.76 (m, 1 H, H-1), 1.74 (m, 1 H, H-16), 1.72 (m, 1 H, H-11), 1.65 (m, 1 H, H-15), 1.60 (m, 2 H, H-7, H-14), 1.56 (m, 1 H, H-2), 1.51 (m, 1 H, H-15), 1.36 (m, 1 H, H-8), 1.33 (m, 1 H, H-9), 1.28 (t, *J* = 7.1 Hz, 3 H, CH_3 Et), 1.12 (dt, *J* = 13.6, 3.6 Hz, 1 H, H-1), 0.98 (s, 3 H, H-19); ^{13}C (75 MHz, $CDCl_3$) δ 170.5 (C-24), 152.9 (C-13), 142.2 (C-5), 139.2 (ipso-C Bn), 128.5 (meta-C Bn), 127.7 (ortho-C Bn), 127.5 (para-C Bn), 122.0 (C-6), 107.4 (C-18), 85.6 (C-17), 78.8 (C-3), 78.0 (C-22), 70.1 (benzyl. C Bn), 64.1 (C-21), 60.9 (CH_2 Et), 53.7 (C-9), 46.1 (C-14), 42.1 (C-20), 41.9 (C-12), 38.8 (C-23), 38.7 (C-4), 38.4 (C-8), 38.3 (C-1), 37.5 (C-10), 36.7 (C-16), 31.1 (C-7), 28.3 (C-2), 26.8 (C-11), 23.7 (C-15), 19.1 (C-19), 14.3 (CH_3 Et); HRMS (*m/z*): $[M+Na]^+$ calcd for $C_{33}H_{43}N_3O_4Na$: 568.31567, found: 568.31524, $[2M+Na]^+$ calcd for $C_{66}H_{86}N_6O_8Na$: 1113.63698, found: 1113.63753.

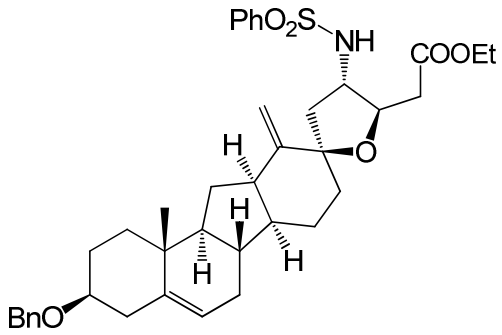

28

(+)-sulfonamide 28: A solution of the azide **20** (54.0 mg, 99.0 µmol) in THF (3.7 mL) was treated sequentially with water (18 µL, 100 mmol) and triphenylphosphine (28.8 mg, 110.0 µmol) under stirring at room temperature. The solution was warmed to 50°C and kept there for 24 h. After allowing to cool to room temperature, all volatiles were evaporated and the crude amine was azeotropically dried with THF (5 mL) two times. After drying under 0.01 mbar pressure for several hours, the crude amine was dissolved in CH_2Cl_2 (3.1 mL) and cooled to 0°C. Et_3N (55 µL, 343 µmol) and benzenesulfonyl chloride (33 µL, 257 µmol) were added sequentially, and the mixture was heated to reflux for 5 h. The solution was cooled to room temperature, diluted with CH_2Cl_2 (10 mL) and washed with saturated aqueous NH_4Cl (5 mL). The phases were separated and the aqueous layer was extracted with CH_2Cl_2 (5 mL). The combined organic extracts were washed with brine (5 mL), dried ($MgSO_4$) and the solvent was rotary evaporated. Purification by silica gel chromatography (*n*-hexane/EtOAc, 3:1 v/v) yielded pure **28** (36 mg, 46 µmol, 78%) as a colourless oil; TLC (*n*-hexane/EtOAc, 3:1 v/v): R_F = 0.25; $[\alpha]_D^{26}$ (deg cm^3 g^{-1} dm^{-1}) = + 2.0 (c = 0.0134 g cm^{-3} in $CHCl_3$); IR (CCl_4): ν_{max} 2924, 2359, 2340, 1632, 1453, 1384, 1164, 1093, 689 cm^{-1}; ^1H

NMR (400 MHz, $CDCl_3$) δ7.86 (d, *J* = 6.9 Hz, 2 H), 7.61 (t, *J* = 7.2 Hz, 1 H), 7.51 (t, *J* = 7.2 Hz, 2 H), δ 7.35 (m, 2 H), 7.33 (m, 2 H), 7.28 (m, 1 H), 5.39 (d, *J* = 5.4 Hz, 1 H), 5.34 (m, 1 H), 5.16 (s, 1 H), 4.81 (s, 1 H), 4.56 (s, 2 H), 4.14 (m, 1 H), 4.08 (q, *J* = 7.1 Hz, 2 H), 3.40 (q, *J* = 7.2 Hz, 1 H), 3.28 (tt, *J* = 11.1, 4.5 Hz, 1 H), 2.60 (m, 1 H), 2.65 (m, 2 H), 2.49 (ddd, *J* = 13.1, 4.6, 2.0 Hz, 1 H), 2.31 (m, 1 H), 2.25 (m, 1 H), 2.11 (m, 1 H), 1.99 (m, 1 H), 1.95 (m, 1 H), 1.81 (m, 1 H), 1.77 (m, 1 H), 1.76 (m, 1 H), 1.74 (m, 1 H), 1.72 (m, 1 H), 1.65 (m, 1 H), 1.60 (m, 2 H, H-7), 1.56 (m, 1 H), 1.51 (m, 1 H), 1.36 (m, 1 H), 1.33 (m, 1 H), 1.28 (t, *J* = 7.1 Hz, 3 H), 1.12 (dt, *J* = 13.6, 3.6 Hz, 1 H), 0.96 (s, 3 H); ^{13}C NMR (75 MHz, $CDCl_3$) δ 171.7, 152.9, 139.2, 135.2, 133.2, 129.3, 128.5, 128.1, 127.7, 127.6, 122.0, 107.5, 85.4, 78.8, 78.0, 70.1, 61.1, 57.8, 53.7, 46.0, 44.2, 41.8, 38.7, 38.4, 38.3, 37.6, 37.1, 31.1, 28.3, 26.9, 23.6, 19.1, 14.3. HRMS (*m/z*): $[M+Na]^+$ calcd for $C_{39}H_{49}NO_6SNa$: 682.31783, found: 682.31728; $[2M+Na]^+$ calcd for $C_{78}H_{98}NO_{12}S_2$: 1341.64589, found: 1341.64534.

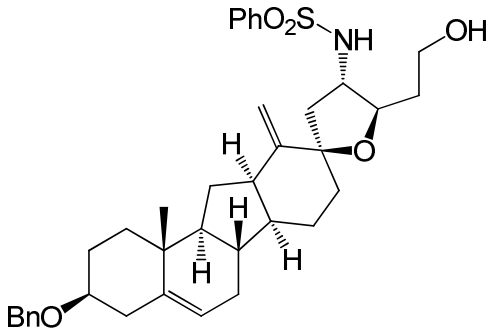

29

(+)-alcohol 29: To a stirred solution of the sulfonamide **28** (50 mg, 76 µmol) in THF (7 mL) was added diisobutylaluminiumhydrid (1.2 M in toluene, 330 µL, 312.8 µmol) dropwise at -78°C and stirring was continued at this temperature for 1 h and thereafter at -40°C for 2 h. The reaction mixture was quenched with MeOH (31 µL), diluted with CH_2Cl_2 (20 mL) and Rochelle-salt (10 wt% in H_2O, 20 mL) and warmed to room temperature. After stirring for 1 h the phases were separated and the aqueous layer was extracted with CH_2Cl_2 (2 x 20 mL). The combined organic extracts were dried ($MgSO_4$) and the solvents were rotary evaporated. Purification by silica gel chromatography (*n*-hexane/EtOAc, 2:1 v/v) yielded pure **29** (45.5 mg, 74 µmol, 97%) as a colourless film; TLC (*n*-hexane/EtOAc, 1:1 v/v): R_F = 0.27; $[\alpha]_D^{22}$ (deg cm^3 g^{-1} dm^{-1}) = + 3.8 (c = 0.0099 g cm^{-3} in $CHCl_3$); IR (CCl_4): ν_{max} 3440, 2929, 2102, 1631, 1447, 1343, 1162, 1093, 788, 756 cm^{-1}; ^1H NMR (400 MHz, $CDCl_3$): δ 7.86 (d, *J* = 6.9 Hz, 2 H), 7.59 (t, *J* = 7.2 Hz, 1 H), 7.51 (t, *J* = 7.2 Hz, 2 H), δ 7.34 (m, 2 H), 7.33 (m, 2 H), 7.26 (m, 1 H), 5.49 (m, 1 H), 5.32 (m, 1 H), 5.19 (s, 1 H), 4.81 (s, 1 H), 4.56 (s, 2 H), 4.08 (q, *J* = 7.1 Hz, 2 H), 3.78 (q, *J* = 3 Hz , 1H), 3.72 (m, 2 H), 3.45 (q, *J* =

7.2 Hz, 1 H), 3.27 (tt, *J* = 11.1, 4.5 Hz, 1 H), 2.65 (m, 2 H), 2.60 (m, 1 H), 2.49 (ddd, *J* = 13.1, 4.6, 2.0 Hz, 1 H), 2.31 (m, 1 H), 2.25 (m, 1 H), 2.11 (m, 1 H), 1.99 (m, 1 H), 1.95 (m, 1 H), 1.81 (m, 1 H), 1.77 (m, 1 H), 1.76 (m, 1 H), 1.74 (m, 1 H), 1.72 (m, 1 H), 1.65 (m, 1 H), 1.60 (m, 2 H, H-7), 1.56 (m, 1 H), 1.51 (m, 1 H), 1.36 (m, 1 H), 1.33 (m, 1 H), 1.12 (dt, *J* = 13.6, 3.6 Hz, 1 H), 0.96 (s, 3 H); ^{13}C NMR (100 MHz, $CDCl_3$) δ 152.9, 142.2, 140.3, 135.2, 133.2, 129.4, 128.5, 128.0, 127.7, 127.6, 122.0 , 107.8 , 85.5 , 81.0, 78.8, 70.1, 67.8, 61.1, 57.6, 53.7, 46.1, 43.8, 41.7, 38.7, 38.4, 37.5, 37.4, 35.0, 31.1, 28.3, 26.9, 23.5, 19.1. HRMS (*m/z*): $[M+Na]^+$ calcd for $C_{37}H_{47}NO_5Na$: 640.30726, found: 640.30703.

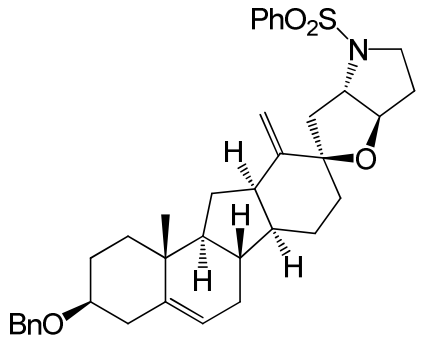

30

(+)-Pyrrolidine 30. To a solution of alcohol **29** (20 mg, 32 µmol) in toluene (1.6 mL) were added in one portion tributylphosphine (34.0 µL, 134 µmol) and azodicarboxylic dipiperidide (31.4 mg, 123 µmol) at 0°C. After warming to room temperature stirring was continued for another 24 h. The reaction mixture was rotary evaporated and the crude product was purified by silica gel chromatography (*n*-hexane/EtOAc, 6:1 v/v) to yield pure **30** (15.4 mg, 25.9 µmol, 81%) as colourless plates; TLC (*n*-hexane/EtOAc, 3:1 v/v): R_F = 0.36; $[\alpha]_D^{24}$ (deg cm^3 g^{-1} dm^{-1}) = + 50.4 (c = 0.0099 g cm^{-3} in $CHCl_3$); IR (KBr): ν_{max} 2925, 2884, 1718, 1446, 1347, 1175, 1092, 905, 798, 694, 598 cm^{-1}; ^{1}H NMR (400 MHz, $CDCl_3$): δ 7.78 (d, *J* = 6.9 Hz, 2 H, ortho-H Bs), 7.64 (t, *J* = 7.2 Hz, 1 H, para-H Bs), 7.56 (t, *J* = 7.2 Hz, 2 H, meta-H Bs), 7.35 (m, 2 H, ortho-H Bn), 7.32 (m, 2 H, meta-H Bn), 7.28 (m, 1 H, para-H Bn), 5.34 (m, 1 H, H-6), 5.20 (s, 1 H, H-18), 4.89 (s, 1 H, H-18), 4.57 (s, 2 H, benzyl. H), 4.09 (m, 1 H, H-22), 3.85 (q, *J* = 9 Hz, 1 H, H-23), 3.55 (t, *J* = 9 Hz, 1 H, H-23), 3.28 (tt, *J* = 11.1, 4.5 Hz, 1 H, H-3), 2.92 (m, 1H, H-21), 2.76 (m, 1 H, H-12), 2.49 (ddd, *J* = 13.1, 4.6, 2.0 Hz, 1 H, H-4), 2.34 (m, 1 H, H-19), 2.25 (m, 1 H, H-4), 2.08 (m, 1 H, H-7), 2.06 (m, 1 H, H-23), 1.95 (m, 1 H, H-2), 1.93 (m, 1 H, H-19), 1.81 (m, 1 H, H-11), 1.77 (m, 1 H, H-16), 1.76 (m, 1 H, H-1), 1.74 (m, 1 H, H-16), 1.72 (m, 1 H, H-11), 1.68 (m, 1 H, H-22), 1.65 (m, 1 H, H-15), 1.60 (m, 2 H, H-7, H-14), 1.58 (m, 1 H, H-2), 1.51 (m, 1 H, H-15), 1.36 (m, 1 H, H-8), 1.33 (m, 1 H, H-9), 1.12 (dt, *J* = 13.6, 3.6 Hz, 1 H, H-1), 0.96 (s, 3 H, H-19); ^{13}C NMR (100 MHz, $CDCl_3$): δ 154.9 (C-13), 142.2 (C-5), 139.2 (ipso-C Bn), 135.2

(ipso-C Bs), 133.2 (para-C Bs), 129.3 (meta-C Bs), 128.1 (ortho-C Bs), 128.5 (meta-C Bn), 127.7 (ortho-C Bn), 127.6 (para-C Bn), 122.0 (C-6), 108.5 (C-18), 96.6 (C-17), 82.9 (C-22), 78.8 (C-3), 70.1 (benzyl. C), 66.3 (C-21), 53.6 (C-9), 53.6 (C-23), 46.5 (C-14), 41.0 (C-12), 40.2 (C-20), 38.8 (C-4), 38.3 (C-19), 38.2 (C-8), 37.7 (C-1), 37.5 (C-10), 31.0 (C-16), 31.0 (C-7), 28.3 (C-2), 26.8 (C-13) ,26.4 (C-11), 22.7 (C-15), 19.2 (C-19); HRMS (*m/z*): $[M+Na]^+$ calcd for $C_{37}H_{45}NO_4SNa$: 662.29670, found: 622.29614; $[2M+Na]^+$ calcd for $C_{74}H_{90}N_2O_8S_2Na$: 1221.60163, found: 1221.60240.

Tetrakis(acetonitrile)copper(I) hexafluorophosphate: To a good stirred suspension of CuO_2 (32.0 g, 224 mmol) in acetonitrile (640 mL) was added hexafluorophosphoric acid (aq. 60-65%, 40 mL, 450 mmol) in portions and after complete addition the resulting green solution was stirred for additional 3 min. The solution was filtered still hot with a Gooch (G3 pore size), washed with a little amount of CH_3CN and stored at -20°C for 15 h. The resulting crystals were collected, washed with Et_2O (3 x 20 mL), dissolved in CH_3CN (900 mL) and the solution was filtered (Gooch G3 pore size). After adding Et_2O (800 mL), the solution was stored at -20°C for 15 h. The resulting crystals were collected, washed with Et_2O (3 x 20 mL) and dried under 0.1 mbar pressure for 1 h to yield tetrakis(acetonitrile)copper(I) hexafluorophosphate (138.4 g, 371.3 mmol, 83%) as a white powder.

References

[1] James, L.F.; Panter, K.E.; Gaffield, W.; Molyneux, R.J.; Biomedical Applications of Poisonous Plant Research, *J. Agric. Food Chem*. **2004**, *52*: 3211–3230.

[2] Keeler, R.F.; Toxic and teratogenic alkaloids of western range plants, *J. Agric. Food Chem.* **1969**, *17*: 473–482.

[3] Keeler, R.F.; Teratogenic compounds of Veratrum californicum Durand-IV, *Phytochemistry* **1968**, *7*: 303–306.

[4] Keeler, R.F.; Binns, W.; Teratogenic Compounds of Veratrum californicum - comparison of cyclopian effects of steroidal alkaloids from the plant and structurally related compounds from other sources, *Teratology* **1968**, *1*: 5–10.

[5] Nüsslein-Volhard, C.; Wieschaus, E.; Mutations affecting segment number and polarity in *Drosophila, Nature* **1980***, 287*: 795-801.

[6] Chiang, C.; Litingtung, Y.; Lee, E.; Young, K.E.; Cordon, J.L.; Westphal, H.; Beachy, P.A.; Cyclopia and defective axial patterning in mice lacking *Sonic hedgehog* gene function, *Nature* **1996**, *383*: 407-413.

[7] Incardona, J.P.; Gaffield, W.; Kapur, R.P.; Roelink, H.; The teratogenic Veratrum alkaloid cyclopamine inhibits Sonic hedgehog signal transduction, *Development* **1998**, *125*: 3553-3562 .

[8] Riddle, R.D.; Johnson, R.L.; Laufer, E.; Tabin, C.; Sonic hedgehog mediates the polarizing activity of the ZPA, *Cell* **1993**, *75*: 1401-1416.

[9] Varjosalo, M.; Taipale, J.; Hedgehog: functions and mechanisms, *Genes Dev.* **2008**, *22*: 2454–2472.

[10] Cooker, M.K.; Porter, J.A.; Young, K.E.; Beachy, P.A.; Teratogen-mediated inhibition of target tissue response to Shh signaling, *Science* **1998**, *280*: 1603-1607.

[11] Lee, J.J.; Ekker, S.C.; von Kessler, D.P.; Porter, J.A.; Sun, B.I.; Beachy, P.A.; Autoproteolysis in hedgehog protein biogenesis, *Science* **1994**, *266*: 1528-1537.

[12] Bumcrot, D.A.; Ritsuko, T.; McMahon, A.P.; Proteolytic processing yields two secreted forms of Sonic hedgehog, *Mol. Cell. Biol.* **1995**, *15*: 2294-2303.

[13] Porter, J.A.; Young, K.E.; Beachy, P.A.; Cholesterol modification of Hedgehog signaling proteins in animal development, *Science* **1996**, *274*: 255-259.

[14] Chamoun, Z.; Mann, R.K.; Nellen, D.; von Kessler, D.P.; Belotto, M.; Beachy, P.A.; Basler, K.; Skinny hedgehog, an acetyltransferase required for plamitoylation and activity of the hedgehog signal, *Science* **2001**, *293*: 2080-2084.

[15] Burke, R.; Nellen, D.; Bellotto, M.; Hafen, E.; Senti, K.A.; Dickson, B.J.; Basler, K.; Dispatched, a novel sterol-sensing domain protein dedicated to the release of cholesterol-modified hedgehog from signaling cells, *Cell* **1999**, *99*: 803-815.

[16] Ma, Y.; Erker, A.; Gong, R.; Yao, S.; Taipele, J.; Basler, K.; Beachy, P.A.; Hedgehog-mediated patterning of the mammalian embryo requires transporter-like function of dispatched, *Cell,* **2002**, *111*: 63-75.

[17] Zhu, A.J.; Scott, M.P.; Incredible journey: How do developmental signals travel through tissue?, *Genes & Dev*. **2004**, *18*: 2985-2997.

[18] Goetz, J.A.; Singh, S.; Suber, L.M.; F. Kull, F.J.; Robbins, D.J.; A Highly Conserved Amino-terminal Region of Sonic Hedgehog Is Required for the Formation of Its Freely Diffusible Multimeric Form, *J. Biol. Chem.* **2006**, *281*: 4087-4093.

[19] Eaton, S.; Multiple roles for lipids in the Hedgehog signalling pathway, *Nature Reviews* 2008, *9*: 437-445.

[20] Chamberlain, C.E; Jeong, J.; Guo, C.; Allen, B.L.; McMahon, A.P.; Notochord-derived Shh concentrates in close association with the apically positioned basal body in neural target cells and forms a dynamic gradient during neural patterning, *Development* **2008**, *135*: 1097-1106.

[21] Zhang, C.; Williams, E.H.; Guo, Y.; Lum, L.; Beachy, P.A.; Extensive phosphorylation of Smoothened in Hedgehog pathway activation, *Proc. Natl. Acad. Sci.* **2004**, *101*: 17900-17907.

[22] Chen, J.K.; Taipale, J.; Young, K.E.; Maiti, T.; and Beachy, P.A.; Small molecule modulation of Smoothened activity, *Proc. Natl. Acad. Sci.* **2002**, *99*: 14071–14076.

[23] Taipale, J.; Chen, J. K.; Cooper, M. K.; Wang, B.; Mann, R. K.; Milenkovic, L.; Scott, M. P.; Beachy, P.A.; Effects of oncogenic mutations in *Smoothened* and *Patched* can be reversed by cyclopamine, *Nature* **2000**, *406*: 1005–1009.

[24] Mahindroo, N.; Punchihewa, C.; Fujii, N.; Hedgehog-Gli signaling pathway inhibitors as anticancer agents, *J. Med. Chem.* **2009**, *52*: 3830-3845.

[25] Ayers, K.L.; Thèrond, P.P.; Evaluating Smoothened as a G-protein-coupled receptor for Hedgehog signaling, *Trends in Cell Biology*, **2010**, *20*: 287-298.

[26] Chen, J.K.; Taipale, J.; Cooper, M.K.; Beachy, P.A.; Inhibition of Hedgehog signaling by direct binding of cyclopamine to Smoothened, *Genes & Dev.* **2002**, *16*: 2743-2748.

[27] Ingham, P.W.; McMahon, A.P.; Hedgehog signaling in animal development: paradigms and principles, Genes & Dev. **2001**, *15*: 3059–3087.

[28] Scales, S.J.; de Sauvage, F.J.; Mechanism of Hedgehog pathway activation in cancer and implications for therapy, *Trends Pharmacol. Sci.*, **2009**, *30*: 303-312.

[29] Christensen, S.T.; Ott, C.M.; A ciliary signaling switch, *Science* **2007**, *317*: 330-331.

[30] Pasca di Magliano, M.; Hebrock, M.; Hedgehog signalling in cancer formation and maintenance, *Nature Reviews* **2003**, *3*: 903-911.

[31] Rubin, L.L.; de Sauvage, F.J.; Targeting the Hedgehog pathway in cancer, *Nat. Rev. Drug Discov.* **2006**, *5*: 1026-1033.

[32] http://www.clinicaltrials.gov/ct2/results?term)GDC-0449&show_flds=Y (October 7, 2010).

[33] Wilson, S.R.; Strand, M.F.; Krapp, A.; Rise, F.; Petersen, D.; Krauss, S.; Hedgehog antagonist cyclopamine isomerizes to less potent forms when acidified, *J. Pharm. Biomed. Anal.* **2010**, *52*: 707–713.

[34] Heretsch, P.; Tzagkaroulaki, L.; Giannis, A.; Cyclopamine and Hedgehog Signaling: Chemistry, Biology, Medical Perspectives, *Angew. Chem. Int. Ed.* **2010**, *49*: 2–12.

[35] Giannis, A.; Heretsch, P.; Sarli, V.; Stößel, A.; Synthesis of Cyclopamine Using a Biomimetic and Diastereoselective Approach, *Angew. Chem. Int. Ed.* **2009**, *48*: 1-5.

[36] Schönecker, B.; Zheldakova, T.; Liu, Y.; Kötteritzsch, M.; Günther, W.; Görls, H.; Biomimetic Hydroxylation of Nonactivated CH_2 Groups with Copper Complexes and Molecular Oxygen, *Angew. Chem. Int. Ed.* **2003**, *42*: 3240–3244.

[37] Hirschmann, R.; Snoddy Jr., C.S.; Wendler, N.L.; Configuration at C_{12} of 12-hydroxylated sapogenins. Rearrangement of the steroid C/D ring, *J. Am. Chem. Soc.* **1952**, *74*: 2693–2694.

[38] Evans, D.A.; Britton, T.C.; Electrophilic Azide Transfer to Chiral Enolates. A General Approach to the Asymmetric Synthesis of a-Amino Acids, *J. Am. Chem. Soc.* **1987**, *109*: 6881–6883.

[39] Sinisterra, J.V.; Marinas, J.M.; Riquelme, F.; Arias, M.S.; $Ba(OH)_2$ as catalyst in organic reactions – Part XIX – Structure and catalytic activity relationship in the in the Ad_N of several ylids to CH=O group, catalyzed by activated Barium Hydroxide catalyst, *Tetrahedron* **1988**, *44*: 1431-1440.

[40] Johnson, C.R.; Tait, B.D.; A Cerium(III) Modification of the Peterson Reaction: Methylenation of Readily Enolizable Carbonyl Compounds, *J. Org. Chem.* **1987**, *52*: 281–283.

[41] Vaultier, M.; Knouzi, N.; Carrie, R.; Reduction d'azides en amines primaries par une method generale utilisant la reaction de Staudinger, *Tetrahedron Letters* **1983**, *24*: 763-764.

[42] Moran, W.J.; Goodenough, K.M.; Raubo, P.; Harrity, J.P.A.; A Concise Asymmetric Route to *Nuphar* Alkaloids. A Formal Synthesis of (-)-Deoxynupharidine, *Org. Lett.* **2003**, *5*: 3427–3429.

[43] Deleris, G.; Kowalski, J.; Dunogues, J.; Calas, R.; *N*-sulfinyl benzene sulfonamide: un nouvel enophile offrant de larges possibilities synthetiques, *Tetrahedron Letters* **1977**, *48*: 4211-4214.

[44] Paquette, L.A.; Lin, H.-S.; Gunn, B.P.; Coghlan, M.J.; Sequential Annulation Approach to Sterpuric Acid and Sterpurene-3,12,14-triol, Metabolites of the Silver Leaf Fungus *Stereum purpureum*, *J. Am. Chem. Soc.* **1988**, *110*: 5818–5826.

[45] Masamune, T.; Takasugi, M.; Murai, A.; Kobayashi K., *C*-Nor-*D*-homosteroids and related alkaloids. IX. Synthesis of Jervine and Related Alkaloids, *J. Am. Chem. Soc*. **1967**, *89*: 4521-4523.

[46] Winkler, J.D.; Isaacs, A.; Holderbaum, L.; Tatard, V.; Dahmane, N.; Design and Synthesis of Inhibitors of Hedgehog Signaling Based on the Alkaloid Cyclopamine, *Org. Lett*. **2009**, *11*: 2824–2827.

[47] Oatis Jr., J.E.; Brunsfeld, P.; Rushing, J.W.; Moeller, P.D.; Bearden, D.W.; Gallien, T.N.; Cooper IV, G., Isolation, purification, and full NMR assignments of cyclopamine from *Veratrum californicum*, *Chem. Cent. J.* **2008**, *2:* 12.

[48] Tremblay, M.R.; Nevalainen, M.; Nair, S.J.; Porter, J.R.; Castro, A.C.; Behnke, M.L.; Yu, L.-C.; Hagel, M.; White, K.; Faia, K.; Grenier, L.; Campbell, M.J.; Cushing, J.; Woodward, C.N.; Hoyt, J.; Foley, M.A.; Read, M.A.; Sydor, J.R.; Tong, J.K.; Palombella, V.J.; McGovern, K.; Adams, J.; Semisynthetic Cyclopamine Analogues as Potent and Orally Bioavailable Hedgehog Pathway Antagonists, *J. Med. Chem.* **2008**, *51*: 6646–6649.

[49] Zhang, J.; Garrossian, M.; Gardner, D.; Garrossian, A.; Chang, Y.-T.; Kim, Y.K.; Chang, C.-W.T.; Synthesis and anticancer activity studies of cyclopamine derivatives, *Bioorg. Med. Chem. Lett.* **2008**, *18*: 1359–1363.

[50] Büttner, A.; Heretsch, P.; Giannis, A.; Exo-cyclopamine – a new stable and highly potent inhibitor of the hedgehog signaling pathway, *Angew.Chem.* Submitted manuscript

[51] Poon, K.W.C.; Dudley, G.B.; Mix-and-Heat Benzylation of Alcohols Using a Bench-Stable Pyridinium Salt, *J. Org. Chem.* **2006**, *71*: 3923–3927.

[52] Imamoto, T.; Kusumoto, T.; Tawarayama, Y.; Sugiura, Y.; Takeshi, M.; Hatanaka, M.; Yokoyama, M.; *J. Org. Chem.* **1984**, *49*: 3904–3912.

[53] Hansen, T.M.; Florence, G.J.; Lugo-Mas, P.; Chen, J.; Abrams, J.N.; Forsyth, C.J.; Highly chemoselective oxidation of 1,5-diols to δ-lactones with TEMPO/BAIB, *Tetrahedron Letters* **2003**, *44*: 57–59.

[54] Moran, W.J.; Goodenough, K.M.; Raubo, P.; Harrity, J.P.A.; A Concise Asymmetric Route to *Nuphar* Alkaloids. A Formal Synthesis of (-)-Deoxynupharidine, *Org. Lett.* **2003**, *5*: 3427–3429.

[55] Uchida, H.; Nishida, A.; Nakagawa, M.; An Efficient Access to the Optically Active Manzamine Tetracyclic Ring System, *Tetrahedron Lett.* **1999**, *40*: 113–116.

Part B - Enantioselective synthesis of (S)-norcoclaurine

Part of this work has been published as

Alessandra Bonamore, Irene Rovardi, Francesco Gasparrini, Paola Baiocco, Marco Barba, Carmela Molinaro, Bruno Botta, Alberto Boffi and Alberto Macone, An enzymatic, stereoselective synthesis of (S)-norcoclaurine, Green Chem., ***2010****, 12: 1623-1627*

Chapter 6

Benzylisoquinoline alkaloids

6.1. Biosynthetic pathway and pharmacological relevance of benzylisoquinoline alkaloids

The benzylisoquinoline alkaloids (BIAs) are a large group of nitrogen-containing secondary metabolites consisting of more than 2500 defined compounds with widely divergent structural scaffolds and pharmacological properties.[1] They are mainly produced by several related plant families including *Papaveraceae, Funariaceae, Menispermaceae, Ranunculaceae and Berberidaceae* and they are not essential for normal growth and development but appear to function in the defense of plant. The interest of medicine in BIAs activity is of long date because these natural products exhibit biological properties of high value. The antimicrobial agents sanguinarine and berberine have long been used for their pharmacological activities, as well as the muscle relaxant (+)-tubocurarine and the vasodilator papaverine (scheme 6.1). The opiates morphine and codeine, produced exclusively by Opium poppy (*Papaver somniferum*), have been exploited for thousands of years for their powerful analgesic properties and are currently in clinical use. Other interesting examples are noscapine,[2] structurally similar to the antineoplastic podophyllotoxin, which has been used originally as an antitussive drug and recently for cancer treatment as anti-mitotic agent and the bis-benzylisoquinoline compounds like fangchinoline,[3] which proved to have an anti-hyperglycemic effect, potentially useful in diabetes treatment.

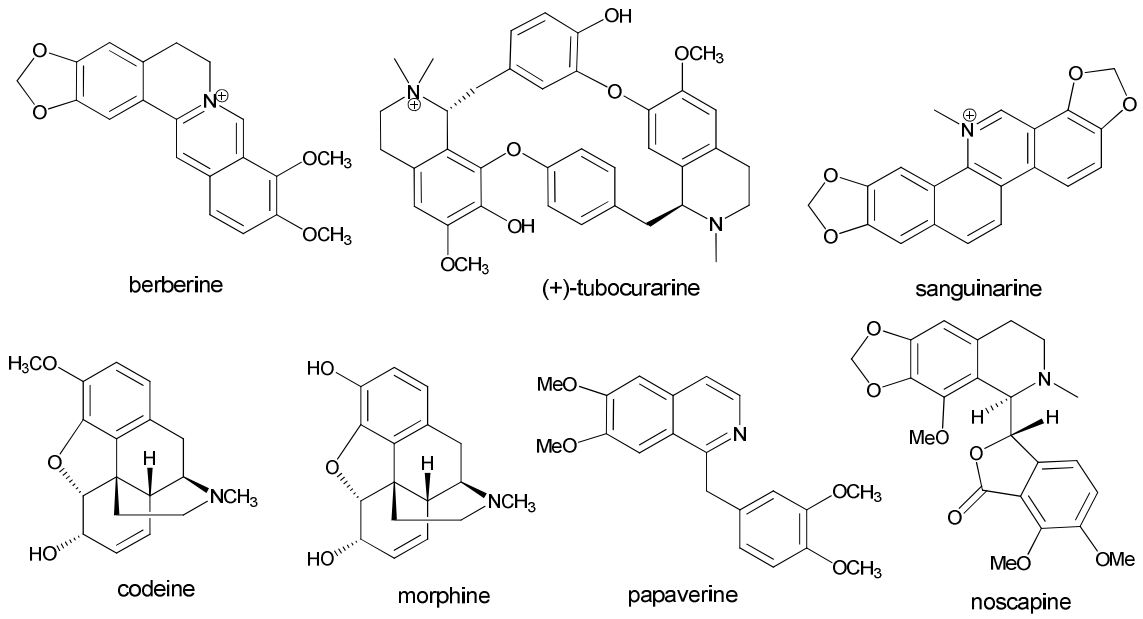

Scheme 6.1 Benzylisoquinoline alkaloids of clinical interest.

Research on BIAs biosynthesis has focused mainly on two model systems as the yellow meadow rue (*Thalictrum flavum*) from *Ranunculaceae* and *Papaver somniferum* from *Papaveraceae*, leading to unravel the complex metabolic networks of BIAs pathway.[4]

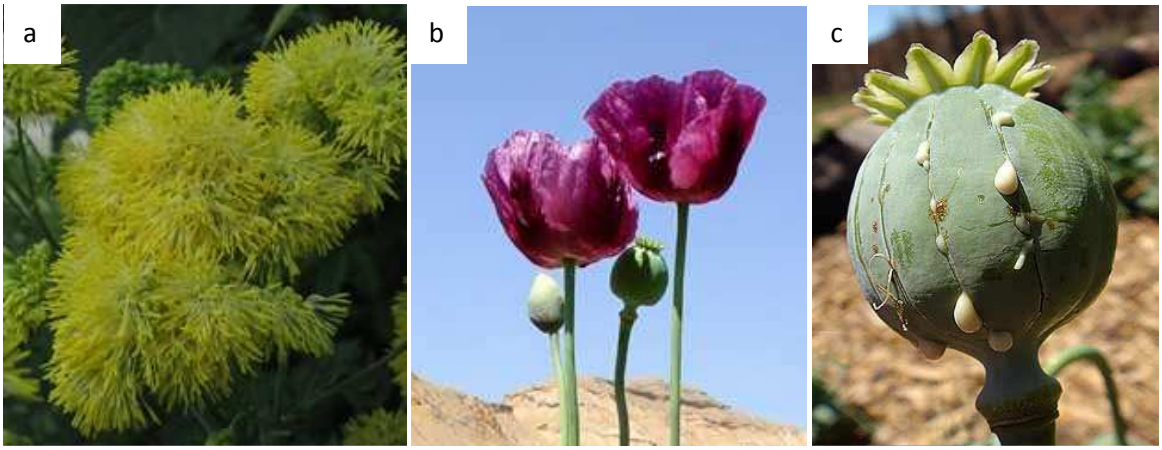

Figure 6.1 a) *Thalictrum flavum, Papaver Somniferum* b) flower and c) capsule.

Despite their wide structural diversity, all BIAs share a common biosynthetic origin beginning with the condensation of 4-hydroxyphenylacetaldehyde (4-HPAA) and dopamine catalyzed by the Pictet-Spenglerase (S)-norcoclaurine synthase (SNCS) yielding (S)-norcoclaurine (SNC) (Figure 6.2) (see chapter 7.1), which is *O*-methylated by (S)-norcoclaurine 6-*O*-methyltransferase (6OMT), and subsequently *N*-methylated by coclaurine N-methyltransferase (CNMT) to afford (S)-*N*-methylcoclaurine. Hydroxylation by (S)-N-methylcoclaurine-3-hydroxylase (NMCH), followed by 3-hydroxy-N-methylcoclaurine 4'-O-methyltransferase (4'OMT) *O*-methylation, yields (S)-reticuline, a central biosynthetic intermediate which undergoes diverse intramolecular coupling reactions resulting in the formation of various backbone structures, such as protoberberine, benzophenanthridine, morphinan and aporphine alkaloids. Noteworthy, in each biosynthetic branch the (S)-stereochemistry established in the first step by SNCS is retained, except for the morphinan alkaloids, in which the 1,2-dehydroreticuline reductase (DRR) epimerizes the (S)-reticuline to (R)-reticuline.

Several BIAs are used directly as pharmaceuticals while others serve as precursors for the synthesis of semi-synthetic drugs as thebaine, which is a metabolic precursor to morphine and codeine and is used for the synthesis of analgesics such as oxycodone, naltrexone, and buprenorphine. Most of these compounds are not feasible targets for *de novo* chemical synthesis owing primarily to the occurrence of multiple chiral centers; therefore, plants remain the only commercial sources for many pharmaceutical alkaloids.

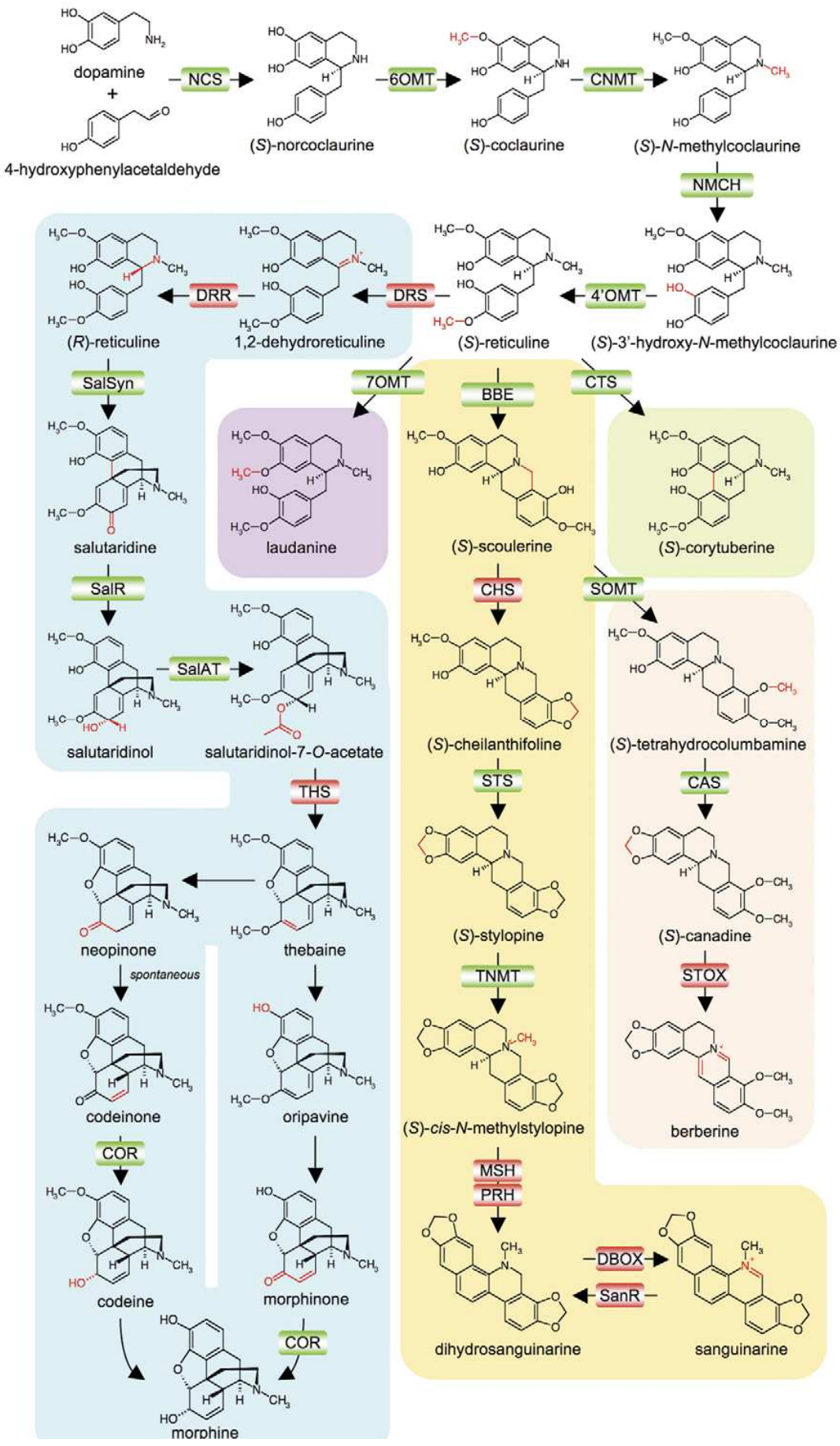
dopamine
4-hydroxyphenylacetaldehyde
NCS
(S)-norcoclaurine
6OMT
(S)-coclaurine
CNMT
(S)-N-methylcoclaurine
NMCH
(S)-3'-hydroxy-N-methylcoclaurine
4'OMT
(S)-reticuline
DRS
1,2-dehydroreticuline
DRR
(R)-reticuline
SalSyn
salutaridine
SalR
salutaridinol
SalAT
salutaridinol-7-O-acetate
7OMT
laudanine
BBE
(S)-scoulerine
CTS
(S)-corytuberine
CHS
(S)-cheilanthifoline
SOMT
(S)-tetrahydrocolumbamine
STS
(S)-stylopine
CAS
(S)-canadine
TNMT
(S)-cis-N-methylstylopine
STOX
berberine
MSH
PRH
dihydrosanguinarine
DBOX
SanR
sanguinarine
THS
neopinone
thebaine
spontaneous
codeinone
oripavine
COR
codeine
morphinone
COR
morphine

Figure 6.2 The biosynthesis of the BIAs. Branch pathways are color-coded. White: simple BIAs; blue: morphinan alkaloids; purple: laudanine; orange: benzophenanthridine alkaloids; pink: protoberberine alkaloids; green: aporphine alkaloids. Enzymes for which cognate cDNAs have been isolated are highlighted in green, while red denotes those with characterized activities. Abbreviations: BBE, berberine bridge enzyme; CAS, canadine synthase; CFS, cheilanthifoline synthase; CNMT, coclaurine *N*-methyltransferase; COR, codeinone reductase; CTS, corytuberine synthase; DBOX, dihydrobenzophenanthridine oxidase; DRR, 1,2-dehydroreticuline reductase; DRS, 1,2-dehydroreticuline synthase; MSH, *N*-methylstylopine 14-hydroxylase; NCS, norcoclaurine synthase; NMCH, *N*-methylcoclaurine 3'-hydroxylase; 4'OMT, 3'-hydroxy-*N*-methylcoclaurine 4'-*O*-methyltransferase; 6OMT, norcoclaurine 6-*O*-methyltransferase; 7OMT, reticuline 7-*O*-methyltransferase; PRH, protopine 6-hydroxylase; SalAT, salutaridinol-7-*O*-acetyltransferase; SalR, salutaridine: NADPH 7-oxidoreductase; SalSyn, salutaridine synthase; SanR, sanguinarine reductase; SOMT, scoulerine-9-*O*-methyltransferase; STOX, (S)-tetrahydroprotoberberine oxidase; STS, stylopine synthase; THS, thebaine synthase; TNMT, tetrahydroprotoberberine *cis*-*N*-methyltransferase.

Despite the fact that plants are the main source of alkaloids, several evidences demonstrated that such compounds do not occur exclusively in plant but also in humans. Following the human labeled alkaloids, It was clearly demonstrated that morphine is biosynthesized *de novo* by mammals and that both (S)-norlaudanosoline[5] and (S)-reticuline[6] are its endogenous precursors (scheme 6.2). The enantioselective occurrence was confirmed in many tissues, as brain for (S)-norlaudanosoline,[7] and human neuroblastoma and pancreas carcinoma cells for (S)-reticuline and (R)-morphine suggesting their enantioselective enzymatic synthesis in such districts.

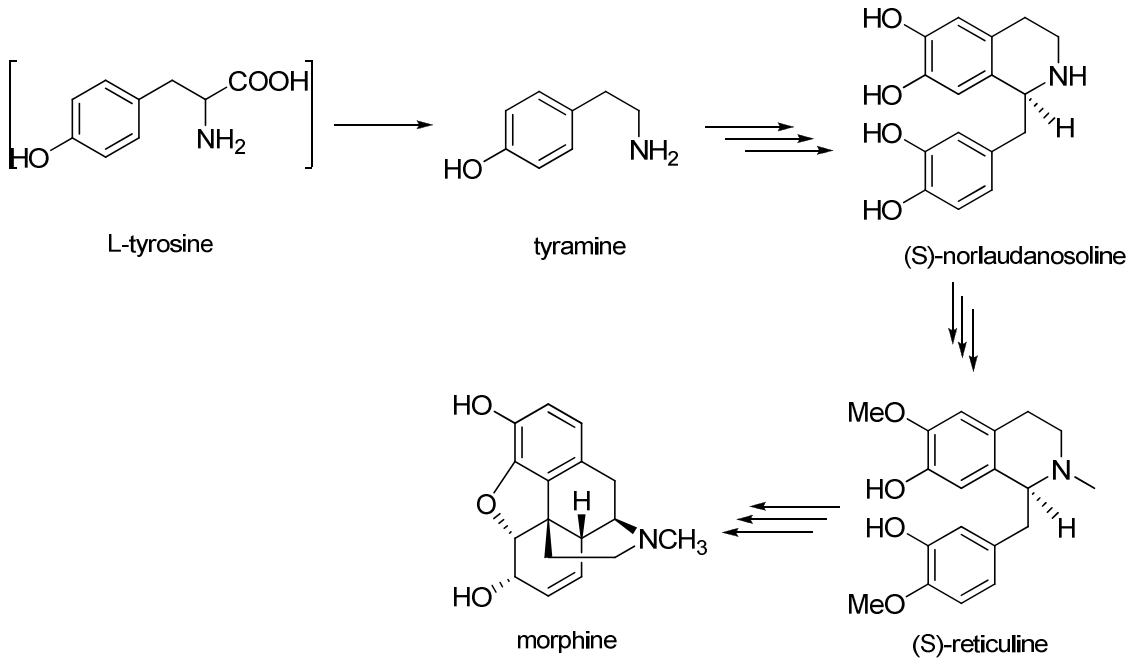

Scheme 6.2 Biosynthetic pathway of morphine in humans.

Morphine biosynthesis in humans is accomplished in at least 19 steps, reflecting for the most part its biogenesis in the plant kingdom; however, there is a fundamental difference in the formation of the key intermediate (S)-reticuline: it proceeds via the tetraoxygenated initial isoquinoline alkaloid (*S*)-norlaudanosoline, whereas the plant morphine biosynthesis proceeds via the trioxygenated (*S*)-norcoclaurine, confirming that the latter is the common intermediate of all BIAs exclusively in the plant kingdom.

6.2. Biological activity of norcoclaurine

The tetrahydroisoquinoline (THIQ) alkaloid norcoclaurine, also named higenamine, exists as optically inert racemic mixture, isolated from many natural sources including *Aconitum japonicum*[8,9], *Annona squamosa*[10] and *Gnetum parvifolium*[11], and as (R)- or (S)-enantiomer, extracted from *Argemone mexicana*[12] and *Nelumbo nucifera*[13], respectively. Norcoclaurine, mostly examined as a racemic mixture, was reported to possess an array of diverse biological activities. With its catecholamine moiety, it was expected to act on the adrenergic receptors: in several studies, indeed, it has been demonstrated to exert cardiac positive inotropic and chronotropic actions through β-adrenoceptor stimulation. Specifically, the β_1-antagonist practolol inhibited the positive chronotropic effect of norcoclaurine in murine atria, indicating that norcoclaurine acts as a selective β_1-adrenoceptor agonist.[14] Moreover, its additional ability in acting as an antagonist on α_1-adrenoceptor in the vascular smooth muscle, is clinically useful in reducing afterload to the heart suggesting a possible beneficial use of norcoclaurine on congestive heart failure.[15] Such coexisting α- and β-adrenoceptor affinity is well characterized in a norcoclaurine structurally related compound, dubutamine (scheme 6.3), a drug currently used for the congestive heart failure: a comparison between the two compounds, both as racemic mixtures, provided similar inotropic, chronotropic and vasorelaxant effects.

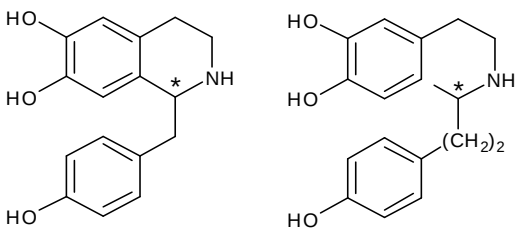

Scheme 6.3 Chemical structures of norcoclaurine and dobutamine.

A further adrenergic action of norcoclaurine has been detected by a comparison with salbutamol, a selective β_2-agonist: the reported β_2-adrenoceptor stimulating effects

identified at the cellular level, were subsequently verified *in vitro* and *in vivo* models confirming that norcoclaurine relaxes tracheal muscle, providing a potential efficient tool to reduce the severity of bronchoconstrictions.[16]

The cardioprotective benefits of norcoclaurine were recognized to be linked not only to the cardiotonic activity but also to an antithrombotic effect. Norcoclaurine strongly inhibits the arachidonic-acid-mediated platelet aggregation: the thromboxane A_2 (TXA_2), produced from arachidonic acid by COX and thromboxane synthase, drive platelet aggregation binding the TXA_2 receptor (TP) while norcoclaurine, acting as an antagonist, directly blocking it.[17,18] Since TP receptor is widely distributed among different organ systems, it was supposed to be involved not only in platelet aggregation but also in several diseases as hypertension, smooth muscle constriction, inflammatory lung disease, nephritic disease and many others, contributing to explain the previously reported pharmacological effects of norcoclaurine.

Remarkably, in an anti-platelet aggregating activity test, the two isomers of norcoclaurine were proven to differ significantly: the (S)-norcoclaurine was approximately 10-fold stronger anti-aggregation inhibitor than the corresponding isomer suggesting that they interfere in a different way, at least partly, with the adrenergic α-receptor. (S)-isomer was also superior in attenuating all of the disseminated intravascular coagulation (DIC) and multiple organ failure (MOF) parameters tested. Many ligands of α- and β-adrenergic receptors exert an influence in the cell response mechanism to endotoxin, bacterial lipopolysaccharide (LPS), which triggers the development of the Gram-negative septicemia effects and contributes to symptoms of sepsis-related DIC and MOF. LPS activates the cell release of inflammatory cytokines and increases the inducible nitric oxide synthase (iNOS) expression, which, in turn, enhances the production of nitric oxide (NO), an important promoter of hypotension, vascular hyporeactivity to vasoconstrictor agents in endotoxaemia, and systemic inflammatory response syndrome in humans. Inducible NOS activity during an inflammatory response is predominantly regulated at the transcriptional level, in which several transcription factors, as NF-κB, IRF-1, Stat1α, and Oct-1, act upon the iNOS gene promoter to activate transcription. Since norcoclaurine effectively inhibits iNOS expression through inhibition of NF-κB-mediated transcription of iNOS gene, it may be beneficial in the treatment of septic shock and inflammatory diseases in which enhanced formation of NO, clearly driven by iNOS, is a main causative factor.[19,20] Even in this case the effects of the racemic mixture were compared with those of each synthetic enantiomer: (S)-, (R)-, and (R,S)-norcoclaurine inhibited iNOS expression and reduced NO production in LPS-treated cells with IC_{50} of 26.2, 86.3, and 53.4 μM, respectively, showing that the (S)-isomer is 30% more potent that (R)-isomer.

Additionally, the *in vitro* results were well correlated with *in vivo* experiments, that is, (S)-norcoclaurine was demonstrated to significantly reduce serum NOx level and to increase survival rates in LPS-treated mice. In contrast, (R)-isomer only showed tendency to increase the survival rates which was not statistically significant when compared to controls, confirming that (S)-norcoclaurine may be more beneficial than (R)-enantiomer in diseases associated with iNOS overexpression.[21]

Finally, the optically active (S)-norcoclaurine extracted from *Nelumbo nucifera* was analyzed as a single enantiomer in HIV-infected cells.[14] Surprisingly, (S)-norcoclaurine demonstrated potent anti-HIV activity compared to AZT (Zidovudine) as showed in table 6.1 providing new pharmacological possibilities to be evaluated in HIV treatment.

Compound	IC_{50} (µg/ml)[a]	EC_{50} (µg/ml)[b,c]	TI[d]
(S)-norcoclaurine	20	<0,8	>25
AZT	1871	0,045±0,056	41,667

Table 6.1 Anti-HIV activity of (S)-norcoclaurine and AZT, an antiretroviral drug used for the treatment of HIV. a: the agent concentration that inhibited H9 cell growth by 50%. b: the agent concentration that inhibited viral replication in H9 cell by 50%. c: in vitro therapeutic index (TI) ratio: IC_{50}/EC_{50}. d: this EC_{50} value represents the mean and standard deviation of 65 experimentally determined EC_{50} values for AZT.

6.3. Synthetic access to norcoclaurine

Optically inert norcoclaurine could be either partially synthesized by demethylation of racemic coclaurine (6-*O*-methylhigenamine) obtained from the plant or by total synthesis,[22] using the sequential Bischler-Napieralsky cyclization/reduction, the most frequently explored approach in the past decade towards the synthesis of isoquinoline alkaloids. A β-arylethylamide undergoes an intramolecular electrophilic aromatic substitution to 1-substituted 3,4-dihydroisoquinoline or a corresponding isoquinolinium salt, which is then reduced in the next step to the 1,2,3,4-tetrahydro derivative affording an optically inert compound. However, as previously discussed, (S)-norcoclaurine was demonstrated to be more beneficial than both the corresponding isomer and the racemic mixture in the treatment of several diseases, encouraging the development of a synthetic enantioselective route. In an early attempt, (S)-norcoclaurine was prepared by chemical resolution of the racemic norarmepavine (6,7-di-O-methylhigenamine) followed by demethylation (scheme 6.4).[9] The two diastereomers obtained from (±)-armepavine and 1-phenylethylisocyanate were easily separated without any chromatographic method and subsequently deprotected furnishing the two enantiomers as HBr salts.

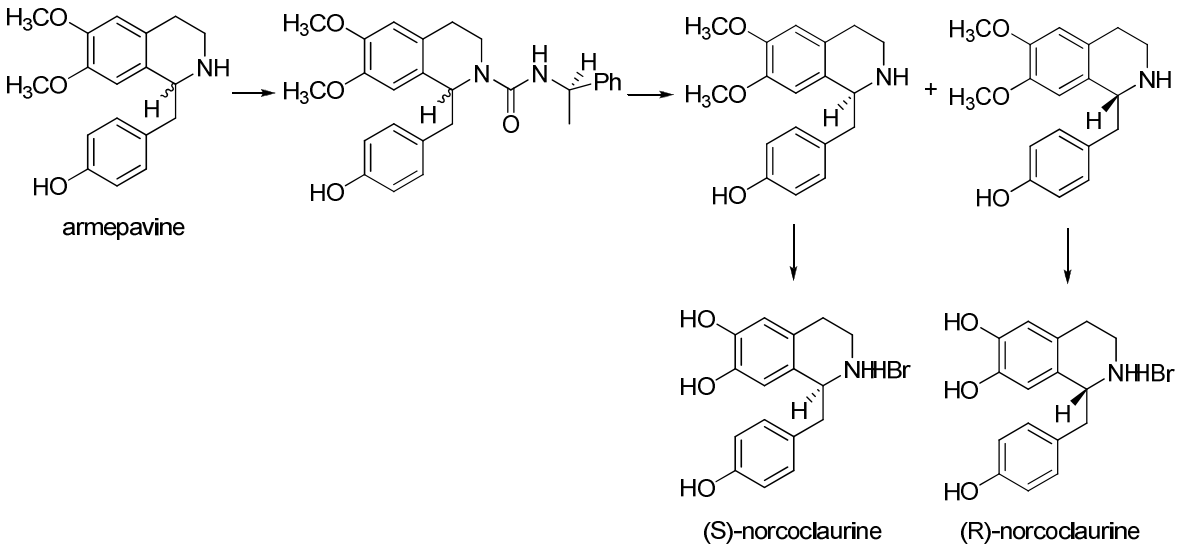

Scheme 6.4 Semisynthetic approach to (S)- and (R)-norcoclaurine

Despite the expeditious route established by this approach, an enantioselective total syntheses of both (R)-(+)- and (S)-(-)-enantiomers of norcoclaurine has been reported only in 2008 exploiting again the sequential Bischler-Napieralski cyclization/reduction but driving the stereochemical outcome through an asymmetric catalytic reduction.[23] In a five steps sequence, the amide **6** was subjected to cyclization to obtain the imine **7**, which in the next step underwent asymmetric reduction to the 1,2,3,4-tetrahydro derivative **9**, by Noyori's hydrogenation protocol, using RuCl[(S,S)-TsDPEN](p-cymene)] (8*R*) (1 mol%) as a catalyst (scheme 6.5).

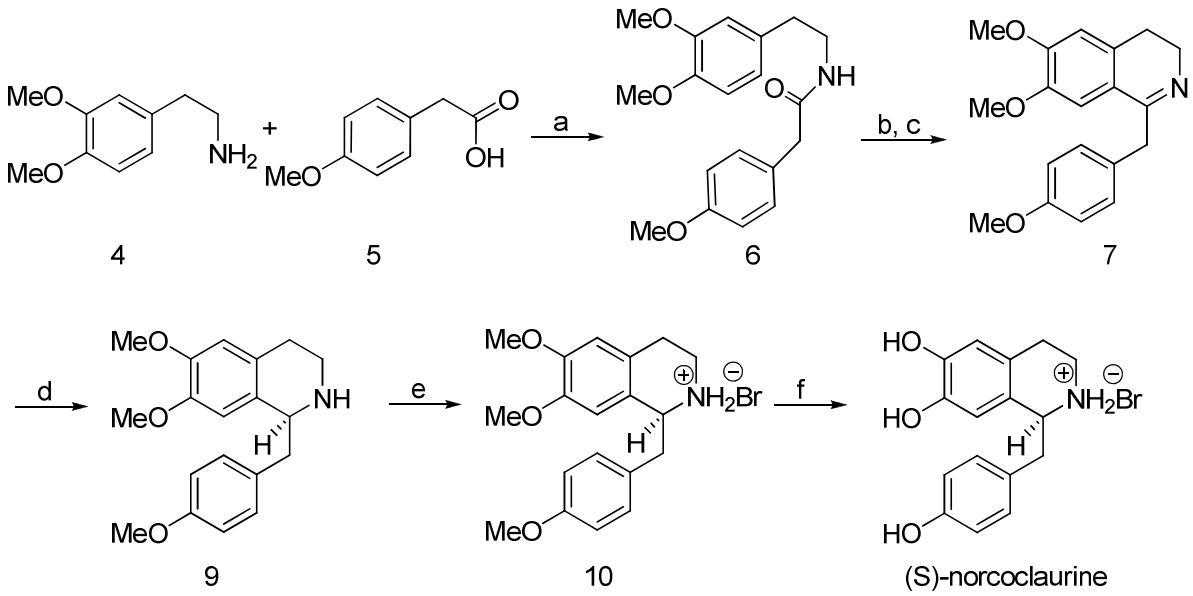

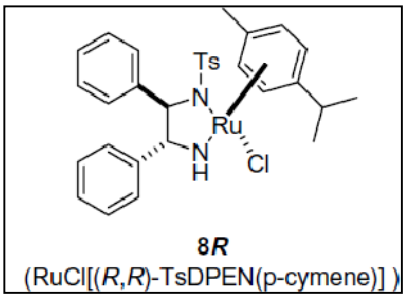

8*R*
(RuCl[(*R*,*R*)-TsDPEN(p-cymene)])

Scheme 6.5 Synthesis of (S)-norcoclaurine (1R). Reagents and conditions: (a) 20-0°C, neat, 4 h, 94%; (b) $POCl_3$, $CHCl_3$, reflux, 12 h; (c) saturated $NaHCO_3$, 0°C, 98% overall yield; (d) (i) RuCl[(S,S)-TsDPEN(p-cymene)] (**8R**) (1 mol%), HCO_2H/TEA = 5:2, DMF, rt, 12 h; (ii) purification, 62%; (e) 48% HBr, AcOH, rt, 84%; (f) CH_2Cl_2, BBr_3, -78 to 0°C, 3 h, 78%.

(S)-norcoclaurine synthesis was therefore successfully accomplished in an overall yield of 27,6% and an enantioselectivity >99% through a Ruthenium-based asymmetric catalyst.

6.4. The Pictet-Spengler reaction

6.4.1. Pictet-Spengler reaction: an overview

The synthesis of complex alkaloids architectures has been a field of great interest in synthetic organic chemistry as reflected in the huge spectrum of published strategies that report syntheses of both the alkaloid cores, the tetrahydroisoquinolines and tetrahydro-β-carbolines (THBCs) with different substitution patterns at the heterocyclic ring system. Among the existing strategies, the Pictet-Spengler (PS) has long been a classical synthetic approach towards both isoquinoline and β-carboline skeleton.[24] It was discovered in 1911 by Amé Pictet and Theodor Spengler, when they isolated 1-methyl-1,2,3,4-tetrahydroisoquinoline (**3**) from the condensation of β-phenethylamine (**1**) with formaldehyde dimethyl acetal (**2**) in the presence of hydrochloric acid. The reaction can be regarded as a kind of Mannich reaction, proceeding through the Schiff base formation (**4**) and subsequent intramolecular electrophilic substitution. It was originally utilized exclusively to prepare tetrahydroisoquinolines (THIQ) but soon after it was modified to accept N-substituted β-phenethylamines, as shown in scheme 6.6.

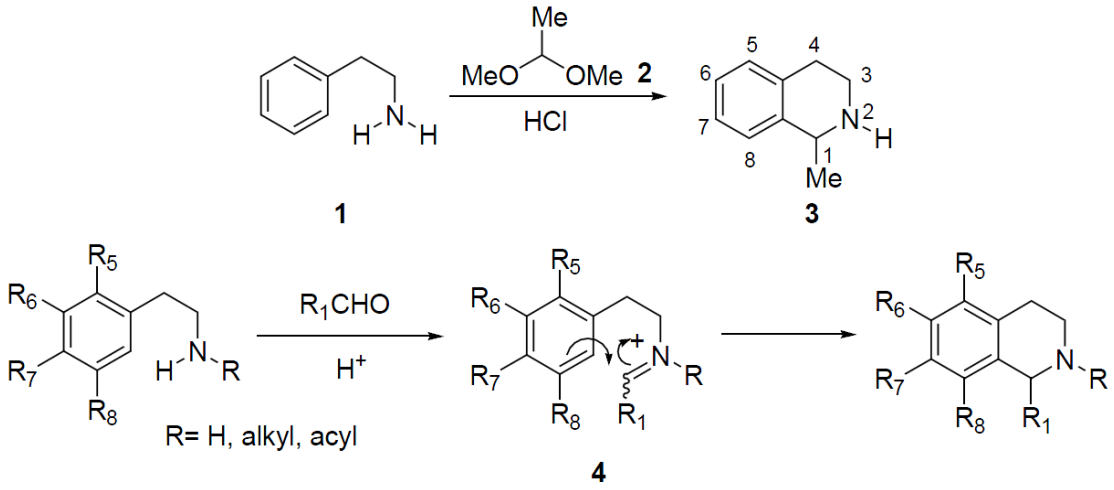

Scheme 6.6 The Pictet-Spengler reaction mechanism.

Since 1928, when Tatsui demonstrated that the reaction could efficiently yield tetrahydro-β-carbolines (THBC) (**6**) from tryptamine (**5**) (scheme 6.7), the PS condensation became the method of choice for the construction of both THBC and THIQ since naturally occurring indole and isoquinoline alkaloids, with a wide range of important biological activities bear this framework.

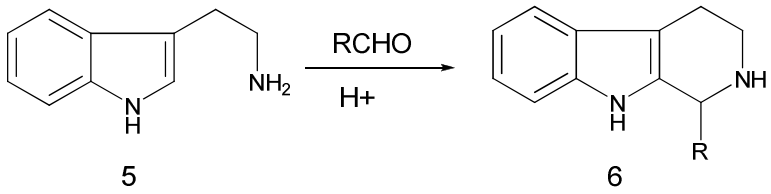

Scheme 6.7 The Pictet-Spengler reaction towards THBC.

Later, this strategy has been applied with great success also to synthesize many other related heterocycles, natural and synthetic organic compounds (scheme 6.8):[25,26,27] among them, the isochromans were easily obtained by the related oxa-Pictet-Spengler condensation.[28]

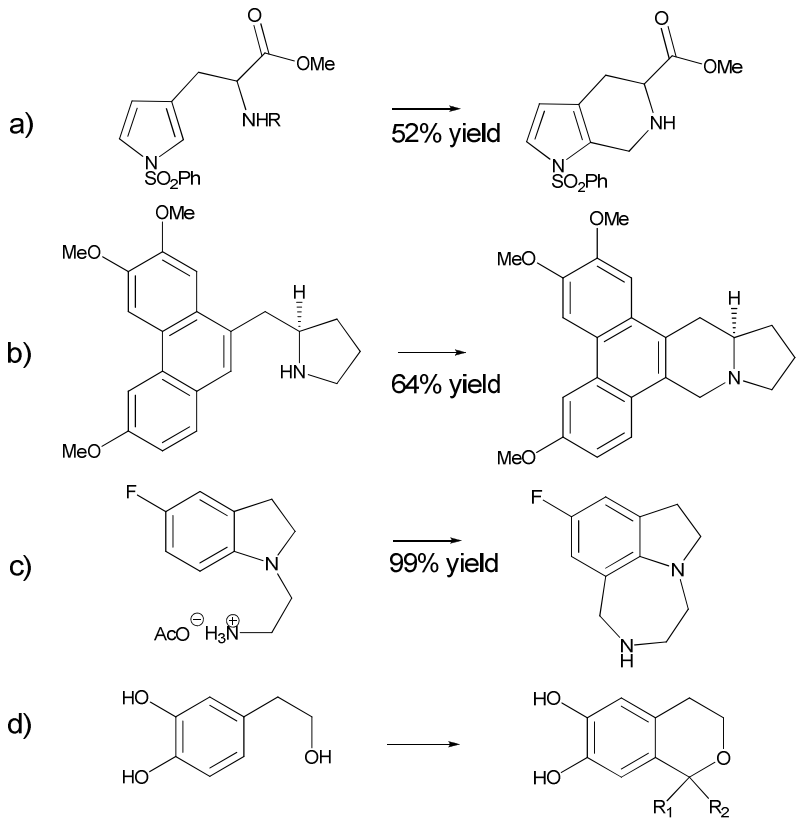

Scheme 6.8 PS based formation of a) 6-azaindoles, b) antofine and c) indolines. d) Oxa-Pictet-Spengler reaction towards isochromans.

Since a great number of chiral natural alkaloids owe their chirality to the stereogenic center correspondent to that formed during the PS condensation (C-1 in THIQ and THBC), the possibility to exploit an enantioselective variant of this reaction has long been an attractive target, promising an easy synthetic access even to the more complex alkaloids architectures. While in the last years many asymmetric organic synthesis have been developed, a newly discovered class of enzyme discussed in chapter 6.4.3 was found to catalyze the enantioselective Pictet-Spengler reaction.

6.4.2. Asymmetric organic Pictet-Spengler reaction

Several asymmetric procedures have been reported to date. In former times, asymmetric reactions could be accomplished only using enantiopure starting material,[29,30,31] i.e. chiral auxiliary groups attached to the side chain or to the nitrogen (N_b) of tryptamine controlled the stereochemistry of the newly formed C-1 stereogenic center in the acid-catalyzed procedure with up to 72% de.

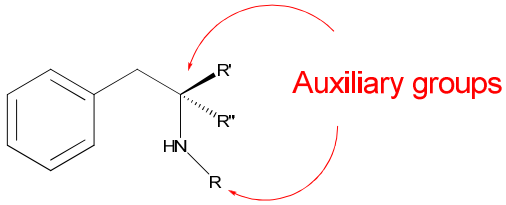

Recently, several interesting examples of chirality transfer 1→3 were reported by Zhu et al.: [32,33] in the synthetic route towards (-)-Renieramycin M and G and (-)-Jorumycin, the two THIQ ring systems were obtained through sequential asymmetric Pictet-Spengler reactions based on the stereodirecting effect of the synthetic intermediates (scheme 6.9).

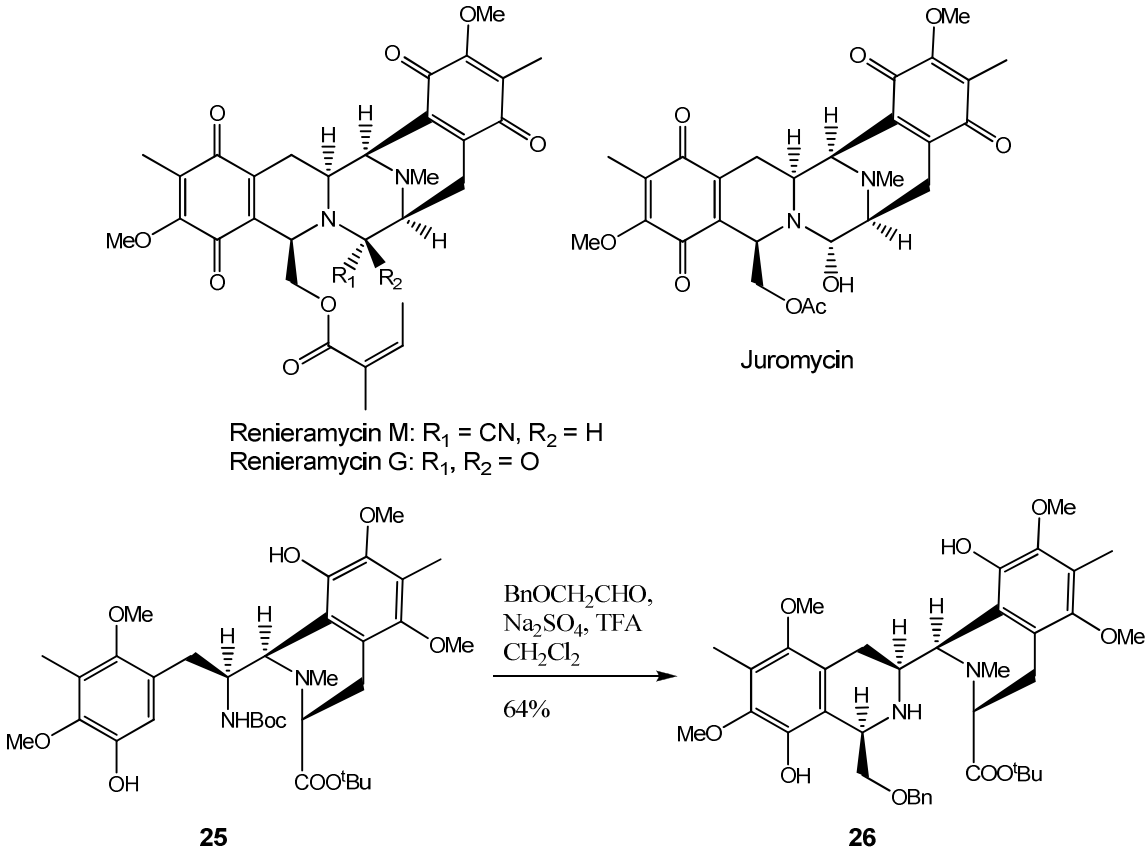

Scheme 6.9 Structures of (-)-Renieramycin M and G and (-)-Jorumycin and synthetic intermediates **25** and **26**.

The first example of a reagent–controlled enantioselective Pictet-Spengler reaction was developed by Nagakawa et al. using (+)-diisopinocampheylchloroborane ((+)-Ipc$_2$BCl) (**1**) or binaphthol-based chiral borane **24** as catalysts, with N$_b$-hydroxytryptamine and several aldehydes to obtain the corresponding 2-hydroxytetrahydro-β-carbolines in up to 91% *ee* (scheme 6.10).[34]

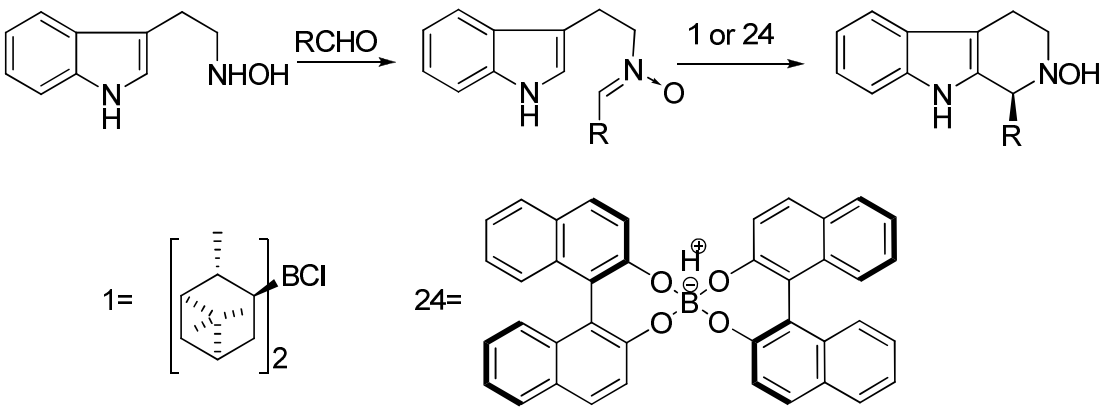

Scheme 6.10 The reagent–controlled enantioselective Pictet-Spengler reaction developed by Nagakawa.

Another similar asymmetric PS reaction has been reported on N-acylderivatives using a thiourea-based chiral catalyst providing quite high selectivity.[35,36] However, even though the described methods are impressive examples of asymmetric organocatalysis, in several cases introduction of a chiral auxiliary does not induce diastereoselectivity. Besides, a general drawback of these procedures is that removal of the chiral auxiliaries is often difficult and causes racemization because of the harsh conditions required for cleavage.

Recently, a new powerful asymmetric approach was developed by Hiemstra et al. combining the use of the binaphtylphosphoric acid **9** and a *N*-sulfenyl substituted triptamine which was found to stabilize the iminium ion thus favoring the cyclization of the intermediate (scheme 6.11).[37] Moreover, the sulfenyl substituent could be easily removed furnishing, in the best case, the THBC in 90% yield and 87% *ee*.

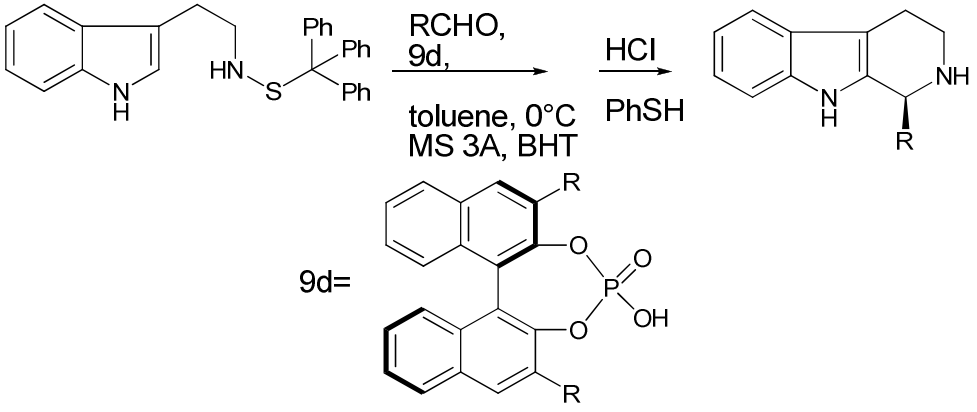

Scheme 6.11 The enantioselective Pictet-Spengler approach on N-sulfenyl triptamine.

Although these reactions are impressive examples of highly asymmetric organocatalysis, many of these reagent-controlled enantioselective methods have been successfully applied so far only to THBCs; asymmetric THIQ synthesis, indeed, has been

accomplished through the Pictet-Spengler reaction only under the stereodirecting control of the substrate.[38]

6.4.3. Pictet-Spenglerase: a biocatalytic asymmetric route to alkaloids synthesis

Enzymes are known to be chemoselective, regioselective and enantioselective and these features renders them ideal catalysts in chiral synthesis. For this reason many organic chemists have recently focused their attention in the use of enzymes as catalysts, now widely recognized as practical alternatives to traditional (non-biological) organic synthesis. In recent years, many plant biosynthetic pathways have been characterized, particularly the ones responsible for alkaloid biosynthesis. The Pictet-Spenglerases are involved in the first committed step of THBC and THIQ biosynthetic pathways in plant kingdom as well as in mammals and their catalytic mechanism is based on an asymmetric Pictet-Spengler reaction. Four such enzymes have been identified, among which three have been partially characterized: strictosidine synthase, salsolonol synthase and (S)-norcoclaurine synthase (which will be discussed in chapter 7.1). Notably, despite the fact that all of these enzymes catalyze the same reaction, they show no sequence homology,[39] representing an interesting example of evolutive convergence.

Strictosidine synthase

The enzyme strictosidine synthase (STR1), originally detected in *Catharanthus roseus* and *Rauwolfia serpentina*, is one of the most well-characterized alkaloid biosynthetic enzymes involved in the biosynthesis of monoterpene indole alkaloids, a large and structurally diverse family of natural products that include vinblastine, yohimbine, ajmaline, camptothecin, and strychnine. The first committed step of the biosynthetic pathway is catalyzed by STR1 and consists of the Pictet–Spengler condensation between tryptamine and secologanin to yield strictosidine (scheme 6.12) .

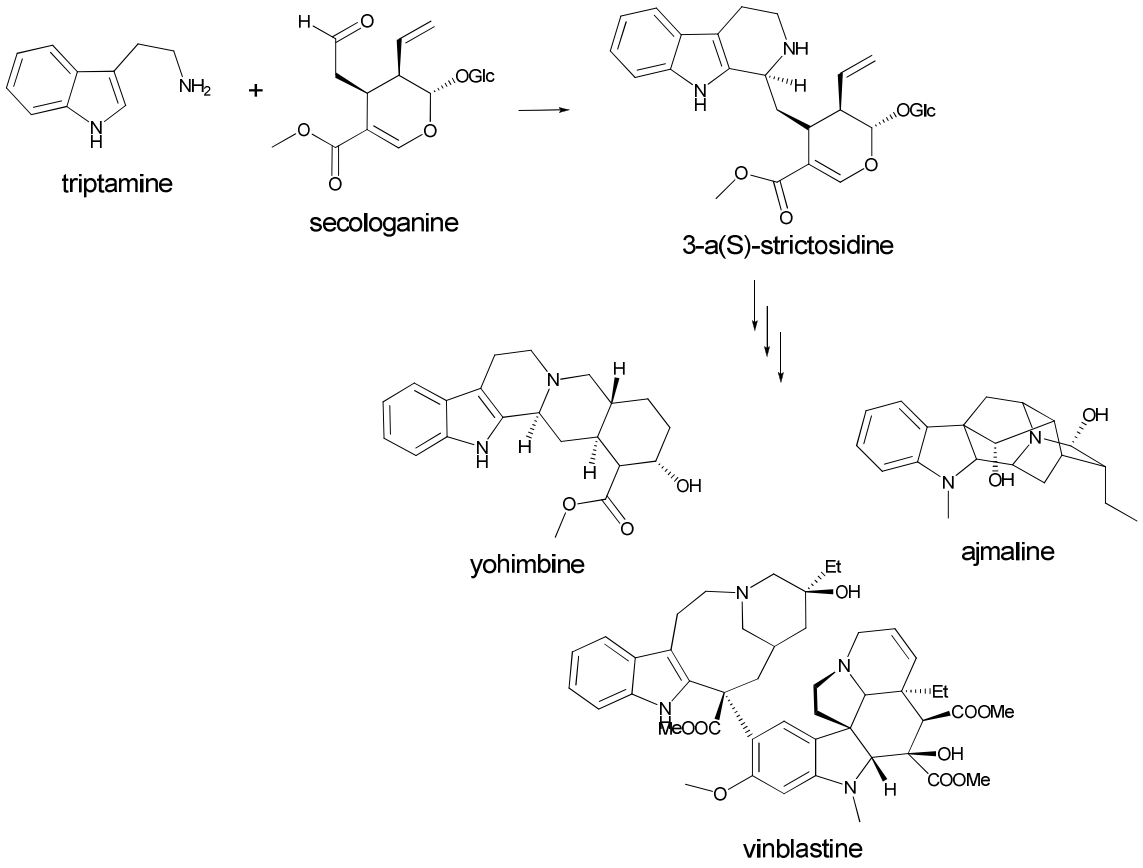

Scheme 6.12 STR1 catalyzes the stereo-specific condensation of tryptamine and secologanin leading to 3α(S)-strictosidine: a central reaction in the biosynthesis of the monoterpenoid indole alkaloids in plants.

The crystal structure of strictosidine synthase was recently solved,[40] paving the way for mechanistic studies. Glu309 (scheme 6.13) has been shown by both structural analysis and site-directed mutagenesis experiments to be the key residue required for acid–base catalysis in the Pictet–Spengler reaction.[41] Glu309 probably hydrogen-bonds to the primary amino group of tryptamine, ensuring that it is neutral and therefore nucleophilic. This primary amine attacks the aldehyde of secologanin to form an iminium ion. The indole moiety then attacks at the iminium in an electrophilic aromatic substitution reaction creating the (S)-stereocenter and, in the final step, deprotonation yields 3-α(S)-strictosidine.

Interestingly, the recently isolated strictosidine synthase from *Ophiorrhiza pumila* is able to utilize a range of simple achiral aldehydes and substituted tryptamines to form highly enantioenriched (*ee* >98%) THBC via a Pictet–Spengler reaction representing a first step toward developing a general biocatalytic strategy to access chiral tetrahydro-β-carboline and suggesting an analogous strategy to be applied towards THIQs though the other Pictet-Spenglerase.

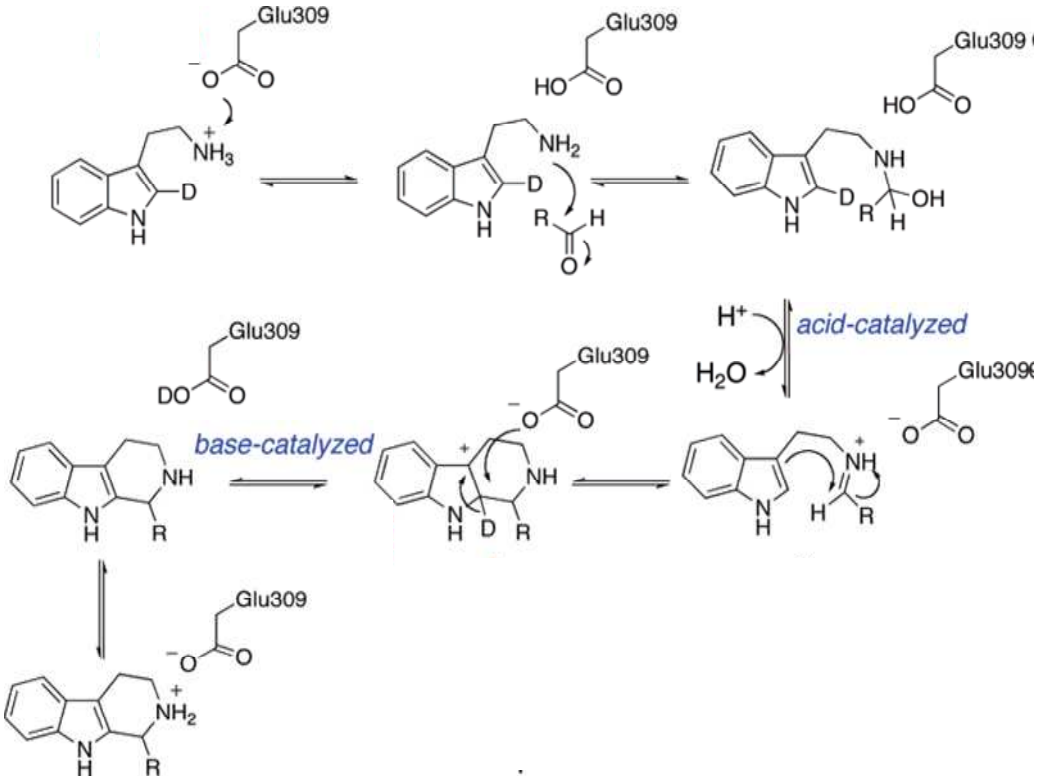

Scheme 6.13 Pictet-Spengler reaction mechanism.

Salsolinol synthase

Until recently, THIQs had been considered to occur only in plants. Anyway, several endogenous alkaloids have been detected in mammals and their enantioselective occurrence suggested an enzymatic biosynthesis: (R)-salsolinol and its neurotoxic derivative *N*-methyl-(R)-salsolinol, were found to derive from the Pictet-Spengler condensation of dopamine and acetaldehyde as showed in scheme 6.14.

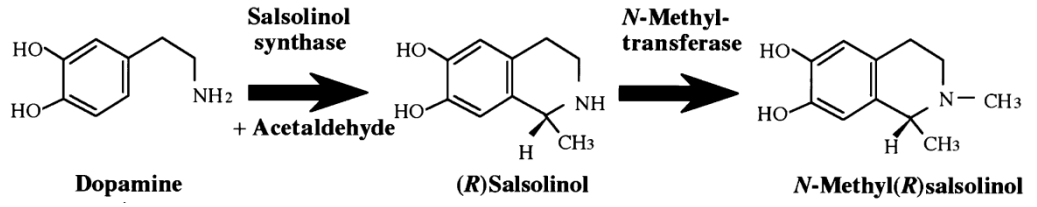

Scheme 6.14 Biosynthetic pathway of (R)-Salsolinol and NM(R)-Salsolinol in human brain.

Specifically, *N*-methyl-(R)-salsolinol, was found to be cytotoxic to dopamine neurons inducing cell apoptosis and playing a key role in the pathogenesis of Parkinson's disease. The products of salsolinol synthase and their role in human diseases have widely been characterized, nevertheless, there is no information currently available about the structure and the catalytic mechanism of the enzyme. However, recent studies seem to rule out the

common biosynthetic pathway of morphine and salsolinol, suggesting the existence of an additional Pictet-Spenglerase involved in the biosynthesis of the human morphine precursor (S)-norlaudanosoline.

6.5. Aim of the study

In therapeutical treatments with chiral drugs there are a number of potential clinical advantages associated with the use of a single isomer instead of the racemic mixture, including improvement in selectivity of the pharmacological profile and increased therapeutic index.[42] The development of an enantioselective route to clinically useful tetrahydroisoquinoline is therefore of interest for both synthetic organic and medicinal chemistry.

The rich biological potential of norcoclaurine was widely investigated in the treatment of several diseases and the pharmacological profile of the (S)-isomer was proved to be more favorable than the one of the (R)-isomer. Nevertheless, the low availability of natural (S)-norcoclaurine and the expensive stereoselective synthesis of this compound, based on the use of metal catalysts and organic solvents, have hampered its clinical development.

On the other side, the structural complexity of many currently used BIAs deriving from (S)-norcoclaurine often renders chemical synthesis impractical as an alternative to extraction of the secondary metabolites from plants for their commercial production. (S)-norcoclaurine, therefore, could be an extremely useful intermediate for the preparation of a wide range of other related alkaloids.

Thus the aim of the study was to:

- characterize the enzymatic activity of the recombinant SNCS from *Thalictrum flavum*

- establish a biotransformation protocol to (S)-norcoclaurine using the catalytic potential of a Pictet-Spenglease;

- expand the scope of the biotransformation from the analytical preparation to the multigram level to develop a green synthetic procedure.

Chapter 7

Results and discussion

7.1. (S)-norcoclaurine synthase

The enzyme (S)-norcoclaurine synthase catalyzes the first committed step of BIAs biosynthetic pathway: it condenses dopamine and 4-hydroxyphenylacetaldehyde to give (S)-norcoclaurine (scheme 7.1) through an asymmetric Pictet-Spengler reaction setting up the characteristic benzylisoquinoline core that defines this family of alkaloids.

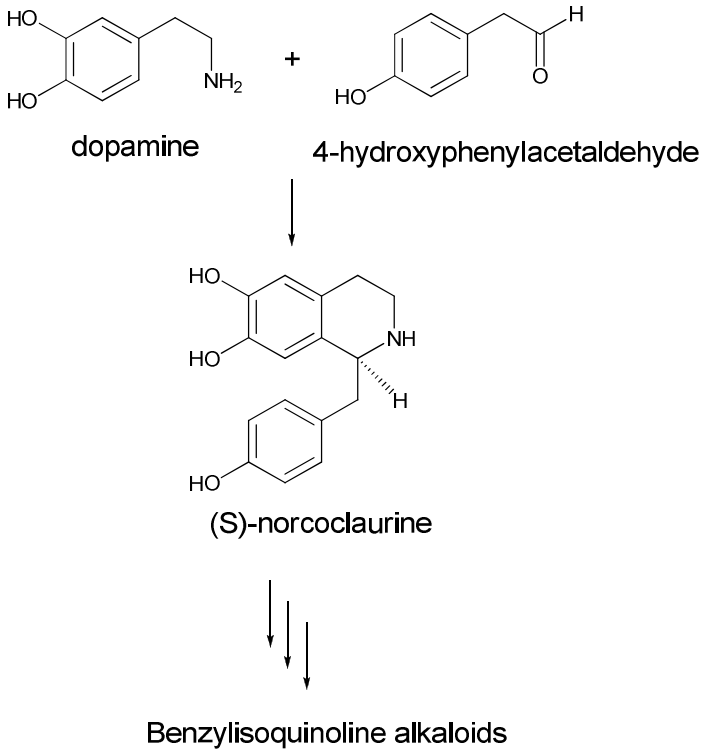

Scheme 7.1 (S)-norcoclaurine synthase catalyzes the condensation of dopamine and 4-hydroxyphenylacetaldehyde to form (S)-norcoclaurine, the common precursor to all BIAs in plants.

Until recently, despite the central role of SNCS in BIAs biosynthesis, very little was known about its structure. Peter J. Facchini for the first time isolated and characterized the enzyme in 2001 demonstrating a positive cooperativity in the binding of dopamine:[43,44] enzymes exhibiting this type of kinetics often have a regulatory role in metabolism, suggesting that (S)-norcoclaurine synthase may play a role in regulating the metabolic flux of the benzylisoquinoline pathway. The subsequent molecular cloning and characterization of SNCS from *Thalictrum flavum ssp.glaucum,* from the family of *Ranunculaceae,* demonstrated similar enzymatic properties of the recombinant enzyme with respect to the natural one. From the NCBI protein database[45] it was found out that (S)-norcoclaurine synthase shares no sequence similarity to the functionally correlated

strictosidine synthases whereas its central part (residues 40–170) displays a high degree of sequence identity (28–44%) to members of class 10 of the pathogenesis-related (PR 10) proteins. The PR proteins are plant products expressed under conditions of stress. They include the family of Bet v 1 homologous allergens that are of medical interest because of their effects on the human immune system: these proteins cause type I allergies involving weaker symptoms such as allergic rhinitis as well as asthma.

Observing the kinetics of the enzyme activity on substrate analogues of dopamine and 4-HPAA, it was proposed a path A enzymatic mechanism and, at the same time, ruled out the Path B implying the spirocyclic intermediate in scheme 7.2.[46] Moreover, the kinetic isotope effect (KIE) observed in a C-5 deuterium-labeled dopamine, indicated that rearomatization is a partially rate determining step of catalysis.

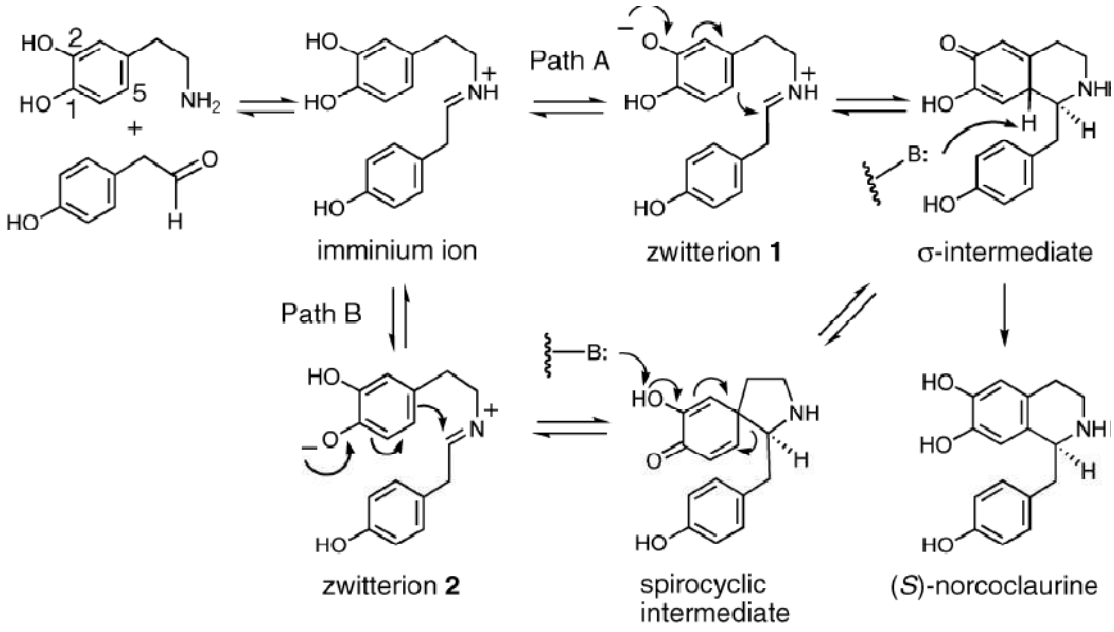

Scheme 7.2 Potential mechanisms for the reaction catalyzed by norcoclaurine synthase.

Finally, in 2009, Boffi et al. solved the first crystallographic structure of SNCS.[40] The histidine tagged enzyme and its selenomethionine-substituted (SeMet) variant were cloned, expressed in *Eschierica coli*, purified and crystallized. The expression of the SeMet variant, which contains four SeMet residues, was necessary since the previous attempt to solve the three-dimentional structure by the molecular replacement method failed. The crystallographic structure has been solved and reported in its complex with dopamine, the natural substrate, and *p*-hydroxybenzaldehyde, a non reactive substrate analogue, and substrate-free, providing a structure of SNCS as showed in figure 7.1[47] thus indicating that the enzyme seems to be a homodimer consisting of two asymmetric units (A1B1 and A2B2).

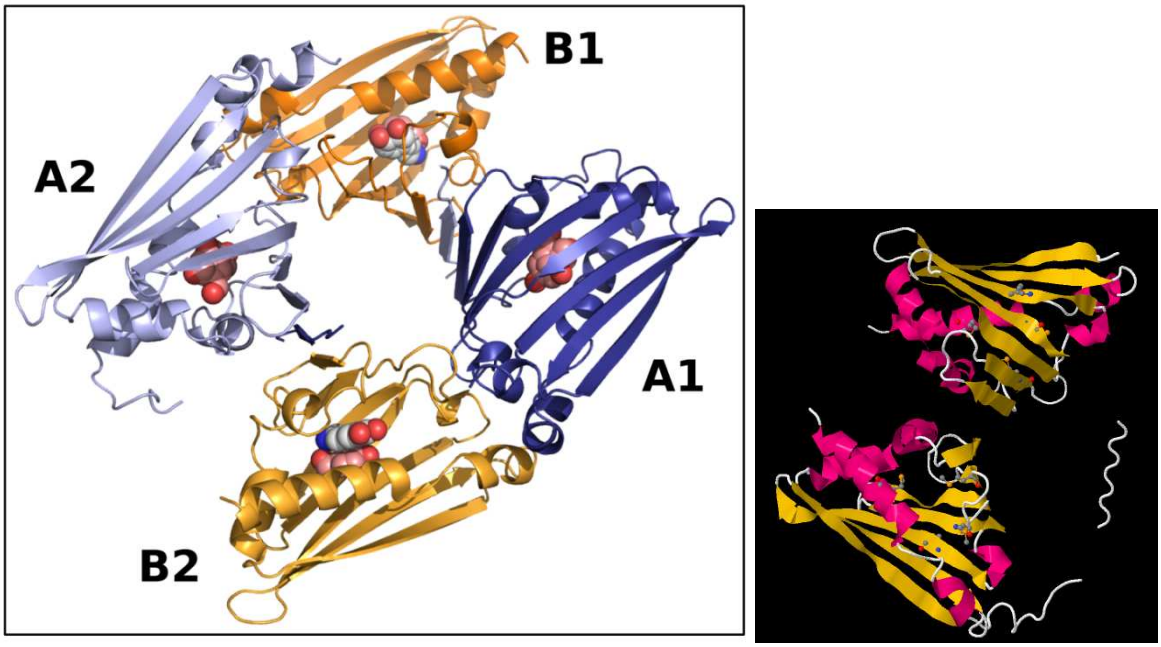

Figure 7.1 Tetrameric packing of SNCS. The monomers indicated in blue (A1 and A2) display a visible N-terminal sequence whereas the monomers indicated in orange (B1 and B2) do not. The picture has been generated in PyMol.[48]

The active site of SNCS is located within a 20 Å long catalytic tunnel (Figure 7.2) and is shaped by the side chains of a tyrosine (Y108), a lysin (K112), an aspartic and a glutamic acid (E110). The geometry of the aminoacid side chains with respect to the substrates reveals the structural determinants that govern the mechanism of the stereoselective Pictet-Spengler cyclization thus establishing a foundation for the understanding of the finer details of the catalytic process.

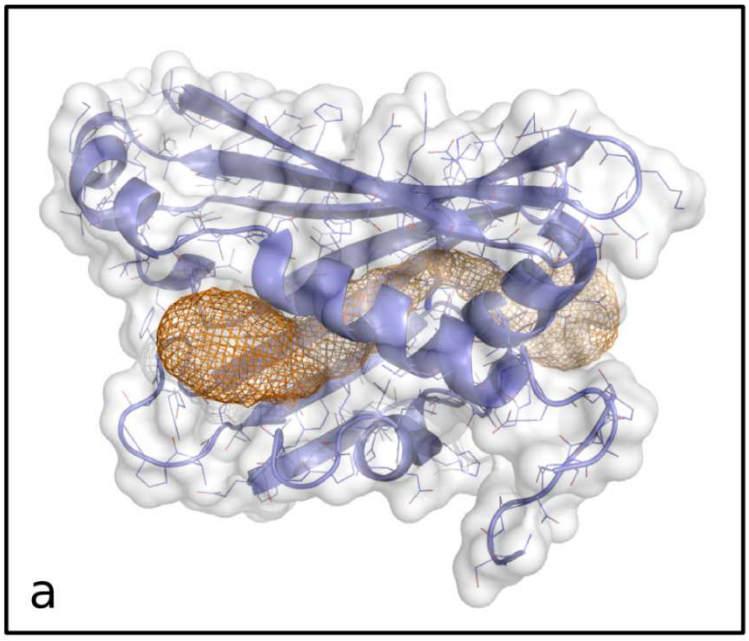

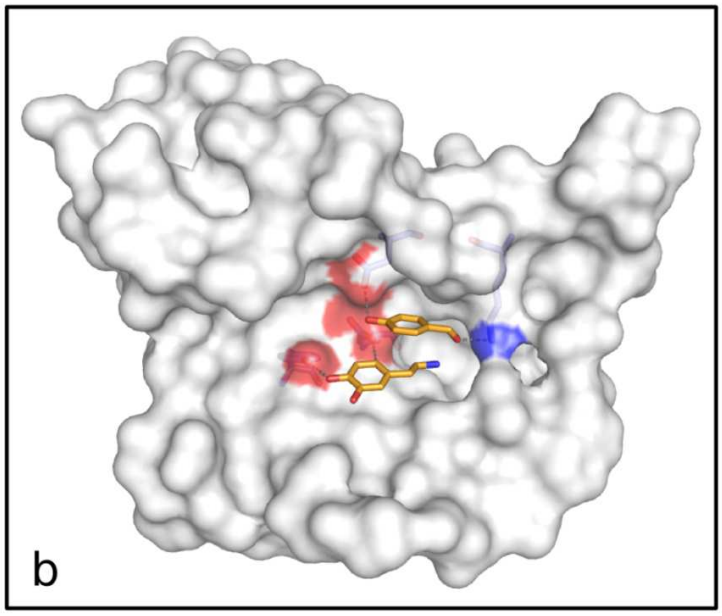

Figure 7.2 SNCS monomer and catalytic tunnel. Protein surface and catalytic tunnel (a) View of the inner surface of the protein (b). Dopamine substrate and p-hydroxybenzaldehyde substrate analogue are indicated. The pictures have been generated in PyMol.[49]

Positively charged K122 is proposed to polarize the carbonyl of the aldehyde substrate (scheme 7.3), making it more susceptible to nucleophilic attack by the primary amine. The lysine residue may also protonate the resulting carbinolamine, driving the loss of water to form the iminium species (scheme 7.3 (c)). The electrophilicity of the imine double bond thus formed is the driving force of the subsequent Pictet-Spengler cyclization. Ring closure entails a rotameric rearrangement of the iminium ion adduct (step (c) to (d) of scheme 7.3) followed by electrophilic substitution at the C5 position (step (d) to (e) of Scheme 7.3). The rotameric arrangement (clockwise rotation of the bond connecting the iminium nitrogen and the adjacent dopamine carbon atom) occurring within steps (c) and (d) is a prerequisite for the effective ring closure in that it brings the iminium carbon atom in proximity of the ring C5 atom. After deprotonation, assisted by the carboxyl moiety of Glu110, the S-stereospecific product is formed (scheme 7.3 (f)). On the basis of the previously discussed kinetic studies on substrate analogues, it seem that the dopamine moiety is deprotonated at the C-2 hydroxyl group, which helps drive the attack on the iminium ion to form the norcoclaurine skeleton. Formation of this phenolate ion has been proposed to be mechanistically essential since analogs lacking a C-2 hydroxyl group are not substrates.[47] However, the residues involved in C-2 hydroxyl group deprotonation, or stabilization of the resulting phenolate ion, have not been definitively identified, though Tyr108 may be involved.

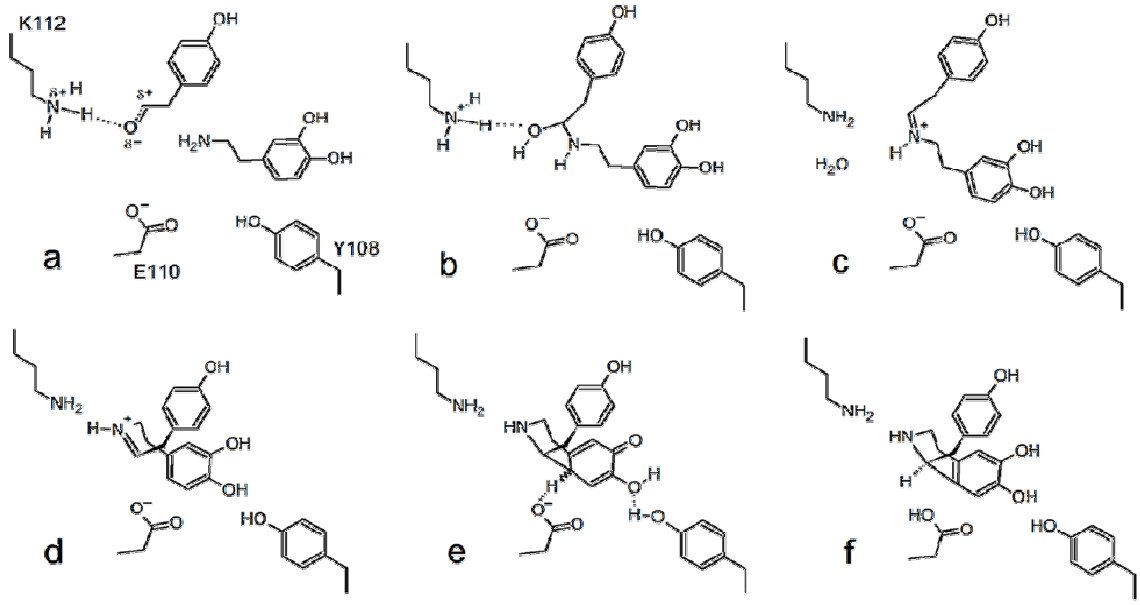

Scheme 7.3 Biocatalytic mechanism proposed for (S)-norcoclaurine formation.

7.2. Enzymatic synthesis of (S)-norcoclaurine

Once the structural basis of SNCS had been identified and characterized, the further step was to set up a biosynthetic procedure to test its enzymatic activity. The major difficulties were in finding a synthetic method to obtain 4-HPAA since it is not commercially available and highly unstable. All the efforts to produce it enzymatically using plant monoamino oxidases starting from tyramine or alcohol dehydrogenase starting from 2-(4-hydroxyphenyl)ethanol were unsuccessful. In turn, after considerable experimentation, it was concluded that chemical synthesis of the pure aldehyde is impractical (scheme 7.4): both attempts made by reduction of methyl 4-hydroxyphenylacetate by DIBAH in dry ether (30% yield estimated by NMR analysis) and oxidation of 2-(4-hydroxyphenyl)ethanol by pyridinium dichromate (PDC)[49] in DCM/EtOAc (1:0,5 v/v) resulted unsuccessful. In each case the resulting product was not enough pure for an enzymatic assay and not stable to be purified and stored since it rapidly undergoes extensive degradation.

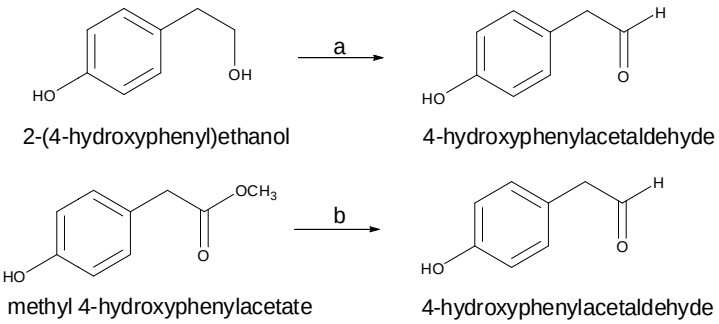

Scheme 7.4 Reaction conditions. a) PDC, DCM/EtOAc (1:0,5 v/v); b) DIBAH, ether, -78°C.

This challenging step was faced exploiting a biological mechanism utilized by activated neutrophils to damage a biological target at the sites of inflammation: they convert L-tyrosine to the highly reactive *p*-hydroxyphenylacetaldehyde through the myeloperoxidase-H_2O_2-chloride system to form Schiff base adducts with cellular targets.[50,51,52] The major oxidant formed was found to be HClO which converts an α-aminoacid to an unstable α-monochloramine, which in turn decomposes loosing in a concerted mechanism CO_2 and Cl^- to yield an aldehyde. Thus, 4-HPAA was conveniently generated directly by oxidative decarboxylation of tyrosine in aqueous solutions in the presence of an equimolar amount of hypochlorite followed by immediate use of the aldehyde for the enzymatic reaction (scheme 7.5). The product formation was followed by GC/MS and the yield was estimated to be greater than 99% with less than 0,1% of chlorinated byproducts (by GC/MS).

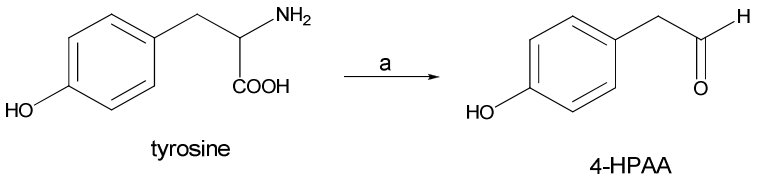

Scheme 7.5 Reaction conditions: NaClO, phosphate buffer 20 mM, pH=7.0; 0°C -> 37°C, 1h, 93%.

The aldehyde was therefore recovered in 93% yield and identified by NMR and Mass spectroscopy and 2,4-dinitrophenylhydrazine assay. Since the reaction was carried out in the same phosphate buffer needed for SNCS catalysis, the whole (S)-norcoclaurine synthesis could be optimized as a one pot reaction by quickly adding dopamine and SNCS to the solution containing the newly synthesized aldehyde. Another critical step is concerning the low stability of dopamine in air equilibrated aqueous solutions which is responsible of the low overall yields of intermediates in benzylisoquinoline alkaloids synthesis.[53] Dopamine is in fact easily oxidized to melanine-like pigments in a second order reaction with oxygen. The dopamine oxidation reaction severely would impair the possibility of reaching synthetically convenient concentrations higher than 1-2 mM in view of a further optimization of (S)-norcoclurine synthesis. Thus, several attempts were made in order to improve the effective concentration of dopamine substrate in solution, including deareation (N_2 purging into the reaction batch) or use of solvent mixtures (water/isopropanol) in the presence of reductants (sodium dithionite, menadiol, vitamin E). Among the different reductants used, ascorbate was observed to be the most efficient, easiest to use and cheapest. Thus, in order to prevent dopamine oxidation during the reaction course, the reaction mix was added with 5 mM ascorbate in the absence of

cosolvents. This strategy would allow even ten folds higher dopamine concentration (10 mM) to be used (see section 7.3).

In a first analytical scale attempt (scheme 7.6) the product formation was followed by circular dichroism and GC/MS, (as reported in figure 7.6), demonstrating that in 30 minutes the reaction was complete. This biotransformation protocol was so applied to a preliminary small scale reaction which afforded 55 mg of norcoclaurine.

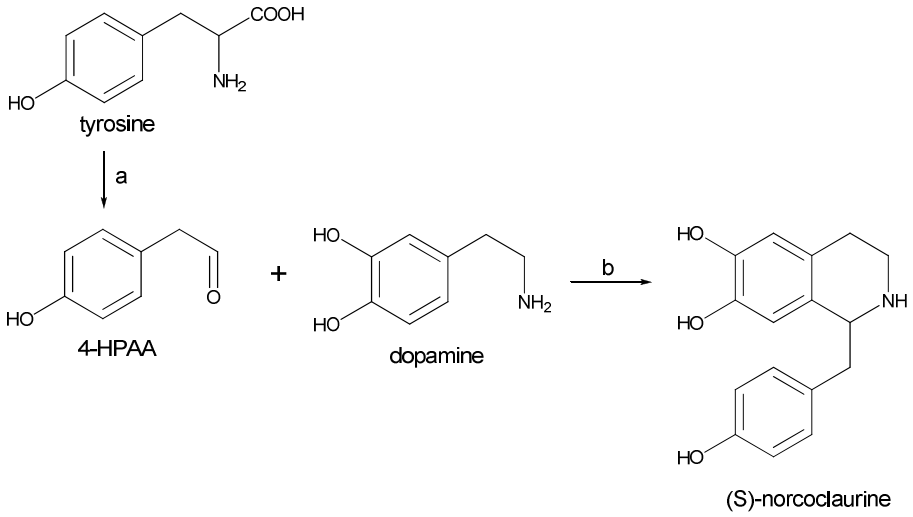

Scheme 7.6 Stereospecific chemoenzymatic synthesis of (S)-norcoclaurine from tyrosine and dopamine. Reagents and conditions: a) NaClO, phosphate buffer, pH=7.0; 0°C → 37°C, 1h; b) SNCS 0.4 μM, ascorbate, phosphate buffer, pH=7, 30 min, 37°C.

In order to distinguish between background reaction contribution and stereoselective catalysis, the enantiomeric excess of (S)-norcoclaurine chiral product vs. the (R)-isomer was determined through a chiral stationary phase with teicoplanin obtained from Gasparrini F.[54] In figure 7.3 the chiral HPLC chromatograms of standard, racemic norcoclaurine and reaction mix are reported and the enantiomeric excess of (S)-norcoclaurine was found to be 93%.

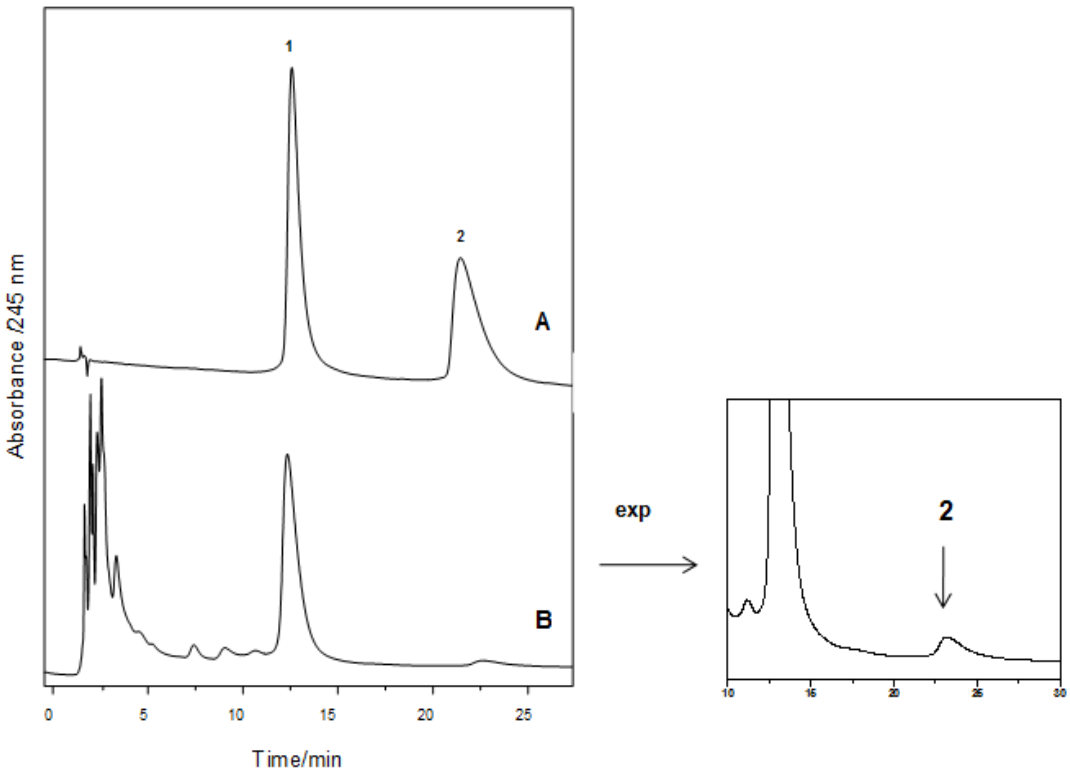

Figure 7.3 A) Chiral HPLC chromatogram of a standard racemic mixture of norcolcaurine. Acquisition was performed with an UV detector at λ = 254 nm. B) HPLC chromatogram of the reaction mix, showing the presence of the expected (S)-norcolaurine enantiomer (peak 1).

This result was confirmed by CD analysis that indicates the presence of two peaks with opposite Cotton effect due to the presence of both enantiomers in standard racemic norcoclaurine (fig. 7.4, A), whereas the reaction mix shows a very large excess of the expected (S)-isomer (fig. 7.4, B). The newly synthesized (S)-norcoclaurine does not racemize after three months when stored as a dry powder at room temperature.

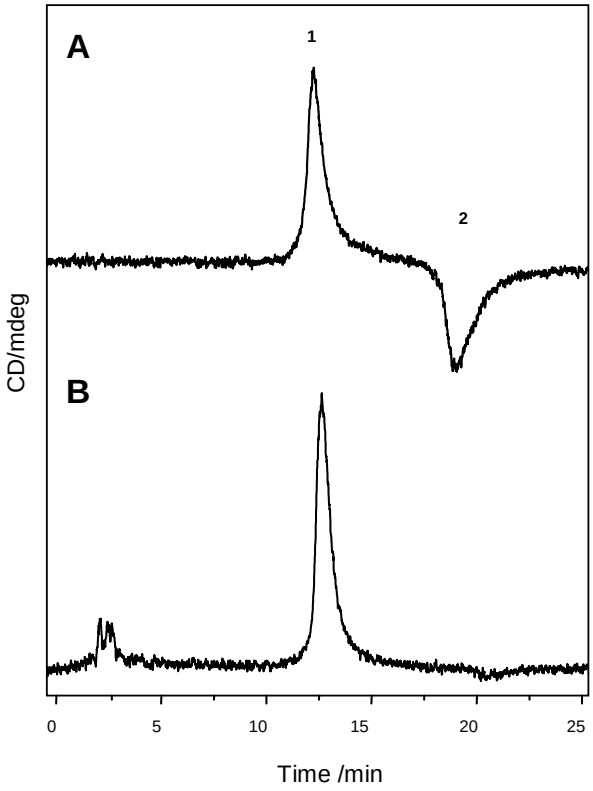

Figure 7.4 A) Chiral HPLC chromatogram of standard racemic mixture of norcolcaurine. Acquisition was performed with a CD detector at λ = 280 nm. B) HPLC chromatogram of the reaction isolated product, showing the presence of the expected (S)-norcolaurine enantiomer (peak 1).

7.3. Easy scalable (S)-norcoclaurine green production

On the basis of the experimental findings outlined above, a green and easily scalable process was set up starting from the small scale biotransformation protocol.

NCS was recombinantly expressed in *Eschericha coli* at high yield using a codon optimized synthetic gene (Geneart AG) as described previously.[40] *E. coli* cells were fermented in a 2 liter Sartorius fermentor with a feed batch procedure in minimal medium at 25 °C. The yield of wet bacterial paste was about 50 g/l fermented medium with a raw yield of 30 mg/protein per gram of bacterial paste. The his-tagged protein was easily purified in batch by standard procedure on a Nickel nitriloacetate resin. The present expression and purification protocol allows one to obtain ten folds larger amount of purified protein with respect to the previously reported methods[40] which consisted of low density growth in shake flasks, suitable for analytical scale preparation. The large amount of enzyme obtained represents the pre-requisite for scaling-up (S)-norcoclaurine production.

Enzyme concentration was adjusted to achieve a relatively fast reaction kinetic in order to limit the competing non enantioselective chemical coupling between dopamine and 4-HPAA, which would dominate the SNCS reaction for longer periods of incubation. The optimal enzyme concentration was found to be 0.5 μM, corresponding to 10 mg enzyme per liter of solution.

Therefore, from dopamine and 4-HPAA, both used in relatively high concentrations (10 mM), (S)-norcoclaurine synthesis was achieved in a one pot two steps synthesis furnishing 2,2 g of isolated product (81% yield) from 1 liter of solution and 30 minutes incubation at 37 °C.

To render the procedure environmental-friendly avoiding the use of organic solvents, an extraction strategy was developed based on the use of activated carbon (NORIT, multipurpose activated charcoal). Adsorption/desorption properties of activated carbon towards phenolic compounds has been widely characterized, and conditions for optimal binding/desorption of (S)-norcoclaurine were investigated as a function of temperature and solvent composition. Absorption was achieved by shaking carbon granules directly added to the aqueous phase at room temperature (30 minutes shaking). Control experiments indicated that dopamine substrate is not absorbed onto the activated carbon beads, whereas aldehyde substrate is strongly absorbed. Best desorption conditions for S-norcoclaurine were obtained in ethanol at 40 °C in the presence of a slight molar excess of NaOH. This procedure allowed to obtain a very good extraction yield of (S)-norcoclaurine in the absence of unreacted aldehyde contaminant that remained adsorbed on the carbon matrix. The yield is comparable to that achieved by extraction with 4 excess volumes of diethylether (81% vs 79%). The procedure based on activated carbon has the notable advantage of recovering about 70% active NCS enzyme from the reaction mix, once carbon has been removed by filtration. In recycling experiments (fig. 7.5), the same enzyme solution has been used up to fivefold with an overall product recovery of about 670 mg of product (isolated) per mg of enzyme.

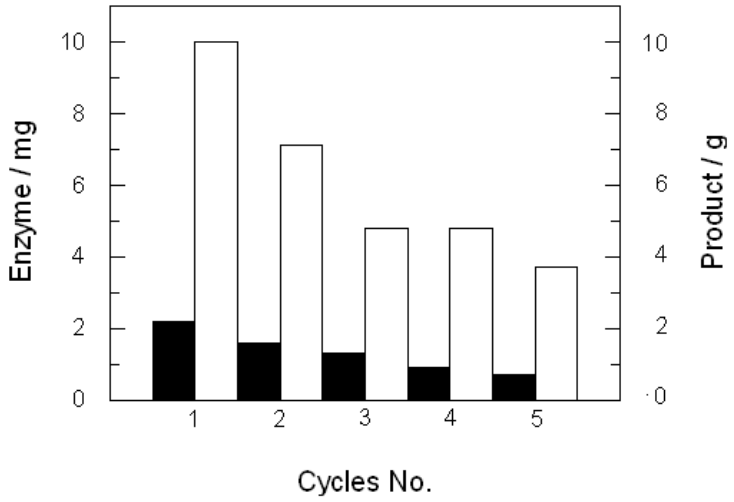

Figure 7.5 Reaction recycling. Five recycling steps have been performed by monitoring enzyme activity after each step (white boxes) and product yield (black boxes). Enzyme concentration on centricon 20 ml tubes had to be performed before each cycle.

Summary

A new, easily scalable process for the synthesis of (S)-norcoclaurine has been developed on the basis of the benzylisoquinoline alkaloids pathway according to one pot-two steps reaction by using (S)-norcoclaurine synthase enzyme, produced in *E. coli* and purified in high yields. Key steps in the biotransformation consist in the oxidative decarboxylation of tyrosine by stoichiometric amounts of sodium hypochlorite in order to generate 4-hydroxyphenylacetadehyde followed by addition of enzyme and dopamine substrate in the presence of ascorbate as antioxidant. The analytical scale reaction furnished the parameters of the catalytic activity of (S)-norcoclaurine synthase while the large scale optimized process afforded enantiomerically pure (S)-norcoclaurine (93%) in reaction yields of about 80%. Additionally, an extraction strategy based on the use of activated carbon allowed to recycle the enzyme and to recover the product by a solvent-free procedure. The reported results represent the first attempt to exploit the potential of a "Pictet-Spengler" enzyme providing an example of a chemo-enzymatic synthetic strategy as a novel, efficient and green tool for manufacturing plant-derived metabolites, particularly benzylisoquinoline alkaloids.

Experimental Part

General procedure. Room temperature refers to 22°C. Reagents obtained from commercial suppliers were used without further purification. (R,S)-norcoclaurine was obtained from Sequoia Research Products (UK). Reactions were monitored by thin layer chromatography using Merck silica gel 60 F_{254} TLC aluminium sheets and products were visualized by UV light, *p*-anisaldehyde, 2,4-dinitrophenylhydrazine.

Ether extracts at the end of the reactions were analyzed by gas chromatography-mass spectrometry using an Agilent 6850A gas chromatograph coupled to a 5973N quadrupole mass selective detector (Agilent Technologies, Palo Alto, CA, USA) was used. Chromatographic separations were carried out an Agilent HP5ms fused-silica capillary column (30 m × 0.25 mm i.d.) coated with polyethylene glycol and 5%- phenyl-95%-dimethylpolysiloxane (film thickness 0.25 µm) as stationary phases for 4-HPAA and (S)-norcoclaurine analysis, respectively. Injection mode: splitless at a temperature of 260 °C. Column temperature program: 100 °C (1 min) then to 300 °C at a rate of 15 °C/min and held for 5 min. The carrier gas was helium at a constant flow of 1.0 ml/min. The spectra were obtained in the electron impact mode at 70 eV ionization energy and a mass range scan from m/z 50 to 500; ion source 280 °C; ion source vacuum 10^{-5} Torr.

^{1}H NMR and ^{13}C NMR spectra were recorded at room temperature on a Bruker Avance at 400 MHz. Chemical shifts are expressed in δ (ppm) values relative to tetramethylsilane (TMS) or residual nondeuterated solvent as an internal standard.

Specific rotation of MeOH solutions of norcoclaurine was measured with a JASCO P-1030 polarimeter at 25 °C (cell path 10 cm).

Preparation of 4-hydroxyphenylacetaldehyde from tyrosine.

To a solution of tyrosine (10 mg, 0,055 mmol) in 5 ml of phosphate buffer 20mM pH 7.0, was added NaClO (solution 10%, 31 µl, 0,055 mmol) dropwise at 0°C. The solution was warmed to 37°C and kept there for 1h. The ether extracts afforded 4-hydroxyphenylacetaldehyde as a colourless oil (7 mg, 93%); TLC ((*n*-hexane/EtOAc, 6:4 v/v): R_F = 0.38; ^{1}H NMR (400 MHz, acetone) δ 9.66 (s, 1 H), 7.09 (m, 2 H), 6.83 (d, J = 8.4 Hz, 2 H), 3.60 (m, 2 H).

GC/MS spectra of 4-HPAA substrate.

100 µL of the reaction mix extracted with 400 µL diethylether were directly injected in GC/MS (1µL). The reaction product is estimated to about 99% of initial tyrosine substrate. The product is devoid of chlorinated byproducts. The GC/MS profile (in sim mode) is shown.

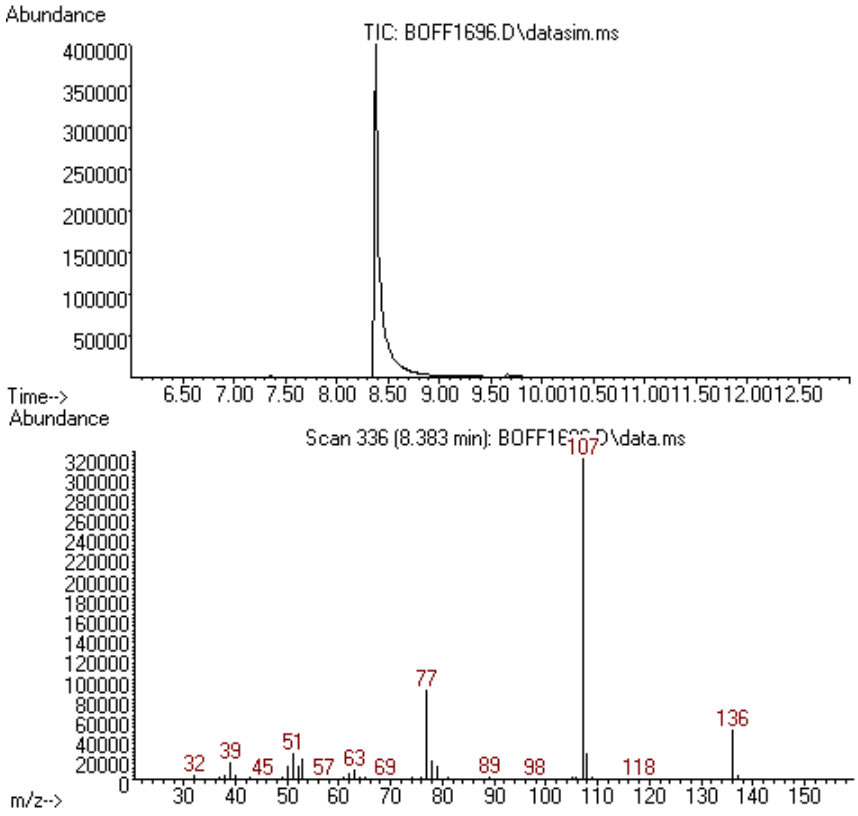

Time courses of (S)-norcoclaurine formation in CD kinetic experiments.

Experiments were carried out by following the increase in ellipticity at 285 nm, corresponding to the formation of the S-norcoclaurine product. The value of molar ellipticity 12541 mdeg cm^{-1} M^{-1} was used to calculate effective concentration of the product. Dopamine and 4-HPAA in a concentration range from 50 µM to 1 mM each were placed in a quartz cell (from 0.1 to 1 cm) and equilibrated 1 minute at 37 °C in 0.1 M phosphate buffer at pH 7.5. Then, 5 µl of a SNCS solution was added to a final protein

concentration of 0.4 μM. Protein concentration was determined by the Bradford method (Sigma Aldrich kit).

UV difference (top) and CD (bottom) spectral time courses of (S)-norcoclaurine formation.

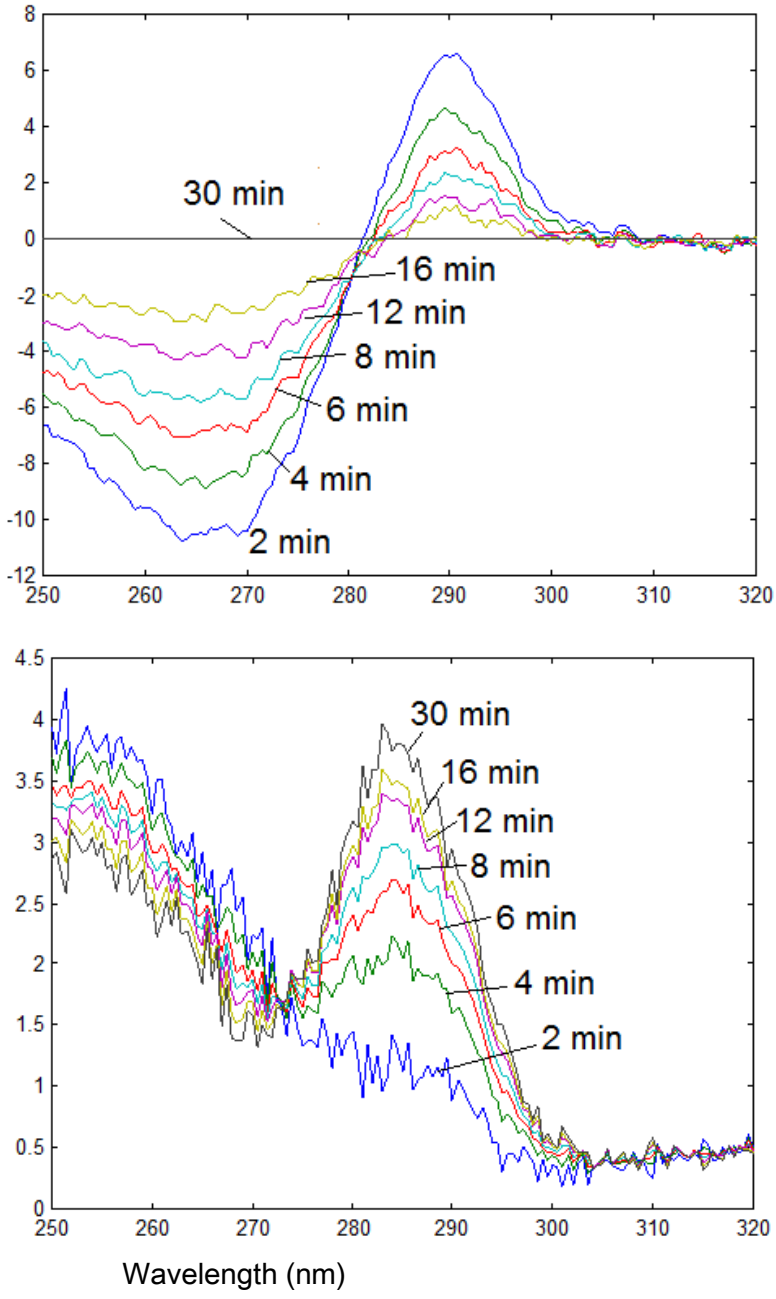

Spectra were simultaneously acquired in the spectropolarimeter in the CD mode and PM voltage (HT) mode. Wavelengths (at the rate of 100 nm/min) are thus reported as a function of PM voltage (top) or mdeg (bottom). 4 mM dopamine and 4 mM 4-HPAA were mixed in a 0.1 cm cell in the presence of 0.4 μM enzyme at 37 °C, in 0.1 M phosphate buffer at pH 7.5.

ESI-MS

1 mg of (S)-norcoclaurine obtained as described above was dissolved in 1 ml of acetonitrile and analyzed by ESI-MS (Thermo Finnigan LXQ). The spectrometer has an electrospray ion source and a linear ion trap analyzer. The ESI capillary temperature is 275°C and the analysis flow is 5 µl/min. The positive ESI-MS of norcoclaurine was observed with an m/z = 272,3 $[M+H]^+$.

GC/MS analysis

(S)-norcoclaurine formation was followed by withdrawing aliquots of reaction mixture (20 µl) until the increase in yield was negligible. Each aliquot was dried under N_2 stream and directly derivatized with trimethylsysil chloride in order to obtain trimethylsilyl ether (Figure 7.6 and 7.7).

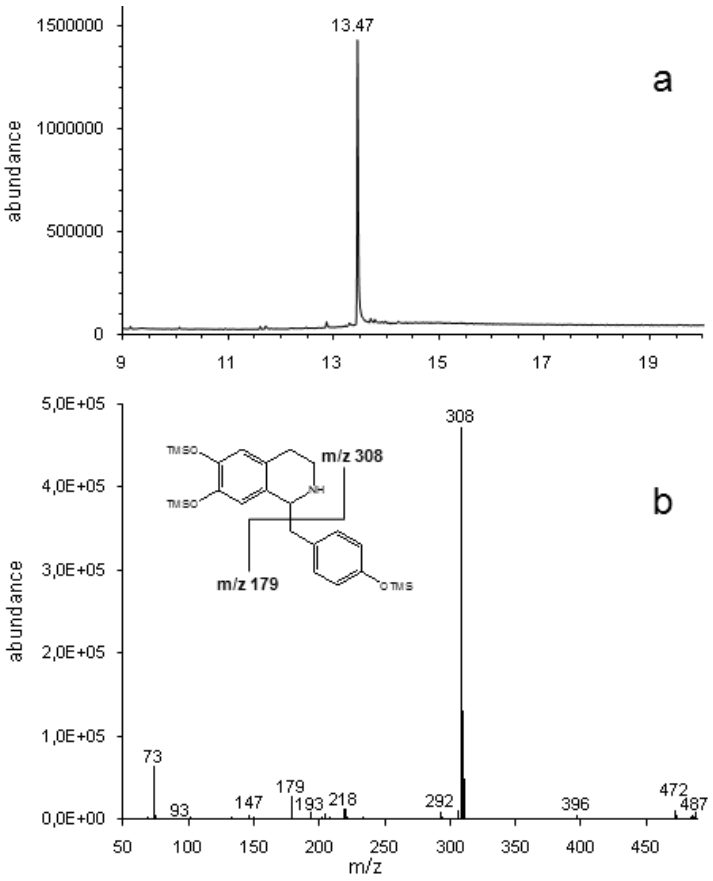

Figure 7.6 a) GC/MS chromatogram of the reaction mix after extraction and derivatization with TMS-chloride. b) EI mass spectrum of TMS-derivatized norcolaurine. The inset shows the two major ions deriving from TMS-norcolaurine fragmentation (m/z 308 and 179).

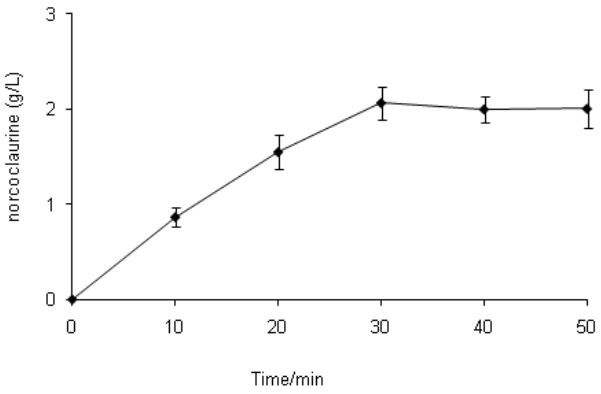

Figure 7.7 Time course of (S)-norcolcaurine formation. The error bars represent the standard deviation of three independent measurements.

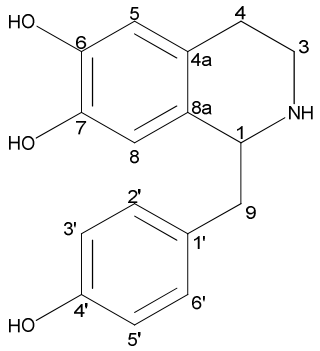

Small scale assay for (S)-norcoclaurine activity

Assay for the SNCS-catalyzed reaction was carried out in 20 mM phosphate (pH 7.0), 5 mM 4-HPAA obtained as described above, 5 mM dopamine, 0.4 µM enzyme in a total volume of 50 ml. The reaction mixture was incubated at 25 °C for 30 min. Extraction with diethyl ether yielded 55 mg (0.19mmol, 80%) of norcoclaurine as a white solid; ^{1}H NMR (CD_3OD, 400 MHz): δ 7.09 (d, J=7.5 Hz; H-2', H-6'), 6.77 (d, J=7.5 Hz; H-3', H-5'), 6.64 (s, H-5) , 6.55 (s, H-8), 4.21 (br s, H-1), 3.21 (m, H_2-3), 2.89 (m, H_2-9), 2.76 (m, H_2-4); ^{13}C NMR (CD_3OD, 400 MHz): δ 156.4 (C-4'), 144.6, 143.8 (C-6, C-7), 130.3 (C-2', C-6'), 127.8, 126.1, 124.3 (C-4a, C-8a, C-1'), 115.4 (C-3', C-5'), 115.1, 113.0 (C-5, C-8), 56.7 (C-1), 40.3, 39.9 (C-3, C-9), 34.0 (C-4). $[\alpha]_D^{25}$ = -24.7 (c = 0,04% in MeOH). The compound is thus assigned to (S)-(-)-norcoclaurine in agreement with ref. [55].

HPLC analysis for enantiomeric excess determination

Separation of the norcoclaurine enantiomers was performed by an HPLC analysis carried out on a chiral stationary phase with Teicoplanin as selector obtained from Gasparrini F. (CSP-Teicoplanin, 250 x 4.0 mm); the mobile phase was methanol/acetonitrile (70/30 v/v)

containing 0.25% Et_3N and 0.25% CH_3COOH; flow rate, 1.00 ml/min at 25 °C. UV and CD detections were performed at λ = 254 nm and λ = 280 nm respectively. The CD spectra on-line were recorded ranging from 220 to 420 nm. The enantiomeric excess of the product as determined by chiral HPLC was found to be 93%. The retention times of (S)- and (R)-norcoclaurine isomers were 12.5 min and 21.5 min respectively.

NCS expression and purification

A synthetic gene coding for norcoclaurine synthase (NCS) from *Thalictrum flavum* has been constructed by GENEART (GmbH, Germany) with optimised *E. coli* codons. The NCS protein truncated at the first 19 aminoacids, with a His-tag at the C-terminus was expressed in *E. coli* BL21 (DE3) cells under fermentative conditions. The cells were harvested by centrifugation (4000 x *g* for 10 min at 4 °C). Cell pellets were frozen overnight, then resuspended and sonicated in 10 ml of 50 mM phosphate buffer, pH 8, containing 300 mM NaCl (buffer A) and 1mM phenylmethylsulfonyl fluoride (PMSF). The extracts were centrifuged at 16000 x *g* for 20 min at 4 °C. NCS was purified in batch using a Nickel-Chelating Resin (Protino, Ni-TED, Macherey-Nagel). After washing with buffer A, the protein was eluted with buffer A added with 500 mM imidazole (buffer B).

One pot preparation of norcoclaurine from 4-hydroxyphenylacetaldehyde and dopamine.

A solution of tyrosine (10 mmol) was mixed with a solution of NaClO (10 mmol) in phosphate buffer 50 mM pH 7.0 (1h a 37°C) in a final volume of 1 L. Aliquots of 50 µl of the reaction mix were extracted with 200 µl diethylether and directly injected in GC/MS (1 µl) to follow the aldehyde formation. Once tyrosine was completely converted in 4-hydroxyphenylacetaldehyde (10 mM final concentration), dopamine (10 mmol) and norcoclaurine synthase (10 mg, corresponding to a final concentration of 0.5 µM) were added to the reaction mixture in the presence of ascorbate (5 mM) and incubated for 30 min at 37 °C. Activated carbon NORIT (Sigma-Aldrich 93067) was used as adsorbent for the purification of (S)-norcoclaurine. Briefly, 10 g of adsorbent were added to the aqueous reaction mixture (1 l). After 30 min shaking at room temperature, the mixture was filtered. The adsorbent was recovered and washed twice with 50 ml distilled water. It was then transferred in a conical flask and treated with 100 ml ethanolic sodium hydroxide (0.005 N NaOH in 99 % ethanol). Desorption was carried out by 2 hours shaking at 40 °C. The

organic fraction was neutralized with 0.005 N HCl and evaporated to dryness under reduced pressure to afford 2,2 g (8.1 mmol) of norcoclaurine.

References

[1] Facchini, P.J.; Alkaloid Biosynthesis in Plants: Biochemistry, Cell Biology, Molecular Regulation, and Metabolic Engineering Applications, *Annu. Rev. Plant Physiol. Plant Mol. Biol.* **2001**, *52*: 29–66.

[2] Mahmoudian, M.; Rahimi-Moghaddam, P.; The Anticancer Activity of Noscapine: A Review, *Recent Patent on Anti-Cancer Drug Discovery* **2009**, *4*: 92-97.

[3] Tsutsumi, T.; Kobayashi, S.; Liu, Y.Y.; Kontani, H.; Anti-hyperglycemic Effect of Fangchinoline Isolated from Stephania Tetrandra Radix in Streptozotocin-Diabetic Mice, *Biol. Pharm. Bull.* **2003**, *26*: 313—317.

[4] Liscombe, D.K.; Facchini, P.J.; Evolutionary and cellular webs in benzylisoquinoline alkaloid biosynthesis, *Current opinion in Biotechnology* **2008**, *19*: 173–180.

[5] Boettcher, C.; Fellermeier, M.; Boettcher, C.; Dräger, B.; Zenk, M.H.; How human neuroblastoma cells make morphine*, Proc. Natl. Acad. Sci.* **2005**, *102* : 8495–8500.

[6] Poeaknapo, C.; Schmidt, J.; Brandsch, M.; Dräger, B.; Zenk, M.H.; Endogenous formation of morphine in human cells, *Proc. Natl. Acad. Sci.* **2004**, *101*: 14091-14096.

[7] Sango, K.; Maruyama, W.; Matsubara, K.; Dostert, P.; Minami, C.; Kawai, M.; Naoi, M.; Enantio-selective occurrence of (S)-tetrahydropapaveroline in human brain, *Neurosci. Lett.* **2000**, *283*: 224–226.

[8] Sekine, Y.; Brossi, A.; Expedient synthesis of (S)- and (R)-norcoclaurine from (S)- and (R)-armepavine prepared by the 1-phenylethylurea method, *Journal of Natural Products* **1990**, *53*: 533-535.

[9] Kosuge, T.; Yokota, M.; Nagasawa, M.; Studies on cardiac principle in Aconite roots: I. Isolation and structure determination of higenamine, *Yakugaku Zasshi* **1978**, *98*: 1370–1375.

[10] Leboeuf, M.; Cavé, A.; Touché, A.; Provost, J.; Forgacs, P.; Isolement de L'higénamine A Partir de l'Annona squamosa; Interet Des Résines Adsorbantes Macromoléculaires en Chime Végétale Extractive, *J. Nat. Prod.,* **1981**, *44* : 53–60.

[11] Xu, Q.; Lin, M.; Benzylisoquinoline Alkaloids from Gnetum parvifolium, *J. Nat. Prod.* **1999**, *62*: 1025-1027.

[12] Chang, Y.C.; Chang. F.R.; Khalil, A.T.; Hsieh, P.W.; Wu, Y.C.; Cytotoxic benzophenanthridine and benzylisoquinoline alkaloids from Argemone mexicana, *Z Naturforsch C.* **2003**, *58*: 521-526.

[13] Kashiwada, Y.; Aoshima, A.; Ikeshiro, Y.; Chen, Y.-P.; Furukawa, H.; Itoigawa, M.; Fujioka, T.; Mihashi, K.; Cosentino, L.M.; Morris-Natschkeg, L.M.; Leeg, K.H.; Anti-HIV benzylisoquinoline alkaloids and flavonoids from the leaves of Nelumbo nucifera, and structure–activity correlations with related alkaloids, *Bioorganic & Medicinal Chemistry* **2005**, *13* : 443–448.

[14] Kimura, I.; Makino, M.; Takamura, Y.; Islam, Md.A.; Kimura, M.; Positive Chronotropic and Inotropic Effects of Higenamine and Its Enhancing Action on the Aconitine-Induced Tachyarrhythmia in Isolated Murine Atria, *Jpn. J. Pharmacol.* **1994**, *66*: 75-80.

[15] Chong, W.-S.; Lee, Y.-S.; Kang, Y.-J.; Lee, D.-H.; Ryu, J.-C.; Yun-Choi, H.S.; Chang, K.-C.; Comparison of Inodilator Effect of Higenamine, YS49, YS51, Tetrahydroisoquinoline Analogs, and Dobutamine in the Rat, *Korean J. Physiol. Pharmacol.* **1998**, *2*: 323-330.

[16] Bai, G.; Yang, Y.; Shi, Q.; Liu, Z.; Zhang, Q.; Zhu, Y.-Y.; Identification of higenamine in Radix Aconiti *Lateralis Preparata* as a beta$_2$-adrenergic receptor agonist, *Acta Pharmacol. Sin.* **2008**, *29*: 1187–1194.

[17] Yun-Choi, H.S.; Pyo, M.K.; Park, K.M.; Chang, K.C.; Lee, D.H.; Antithrombotic Effects of YS-49 and YS-51—1-Naphthylmethyl Analogs of Higenamine, *Thrombosis Research* **2001**, *104*: 249–255.

[18] Pyoa, M.K.; Kima, J.M.; Jina, J.L.; Chang, K.C.; Lee, D.H.; Yun-Choia, H.S.; Effects of higenamine and its 1-naphthyl analogs, YS-49 and YS-51, on platelet TXA_2 synthesis and aggregation, *Thrombosis Research* **2007**, *120*: 81-86.

[19] Kang, Y.J.; Lee, Y.S.; Lee, G.W.; Lee, D.H.; Ryu, J.C.; Yun-Choi, H.S.; Chang, K.C.; Inhibition of activation of nuclear factor kappaB is responsible for inhibition of inducible nitric oxide synthase expression by higenamine, an active component of aconite root, *J. Pharmacol. Exp. Ther.* **1999**, *291*: 314– 320.

[20] Lee, H.Y.; Lee, J.S.; Kim, E.J.; Han, J.W.; Lee, H.W.; Kang, Y.J.; Chang, K.C.; *Arch. Pharm. Res.* **1999**, *22*: 55-59.

[21] Park, J.E.; Kang, Y.G.; Park, M.K.; Lee, Y.S.; Kim, H.J.; Seo, H.J.; Lee, J.H.; Sook, Y.-C.H.; Shin, J.S.; Lee, H.W.; Ahn, S.K.; Chang, K.C.; Enantiomers of higenamine inhibit LPS-induced iNOS in a macrophage cell line and improve the survival of mice with experimental endotoxemia, *International Immunopharmacol.* **2006**, *6*: 226–233.

[22] Chang, K.-C.; Yun-Choi, H.S.; Lim, J.K.; Park, C.-W.; Synthesis of Higenamine, A Cardiotonic Principle of Aconite Root, *Arch. Pharm. Res.* **1984**, *7*: 133-136.

[23] Pyo, M.K.; Lee, D.H.; Kim, D.H.; Lee, J.H.; Moon, J.C.; Chang, K.C.; Yun-Choi, H.S.; Enantioselective synthesis of (R)-(+)- and (S)-(-)-higenamine and their analogues with effects on platelet aggregation and experimental animal model of disseminated intravascular coagulation, *Bioorg. Med. Chem. Lett.* **2008**, *18*: 4110-4114.

[24] Cox, E.D.; Cook, J.M.; The Pictet-Spengler Condensation: A New Direction for an Old Reaction, *J. Org. Chem.* **1995**, *60*: 1797-1842.

[25] Rousseau, J.-F.; Dodd, R.H.; Synthesis of 3-Deaza-β-hydroxyhistidine Derivatives and Their Use for the Preparation of Substituted Pyrrolo[2,3-c]pyridine-5-carboxylates via the Pictet-Spengler Reaction, *J. Org. Chem.* **1998**, *63*: 2731-2737.

[26] Kim, S.; Lee, J.; Lee, T.; Park, H.-G.; Kim, D.; First Asymmetric Total Synthesis of (-)-Antofine by Using an Enantioselective Catalytic Phase Transfer Alkylation, *Org. Lett.* **2003**, *5*: 2703-2706.

[27] Magnus, N.A.; Ley, C.P.; Pollock, P.M.; Wepsiec J.P.; Pictet-Spengler Based Synthesis of a Bisarylmaleimide Glycogen Synthase Kinase 3 Inhibitor, *Org. Lett.* **2010**, *12*: 3700-3703.

[28] Guiso, M.; Marra, C.; Cavarischia, C.; Isochromans from 2-(3',4'-dihydroxy)phenylethanol, *Tetrahedron Letters* **2001**, *42*: 6531–6534.

[29] Soe, T.; Kawate, T.; Fukui, N.; Nagakawa, M.; Asymmetric Pictet-Spengler Reaction with ChiraI-N-(β-3-indolyl)ethyl-1-methylbenzylamine, *Tetrahedron Letters* **1995**, *36*: 1857-1860.

[30] Gremmen, C.; Willemse, B.; Wanner, M.J.; Koomen, G.-J.; Enantiopure Tetrahydro-β-carbolines via Pictet-Spengler Reactions with N-Sulfinyl Tryptamines, *Org. Lett.* **2000**, *2*: 1955-1958.

[31] Madrigal, A.; Grande, M.; Avendaño, C.; Stereocontrolled Synthesis of 3,6-Dimethyl-2,3,6,7,12,12a-hexahydropyrazino[1,2-b]-β-carboline-1,4-diones, *J. Org. Chem.* **1998**, *63*: 2724-2727.

[32] Wu, Y.-C.; Zhu, J.; Asymmetric Total Syntheses of (-)-Renieramycin M and G and (-)-Jorumycin Using Aziridine as a Lynchpin, *Org. Lett.* **2009**, *11*: 5558-5561.

[33] Chen, J.; Chen, X.; Bois-Choussy, M.; Zhu, J.; Total Synthesis of Ecteinascidin 743, *J. Am. Chem. Soc.* **2006**, *128*: 87–89.

[34] Yamada, H.; Kawate, T.; Matsumizu, M.; Nishida, A.; Yamaguchi, K.; Nakagawa, M.; Chiral Lewis Acid-Mediated Enantioselective Pictet-Spengler Reaction of Nb-Hydroxytryptamine with Aldehydes, *J. Org. Chem.* **1998**, *63*: 6348-6354.

[35] Taylor, M.S.; Jacobsen, E.N.; Highly Enantioselective Catalytic Acyl-Pictet-Spengler Reactions, *J. Am. Chem. Soc.*, **2004**, *126*: 10558–10559.

[36] Seayad, J.; Seayad, A.M.; List, B.; Catalytic Asymmetric Pictet-Spengler Reaction, *J. Am. Chem. Soc.* **2006**, *128*: 1086-1087.

[37] Wanner, M.J.; van der Haas, R.N.S.; de Cuba, K.R.; van Maarseveen, J.H.; Hiemstra, H.; Catalytic Asymmetric Pictet–Spengler Reactions via Sulfenyliminium Ions, *Angew. Chem. Int. Ed.* **2007**, *46*: 7485 –7487.

[38] Comins, D.L.; Thakker, P.M.; Baevsky, M.F.; Badawi, M.M.; Chiral Auxiliary Mediated Pictet-Spengler Reactions: Asymmetric Syntheses of (-)-Laudanosine, (+)-Glaucine and (-)-Xylopinine, *Tetrahedron* **1997**, *53*: 16327-16340.

[39] Ilari, A.; Franceschini, S.; Bonamore, A.; Arenghi, F.; Botta, B.; Macone, A.; Pasquo, A.; Bellucci, L.; Boffi, A.; Structural Basis of Enzymatic S-norcocclaurine Biosynthesis, *J. Biol. Chem.* **2009**, *284*: 897-904.

[40] Ma, X.; Panjikar, S.; Koepke, J.; Loris E.; Stöckigt, J.; The structure of rauvolfia serpentina strictosidine synthase is a novel sixbladed β-propeller fold in plant proteins, *Plant Cell* **2006**, *18*: 907-920.

[41] Maresh, J.J.; Giddings, L.; Friedrich, A.; Loris, E.A.; Panjikar, S.; Trout, B.L.; Stöckigt, J.; Peters, B.; O'Connor, S.E.; Strictosidine synthase: mechanism of a Pictet-Spengler catalyzing enzyme, *J. Am. Chem. Soc.* **2008**, *130*: 710-723.

[42] Hutt, A.J.; Tan, S.C.; Drug chirality and its significance, *Drugs* **1996**, *suppl. 5*: 1-12.

[43] Samanani, N.; Facchini, P.J.; Isolation and partial characterization of norcoclaurine synthase, the first committed step in benzylisoquinoline alkaloid biosynthesis, from opium poppy, *Planta* **2001**, *213*: 898-906.

[44] Samanani, L.; Facchini, P.J.; Purification and Characterization of Norcoclaurine Synthase, *J. Biol. Chem*. **2002**, *277*: 33878-33883.

[45] (http://www.ncbi.nlm.nih.gov/blast)

[46] Luk, L.Y.; Bunn, S.; Liscombe, D.K.; Facchini, P.J.; Tanner, M.E.; Mechanistic Studies on Norcoclaurine Synthase of Benzylisoquinoline Alkaloid Biosynthesis: An Enzymatic Pictet-Spengler Reaction, *Biochemistry* **2007**, *46*: 10153-10161.

[47] Protein Data Bank: accession codes 2VNE (substrates free) and 2VQ5 (in complex with substrates).

[48] 24. DeLano, W.L. (2002) The PyMOL. User's Manual, DeLano Scientific, San Carlos, CA, USA.

[49] Guiso, M.; Bianco, A.; Marra, C.; Chiavarischia, C.; One-Pot Synthesis of 6-hydroxyisochromans: The Example of Demethyl-oxa-coclaurine, *Eur. J. Org. Chem.* **2003**, 3407-3411.

[50] Hazen, S.L.; Hsu, F.F.; Heinecke, J.W.; *p*-Hydroxyphenylacetaldehyde Is the Major Product of L-Tyrosine Oxidation by Activated Human Phagocytes, *J. Biol. Chem.* **1996**, *271*: 1861-1867.

[51] Hazen, S.L.; Gaut, J.P.; Hsu, F.F.; Crowley, J.R.; d'Avignon A.; Heinecke, J.W.; *p*-Hydroxyphenylacetaldehyde, the Major Product of L-Tyrosine Oxidation by the Myeloperoxidase-H_2O_2-Chloride System of Phagocytes, Covalently Modifies ε-Amino Groups of Protein Lysine Residues, *J. Biol. Chem.* **1997**, *272*: 16990-16998.

[52] Hazen, S.L.; d'Avignon A.; Anderson, M.M.; Hsu, F.F.; Heinecke, J.W.; Human Neutrophils Employ the Myeloperoxidase-Hydrogen Peroxide-Chloride System to Oxidize α-Amino Acids to a Family of Reactive Aldehydes; *J. Biol. Chem.* **1998**, *273*: 4997-5005.

[53] Minami, H.; Kim, J.S.; Ikezawa, N.; Takemura, T.; Katayama, T.; Kumagai, H., Sato, F.; Microbial production of plant benzylisoquinoline alkaloids, *Proc. Natl. Acad. Sci. USA*., **2008**, *105*: 7393-7398.

[54] Cavazzini, A.; Pasti, L.; Dondi, F.; Finessi, M.; Costa, V.; Gasparrini, F.; Ciogli, A.; Bedani F.; Binding of Dipeptides and Amino Acids to Teicoplanin Chiral Stationary Phase: Apparent Homogeneity of Some Heterogeneous Systems *Anal. Chem*. **2009**, *81*: 6735–6743.

[55] Chung, K.S.; Yun-Choi, H.S.; Hahn, Y.; High-performance liquid chromatographic analyses of higenamine enantiomers in Aconite roots, *Nat. Prod. Sci*., **2000**, *6*: 20–24.

Pubblications list

1. N. Tocci; F. Ferrari; A. R. Santamaria; A. Valletta; I. Rovardi; G. Pasqua, *Chitosan enhances xanthone production in Hypericum perforatum subsp. angustifolium cell cultures,* Natural Product Research, 2010, vol 24: 286–293;

2. A. Macone, E. Lendaro, A. Comandini, I. Rovardi, R. M. Matarese, A. Carraturo, A. Bonamore, *Chromane derivatives of small aromatic molecules: Chemoenzymatic synthesis and growth inhibitory activity on human tumor cell line LoVo WT,* Bioorganic & Medicinal Chemistry, 2009, vol 17: 6003–6007;

3. A. Bonamore, I. Rovardi, F. Gasparrini, P. Baiocco, M. Barba, C. Molinaro, B. Botta, A. Boffi, A. Macone, *An enzymatic, stereoselective synthesis of (S)-norcoclaurine*, Green Chem., 2010, vol 12: 1623-1627.